REPORT DOCUMENTATION PAGE

1. AGENCY USE ONLY (Leave blank)	2. REPORT DATE	3. REPORT TYPE AND DATES COVERED
	25 Mar 96	

4. TITLE AND SUBTITLE
Guided Bone Regeneration Around Commercially Pure Titanium and Hydroxyapatite-Coated Dental Implants

5. FUNDING NUMBERS

6. AUTHOR(S)

William Cyrus Stentz, Jr.

7. PERFORMING ORGANIZATION NAME(S) AND ADDRESS(ES)

AFIT Student Attending:

University of Texas

8. PERFORMING ORGANIZATION REPORT NUMBER

96-009

9. SPONSORING/MONITORING AGENCY NAME(S) AND ADDRESS(ES)

DEPARTMENT OF THE AIR FORCE
AFIT/CI
2950 P STREET, BLDG 125
WRIGHT-PATTERSON AFB OH 45433-7765

10. SPONSORING/MONITORING AGENCY REPORT NUMBER

11. SUPPLEMENTARY NOTES

12a. DISTRIBUTION/AVAILABILITY STATEMENT

Approved for Public Release IAW AFR 190-1
Distribution Unlimited
BRIAN D. GAUTHIER, MSgt, USAF
Chief Administration

12b. DISTRIBUTION CODE

13. ABSTRACT (Maximum 200 words)

19960531 100

14. SUBJECT TERMS

15. NUMBER OF PAGES
146

16. PRICE CODE

17. SECURITY CLASSIFICATION OF REPORT	18. SECURITY CLASSIFICATION OF THIS PAGE	19. SECURITY CLASSIFICATION OF ABSTRACT	20. LIMITATION OF ABSTRACT

GENERAL INSTRUCTIONS FOR COMPLETING SF 298

The Report Documentation Page (RDP) is used in announcing and cataloging reports. It is important that this information be consistent with the rest of the report, particularly the cover and title page. Instructions for filling in each block of the form follow. It is important to *stay within the lines* to meet *optical scanning requirements*.

Block 1. Agency Use Only *(Leave blank)*.

Block 2. Report Date. Full publication date including day, month, and year, if available (e.g. 1 Jan 88). Must cite at least the year.

Block 3. Type of Report and Dates Covered. State whether report is interim, final, etc. If applicable, enter inclusive report dates (e.g. 10 Jun 87 - 30 Jun 88).

Block 4. Title and Subtitle. A title is taken from the part of the report that provides the most meaningful and complete information. When a report is prepared in more than one volume, repeat the primary title, add volume number, and include subtitle for the specific volume. On classified documents enter the title classification in parentheses.

Block 5. Funding Numbers. To include contract and grant numbers; may include program element number(s), project number(s), task number(s), and work unit number(s). Use the following labels:

C	-	Contract	PR	- Project
G	-	Grant	TA	- Task
PE	-	Program Element	WU	- Work Unit Accession No.

Block 6. Author(s). Name(s) of person(s) responsible for writing the report, performing the research, or credited with the content of the report. If editor or compiler, this should follow the name(s).

Block 7. Performing Organization Name(s) and Address(es). Self-explanatory.

Block 8. Performing Organization Report Number. Enter the unique alphanumeric report number(s) assigned by the organization performing the report.

Block 9. Sponsoring/Monitoring Agency Name(s) and Address(es). Self-explanatory.

Block 10. Sponsoring/Monitoring Agency Report Number. *(If known)*

Block 11. Supplementary Notes. Enter information not included elsewhere such as: Prepared in cooperation with...; Trans. of...; To be published in.... When a report is revised, include a statement whether the new report supersedes or supplements the older report.

Block 12a. Distribution/Availability Statement. Denotes public availability or limitations. Cite any availability to the public. Enter additional limitations or special markings in all capitals (e.g. NOFORN, REL, ITAR).

DOD	- See DoDD 5230.24, "Distribution Statements on Technical Documents."
DOE	- See authorities.
NASA	- See Handbook NHB 2200.2.
NTIS	- Leave blank.

Block 12b. Distribution Code.

DOD	- Leave blank.
DOE	- Enter DOE distribution categories from the Standard Distribution for Unclassified Scientific and Technical Reports.
NASA	- Leave blank.
NTIS	- Leave blank.

Block 13. Abstract. Include a brief *(Maximum 200 words)* factual summary of the most significant information contained in the report.

Block 14. Subject Terms. Keywords or phrases identifying major subjects in the report.

Block 15. Number of Pages. Enter the total number of pages.

Block 16. Price Code. Enter appropriate price code *(NTIS only)*.

Blocks 17. - 19. Security Classifications. Self-explanatory. Enter U.S. Security Classification in accordance with U.S. Security Regulations (i.e., UNCLASSIFIED). If form contains classified information, stamp classification on the top and bottom of the page.

Block 20. Limitation of Abstract. This block must be completed to assign a limitation to the abstract. Enter either UL (unlimited) or SAR (same as report). An entry in this block is necessary if the abstract is to be limited. If blank, the abstract is assumed to be unlimited.

GUIDED BONE REGENERATION AROUND COMMERCIALLY PURE TITANIUM AND HYDROXYAPATITE-COATED DENTAL IMPLANTS

A
THESIS

Presented to the Faculty of
The University of Texas Graduate School of Biomedical Sciences
at San Antonio
in Partial Fulfillment
of the Requirements
for the Degree of

MASTER OF SCIENCE

by

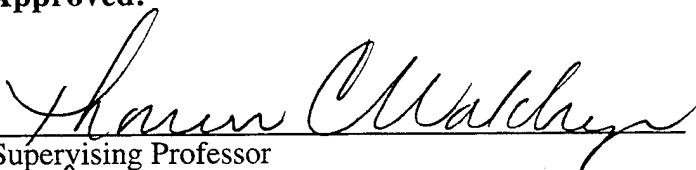## William Cyrus Stentz, Jr., D.D.S.

San Antonio, Texas

March 25, 1996

GUIDED BONE REGENERATION AROUND COMMERCIALLY PURE TITANIUM AND HYDROXYAPATITE COATED DENTAL IMPLANTS

William Cyrus Stentz, Jr.

Approved:

_____
Supervising Professor

_____
Supervising Professor

_____

_____

25 MAR 96
_____
Date

Approved:

_____
Sanford A. Miller, Ph.D.
Dean

DEDICATION

To the many teachers and professors through the years that have nourished my interest in science and medicine, to my mother and my late father who unselfishly provided the support and encouragement during the challenging academic times, to my thesis committee, especially my co-mentors, Dr. Brian Mealey and Dr. Thomas Waldrop, who gave me the latitude to design, orchestrate, and grow in knowledge through study and analysis, this overwhelming project. Finally, to my wife Maria, who sacrificed our time together allowing me to complete this personal goal.
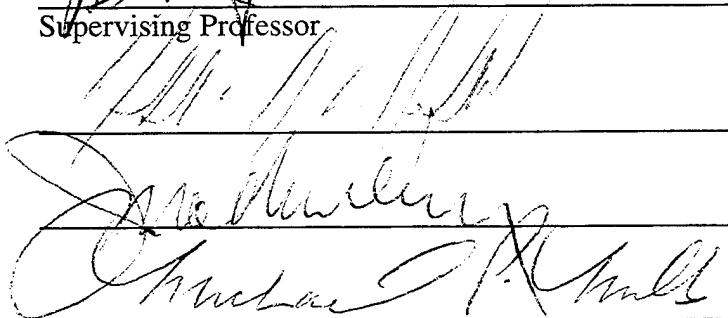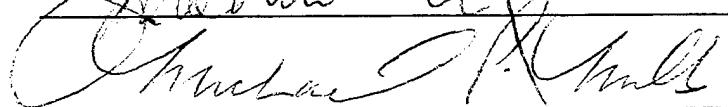
ACKNOWLEDGEMENTS

GUIDED BONE REGENERATION AROUND COMMERCIALLY PURE TITANIUM AND HYDROXYAPATITE COATED DENTAL IMPLANTS
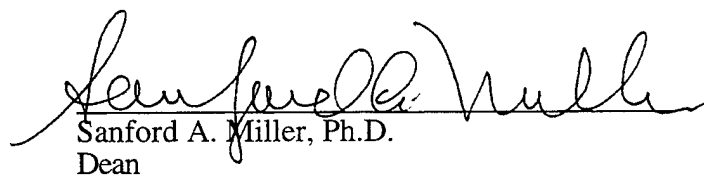
William Cyrus Stentz, Jr., M.S.

The University of Texas Graduate School of Biomedical Sciences
at San Antonio

Supervising Professors: Brian L. Mealey and Thomas C. Waldrop

In a split-mouth design, 6 implants were placed in edentulous mandibular ridges of 10 mongrel dogs after preparation of 6 cylindrical mid-crestal defects, 5 mm in depth and 10 mm in diameter. An implant site was then prepared in the center of each defect to a depth of 5 mm beyond the apical extent of the defect. One mandibular quadrant received three commercially pure titanium screw implants (3.75 x 10 mm), while the contralateral side received three titanium double plasma sprayed hydroxyapatite-coated root-form implants (3.3 x 10 mm). Consequently, the coronal 5 mm of each implant was surrounded by a circumferential surgically created defect approximately 3 mm wide and 5 mm deep. The three dental implants in each quadrant received either canine demineralized freeze-dried bone (DFDBA) and an expanded polytetrafluoroethylene membrane (e-PTFE), membrane alone, or no treatment which served as the control. Standardized radiographs were taken at one week and 4 months post-implant placement. Computer-Assisted Densitometric Image Analysis (CADIA) was performed for each of the implants. After 4 months of healing,

block sections of the mandibles were harvested for light microscopy and histomorphometric analysis.

Clinically, implant sites that received DFDBA/e-PTFE increased in both ridge height and width compared to the e-PTFE alone and controls. e-PTFE alone sites maintained the ridge height; however, the membrane tended to collapse against the implant buccolingually, limiting the potential for osseous regeneration. In the control sites, alveolar height and width resorption occurred in most cases to the depth of the original defect. After tissue reflection, sites receiving DFDBA/e-PTFE or e-PTFE alone appeared to be clinically osseointegrated and were non-mobile.

Radiographically, statistically significant differences in changes in bone density were seen between treatment groups (p<0.0001: DFDBA/e-PTFE > e-PTFE alone > control). There were no significant differences in radiographic bone density changes adjacent to titanium versus hydroxyapatite-coated implants (p=0.14).

Histologically, statistically significant differences in defect osseointegration were seen between treatment groups (p<0.0001: DFDBA/e-PTFE > e-PTFE alone > control). For the non-defect area, no significant difference in osseointegration between treatments was found (p=0.47). Hydroxyapatite-coated implants had significantly greater osseointegration within the defect than titanium implants (p<0.0001). Likewise, non-defect osseointegration was significantly greater for hydroxyapatite-coated implants than for titanium implants (p<0.0001). Average trabeculation of newly formed bone in the defect after healing was significantly greater for hydroxyapatite-coated implants than for titanium (p<0.0001), while the effect between treatments was not significantly different (p=0.17). Average trabeculation in the non-defect area after healing, was not significantly different when the type of implant surface was considered (p=0.21), nor was the effect between treatments (p=0.08). Finally, there were significantly less residual allograft particles in defect areas adjacent to hydroxyapatite implants than titanium implants (p=0.0355).

Radiographically, the use of DFDBA/e-PTFE promoted a denser healing of osseous structure adjacent to implants compared to e-PTFE alone or no treatment. No difference was found by CADIA regarding the choice of implant surface. Histologically, the use of hydroxyapatite coated

implants in large size defects with DFDBA and e-PTFE membranes produced significantly more osseointegration than other treatment options and more than titanium implants with the same treatment combinations. The results of this study indicate that although the implants appeared osseointegrated both clinically and radiographically after 4 months of healing, histologic data suggest that selection of both the implant type and the treatment modality is important in obtaining optimum osseointegration in large size defects.

TABLE OF CONTENTS

LIST OF TABLES

LIST OF FIGURES

LIST OF PLATES

I. <u>INTRODUCTION</u>

Endosseus dental implants have had a dramatic impact on the field of dentistry in the last 20 years. Prior to implant therapy, dental patients who lost one or all of their teeth were relegated to altering adjacent teeth for fixed prosthetics or dealing with the inadequacies of removable prosthetics.

Endosseous implants allow a wide variety of treatment options ranging from the replacement of a single tooth without altering adjacent teeth to the creation of a totally implant born appliance for edentulous patients. In addition, much progress has been made in improving the hard tissue anatomy for patients who have inadequate support or room for implant therapy. These anatomical inadequacies include severe alveolar bone loss in both buccolingual and apical directions and inadequate ridge dimensions for proper prosthodontic alignment with the existing dentition. Many types of implant systems have been devised and tested and have shown long-term success rates of approximately 91% in the mandible and 81% in the maxilla.[1]

Despite all of these improvements in therapy and the inclusion of patients who previously would not have been considered for implant placement, time requirements are still a negative factor. Ideal implant placement requires 4 to 6 months for osseointegration. This assumes an ideal healed ridge prior to endosseous implant placement. Special augmentation procedures, nerve repositioning, or sinus lifts demand extra healing time. Patients naturally do not want to wait these extra months and may conceivably wait more than a year for the final prosthesis to be delivered.

Recently, bone augmentation materials such as demineralized freeze-dried bone allograft (DFDBA) have been used around implants in less than ideal situations such as dehiscences or fenestrations. In addition, implants are being placed in immediate extraction sites to reduce the time to final restoration placement by eliminating the 4 to 6 months required for the ridge to heal post-extraction. More often than not, the socket remaining after extraction is either much larger

1

that the planned implant or the ideal implant location is not coincident with the socket location and does not provide ideal implant emergence.

Placement of DFDBA with or without barrier membranes as used with guided tissue regeneration, has provided successful clinical results; however, actual verification of osseointegration in these "repaired" areas is difficult to obtain. Several authors have presented histology of bone removed over the implant cover screw or where fenestrations or dehiscences were "repaired," but these locations do not give any insight into the quality or quantity of bone at the implant interface. Although some human histology has been obtained following removal of failed implants, most of the information concerning osseointegration has been obtained through animal studies.

The success of two stage immediate implant therapy is based on alveolar ridge appearance and the apparent clinical integration of the implant at abutment connection. It is imperative that the osseointegration be verified in a standardized manner with properly controlled studies where histology can be obtained. The goal of this study was to investigate the quality and quantity of osseointegration for two of the major implant types, commercially pure titanium (Ti) machined screws and Ti double plasma sprayed hydroxyapatite-coated cylinders, when regeneration of a peri-implant defect is required. The implants were placed in surgically created defects simulating a situation analogous to an extraction site since the alveolar housing does not totally encase the implant. Three regeneration techniques were applied: DFDBA and an expanded polytetrafluoroethylene membrane (e-PTFE), e-PTFE alone, or no treatment that served as a control.

II. LITERATURE REVIEW

A. Endosseous Dental Implants

1. Titanium implants

Brånemark and his co-workers published their work with commercially pure Ti for endosseous implants in 1969.[2] Their design, a machined-threaded screw, has become the standard against which implant systems are measured. The surface of Ti implants is considered bioactive in that it reacts to bone even though the metal is considered inert.[3] The Ti surface has a 30 to 150 Å thick layer of TiO_2, which is considered bioactive.[4,5] The surface biocompatibility is derived from the high dielectric constant of the oxide layer resulting in strong Van der Waal's bonds at the surface.[4] Ti and Ti alloys maintain this layer in physiologic conditions without significant breakdown or corrosion.[6] These properties support the phenomenon of direct bone-implant contact or osseointegration.[6,7]

Osseointegration, the anchorage of Ti to bone, as defined by Brånemark is "a direct structural and functional connection between ordered, living bone and the surface of a load-carrying implant."[1,8] Weinlaender[4] summarized this as a firm, direct, and lasting connection between vital bone and implants of defined finish and geometry, with no interposed connective tissue between implant fixture and bone.

Osseointegrated Ti implants were felt to yield the most predictable success for long-term stability in both hard and soft tissue.[8,9] Though Ti is biocompatible, it does not biologically bond to bone and relies solely on mechanical retention or "ankylosis"[10] for stability with undercuts such as threads, grooves, or blade shapes.[11,12]

Three possible host tissue responses are postulated by Brånemark to occur after implant placement.[3] First, acute or chronic inflammation may cause early implant failure. Second, encapsulation of the implant with fibrous tissue may occur (fibro-osseointegration, peri-

implant ligament, or pseudoperiodontium). Third, and most desired, vital bone may be in immediate mechanical contact with the implant, securing anchorage around the implant.

In this immediate mechanical contact, bone is not able to attach directly to Ti implants. Electron microscopy has demonstrated a proteoglycan layer of 40-200 Å in direct contact with the TiO_2 surface.[13] By adding threads, deep grooving, or porosities, the incidence of mechanical retention and available surface area for osseointegration increases. Histomorphometric analysis suggests approximately 40 to 60% of the available implant surface is apposed by mineralized bone. The remainder consists of combinations of nonmineralized tissue such as osteoid, fibrous connective tissue, and marrow space.[14] Ti demonstrates no "osteoconductive" or "osteophilic" properties.[10,12,15-17]

a. Titanium research

Brånemark[18] has demonstrated in different animal models that healthy bone is able to integrate with implants made of pure Ti. Steflik et al.,[14] using Transmission Electron Microscopy (TEM) and High Voltage Electron Microscopy (HVEM), studied bone and osteocyte activity next to Ti implants in dogs. They observed a mineralization pattern of supporting bone that was similar to those events occurring naturally within mandibular bone. Arvidson et al.[19] placed 24 implants in dogs and histologically confirmed the radiographic appearance of implant surface contact with bone tissue. Lum and Beirne researched Ti alloy implants and found histologically new bone against implant surfaces with no intervening fibrous tissue layer at the light level.[20]

Roberts[21] has looked at implant healing in both rabbit femur and dog mandibles. Through multiple fluorochrome labeling he has demonstrated successful integration on 94% of Ti endosseous implants and determined the appropriate times needed for healing.

In a long-term retrospective study, Adell et al.[22] reported in totally edentulous patients an estimated 15 year implant survival rate of 86% in the mandible and 78% in

the maxilla. Zarb *et al.*[23] have also found similar results in prospective studies in edentulous patients. Clinical interest began to turn to treating partially edentulous patients in the mid-1980s. Brånemark implants have demonstrated a mean success rate of greater than 90% in a prospective study of partially edentulous patients.[24]

2. Hydroxyapatite-coated implants

Calcium phosphate ceramics (CPC), such as hydroxyapatite (HA) and tricalcium phosphate, resemble the inorganic phase of the human skeleton and their composition has no toxic components.[3,4] They are considered bioactive since they react with the surrounding environment, and have the apparent ability to become directly bonded to bone.[4,7,12] Unfortunately, CPC's are stronger in compression than tension and have an inherent brittleness that limits their use as implants. By combining the mechanical properties of pure Ti with an over coating of 75 μm of HA, the best properties of each material are employed.[4,7,16,17,25-27]

HA is an osteophilic, osteoconductive, bioactive coating; whereas, Ti and Ti alloy are bioinert.[10] Direct chemical bonding of the HA implant surface to bone along with a dense close mechanical bond of the implant-bone interface is defined as biointegration. The latter is independent of any mechanical interlocking mechanism. Biointegration has been verified at the light and electron microscope level.[3,16,25]

Shear strengths and pull-out forces have been measured for different implant shapes and types. Coating HA on Ti implants increases the shear strength 4.4 to 141 times compared to Ti alone in mandibular bone.[11,25,28-30] HA-coated implant systems have been reported to have greater bone-implant contact compared to Ti.[4,31]

Ultrastructurally, HA-bone interface exhibits a direct chemical bond to bone. This is unlike the Ti-bone interface which has an intervening glycoprotein layer.[28] Evidence exists that bone forms simultaneously at the HA surface and the surrounding bone bed, unlike Ti implants where bone formation is only in one direction, i.e. from the bone bed.[4,32]

Kay[32] has also described this faster adaptation of bone to HA surfaces. Furthermore, there is an absence of fibrous tissue seams due to direct adaptation of bone to the HA surface. Thus, bone adapts more quickly to fill the small defects between the implant surface and bone. Direct bone apposition at the implant interface may offer a better clinical prognosis.[12]

Pillar *et al.*[33] reviewed the literature and suggested that HA coatings on Ti and Ti alloy offer certain advantages. These include more rapid development of strong bonding at porous-coated implant-bone interfaces and greater shear and tensile strengths at non-porous implant-bone interfaces.

Biochemical tests suggest that HA-coated surfaces are superior to Ti alone as to degree and rate of fixation in bone. More load bearing bone on HA-coated surfaces compared to uncoated Ti surfaces may contribute to the implant success.[3]

In review, HA coating on dental implants leads to faster bony adaptation, absence of fibrous tissue seams, firmer implant-bone attachment, reduced healing time, and increased tolerance of surgical inaccuracies, when compared to a bioinert surface such as commercially pure Ti.[11,16,26,28,32,34,35] However, Buser comments in his text that several publications have reported on the instability of the HA surface over time, demonstrating resorption in histologic evaluations. This may be a contributing factor in the increased rate of complications seen with these implants in the 3 to 5 year time frame.[34]

Johnson[36] reviewed concerns with HA coated implants and the apparent increase in failures with time. Although HA coatings have many initial benefits compared to Ti, success rates over a five year period are very similar, greater than or equal to 95%. Johnson concludes there is no benefit to the HA coating in this regard. The bioactive bond between bone and HA coatings involves a continuous ion exchange and may lead to dissolution of the coating and eventual failure of the implant. Cook *et al.*[37] found through push-out studies that the shear strength of HA-coated implants decreased during his study from 10 to 32 weeks. This raises concern for the HA bond over time. Gottlander and

Albrektsson[38] demonstrated at 6 weeks an initially higher bone-to-implant contact for HA-coated implants compared to Ti. However, by 12 months, the Ti surface contact had increased while the HA diminished. This again casts doubt on the long term stability of the HA bond. Microbiologically, the HA coating also comes under attack when failed implants are examined. Krauser *et al.*[39] compared failed HA-coated and Ti implants. He found colonization of the HA surface was common, some of the HA surface was lost, and microcracks and stripping of the HA coating were numerous. Due to the rough surface, exposed HA-coated implants may enhance plaque growth and subsequent peri-implantitis.[40] In a survey of implant practices using Calcitek HA-coated implants, Johnson reported:

> (1) long-term maintenance of HA-coated implants is unpredictable; (2) bone loss around HA-coated implants can occur suddenly and rapidly after an initial period of apparent success; (3) a significant proportion of the HA-coated implant failures show aggressive and destructive bone loss patterns; (4) bleeding and suppuration are common soft tissue signs around HA-coated implants; and (5) the HA-coated implants are usually not mobile even when bone loss has been extreme (>50%).

More long-term research is required concerning these findings.

a. Hydroxyapatite research

Animal studies have found bone healing is enhanced by HA.[10] In a literature review, Denissen *et al.*[11] suggests that the HA coating results in a more rapid bonding to bone than Ti alone in dog femurs. Also, the initial mechanical fit of the implant may not be as critical with HA coating since a strong bond forms very rapidly between bone and the HA coating. The same results were demonstrated in dog mandibles by this group.

Animal studies have shown that the attachment of bone to HA has an increased shear and tensile strength. Cook *et al.*[37] using HA-coated and grit-blasted cylindrical Ti implants in the dog femur, reported a shear strength of 6 to 7 MPa in comparison to 1.2 MPa for uncoated implants. Ducheyne *et al.*[41] and Rivero *et al.*[42] have reported

faster bone ingrowth, resulting in earlier secure implant fixation. De Groot et al.[43] also compared HA-coated and uncoated Ti implants in the dog femur. The tensile bond strength of HA-Ti-bone interface was 85 MPa while uncoated implants were only 0.6 MPa.

Cooley et al.[27] demonstrated that HA-coated implants had twice the percentage of direct bone contact compared to noncoated implants and that the interface bond strength was significantly greater for HA-coated implants. Pilliar et al.[33] in a dog study found that greater bone height was observed mesially and distally with HA-coated implants. In a dog study by Block et al.,[26] HA-coated implants demonstrated statistically significantly greater bone apposition, and at an earlier time point to their axial and apical surfaces, compared to the grit-blasted Ti implants. Bone directly apposed 85% of the HA-coated implants compared to only 62.8% of the grit-blasted implant surface. Animal experiments in alveolar processes and long bones have demonstrated bone deposition is faster and bonds stronger to HA-coated surgical metal than uncoated controls.[3]

Block and Kent have published a prospective clinical analysis of 740 HA-coated implants in 215 patients with a 93.65% success rate.[44] Krauser states several clinical reports demonstrate an improvement in the use of HA cylinders in the maxilla over the Ti screw. The formation of lamellar bone on the HA surface during the healing phase seems to be the key to success in the spongy cancellous bone of the maxilla.[3]

3. Histology of endosseous dental implants

Guided bone regeneration (GBR) using autografts, allografts, or alloplasts, barrier membranes, or combination therapy has been accomplished with what appear to be successful clinical results; however, actual verification of osseointegration through histology in these "repaired" areas is difficult to obtain. Several authors have presented histology of bone removed over the implant cover screw or where fenestrations or

dehiscences were "repaired," but these locations do not give any insight into the quality or quantity of bone at the implant interface.[45-49] Although some human histology has been obtained through removal of Ti miniscrews,[50] failed implants,[51-53] experimental protocols,[54] block sections,[55] or cadaveric specimens;[56,57] most of the information concerning osseointegration in defects and immediate extraction sockets has been obtained through animal studies.[15,58-63]

Normal mandibular bone is comprised of compact bone, which is largely mineralized interstitial bone, encasing a core of spongy bone. Lacunae, uniformly distributed throughout the interstitial substance, are filled completely by a bone cell or osteocyte. Radiating in all directions are slender, branching, tubular passages identified as canaliculi. These canaliculi penetrate the interstitial substance of lamellae, anastomosing with the canaliculi of other lacunae. The passages are considered essential to the nutrition of bone cells.

Messadi et al.[64] summarizes general bone healing as a similar sequence to soft tissue healing. Bone healing is divided into 3 phases with the first being the inflammatory phase, followed by the reparative phase, and finally the remodeling phase. When bone is injured as in a fracture, small blood vessels in the haversian canals, bone marrow, and periosteum are severed. Blood flows into the fracture cleft and a hematoma occurs. A loose fibrin mesh is formed by this blood clot and seals off the fracture site while also serving as a framework for the ingrowth of fibroblasts and new capillary buds. The clot reorganizes and produces a soft tissue callus that provides anchorage for the bony fragments but does not provide structural rigidity. After the first few days, the granulation tissue matures into cartilage and bone matrix forms a fibrocartilaginous callus that bridges the fracture gap. Woven bone is formed by the mineralization of the callus, which develops by endochondral ossification in the callus and by subperiosteal deposition at its periphery. Buser adds that woven bone is primarily seen in embryos and growing children; however, it returns when accelerated bone formation is needed.[65] This immature bone is later replaced by lamellar

bone composed of regularly arranged collagen bundles. Remodeling continues over time and eventually results in dense compact bone.

When a bone bed for implant placement is prepared, the healing sequence is similar to that previously described for general bone healing. It is considered orthotopic bone induction, i.e. ossification in contact with existing bones. The hemorrhaging damaged vessels at the implant site form a blood clot. The periosteum and endosteum respond with proliferation of fibroblasts and osteoprogenitor cells creating direct bone formation by forming a connective tissue callus. There is an initial short lag phase of 1 to 3 days prior to new bone being laid down on existing bone surfaces. The callus is transformed into immature or woven bone by osteoblasts producing osteoid. This osseous matrix becomes mineralized in only 1 to 3 days with calcium and phosphate ions.[4,65] Initiation of woven bone mineralization is by matrix vesicles. Lamellar bone formation progresses at a much slower rate than woven bone, taking 10 days to mineralize. In addition, matrix vesicles are rarely seen along the mineralization front and lamellar bone is not able to construct beams or ridges like woven bone.[65]

HA-coated and Ti implants demonstrate different degrees of healing at their bone-implant interface, which can be determined at the light microscope level.[10,66] Healing of the Ti screw is initiated after 1 week, with primary or woven bone originating from the bone bed surrounding the implant.[4] New bone grows up to and then adapts to the surface of Ti implants.[3] Secondary or lamellar bone forms in 3 to 12 weeks.[4] This bone growth takes the direction from bone bed toward the implant surface.[4,67] After 12 weeks, continuous bone formation with remodeling is subject to occur.[4] Often, intervening fibrous tissue elements can be seen between the implant and bone.

Roberts, studying this Ti-bone interface, has stated 25% of the bone is in direct implant contact, 40-50% is in close apposition with undifferentiated material between the implant and bone, while 20% has fibrous tissue elements between bone and implant.[67] The general appearance of the bone adjacent to Ti implants in a study by Arvidson *et al.*[19] was that of

normal healthy bone. Direct bone contact was seen at the implant surface in the cortical parts of the alveolar bone, while in the trabecular area contact was 61.3% at 6 months. Deporter et al.[68] compared partially porous coated Ti-6Al-4V implants with commercially pure Ti screws. Histologically, the Ti screw threads were embedded in bone and depended on the aspect of implant observed. In buccolingual sections, all remaining threads were fully embedded in bone. In mesiodistal sections, some of the threads were covered with fibrous tissue, with cells and fibers oriented parallel to the surfaces of the affected threads.

With HA-coated implants, the healing observed is different from Ti implants. Simultaneous bone formation occurs at both the HA-coated implant surface and the bone margin. At 1 week, direct lamellar bone formation at the straight implant surface can be observed, which does not occur around Ti implants until the third week. Direct bone formation on the implant surface can be observed in areas where there is no direct contact with the bone bed proper. During the 3-12th week, remodeling of lamellar bone can be observed.[4] With HA-coated implants, bone growth covers a greater percentage of the implant surface and grows more rapidly. There are virtually no fibrous tissue elements between bone and the implant.[3] Histomorphometric analysis of the amount of implant-bone contact zones indicate a higher rate of contact with HA-coated implants versus Ti surfaced implants.[4] Conversely, Kohri et al.[25] histomorphometrically compared HA-coated implants with Ti screws at 2, 4, and 6 months in dogs and found no significant differences in the percent bone contact length between implants or between functional and non-functional implants.

Ohno et al.[29] placed HA-coated implants in dogs and studied the healing histologically. After 1 month new woven bone was seen in the space between the bone socket and apatite. This woven bone was bonded directly to the apatite. Collagen fibers were occasionally observed running parallel to the apatite surface. At 3 months woven bone was found to be replaced by lamellar bone in some areas. At intervals of 7.5, 9, and 12 months, remodeled lamellar bone was found to bond directly to the apatite surface. This apatite bonding

appeared to develop from the top to the bottom with time. Osteogenesis began away from the implant by day 5. Within 1 month, new bone formation filled the interface between the implant and old bone.

Studies by Denissen et al.[11] using dogs and HA-coated implants demonstrated bone was deposited in extraction sockets in direct contact with the HA coating. The bone was of the lamellar type and was mostly laid down as secondary osteons. Bone deposits were also seen directly against HA surfaces.

Kohri et al.[25] with scanning electron microscopy (SEM) compared HA-coated implants with a threaded Ti screw. The HA-coated interface with bone showed no gaps, while the Ti implants always presented gaps. After preparing the samples for histology, the Ti implants were easily removed from the bone while the HA-coated fixtures were strongly adherent. Both implants showed osteogenic ingrowth to the implant surfaces.

Steflik et al.[66] using TEM and HVEM studied bone and osteocyte activity next to Ti implants in dogs. They observed a mineralization pattern of supporting bone that was similar to those events occurring naturally within mandibular bone. SEM studies by Albrektsson et al.[8] show haversian systems with osteocytes closely approaching the Ti surface. Collagen bundles were 100 to 300 nm from the metal surface. Collagen filaments approached the Ti oxide layer and were distanced from it by a 20 nm-thick glycoprotein layer.

In another study by Steflik et al.,[66] SEM showed Ti implants having a thin layer of fibrous connective tissue at various points of interface with the bone. The authors also reported SEM evidence of bone contact to Ti in the coronal half of the implant after 5 months. Bone apposition to the Ti implant was shown by SEM in an area midway down the lingual surface, along with tight adaptation of bone to the implant and the cellular components of the haversian system. A band of fibrous connective tissue interfaced the mandibular bone and the apical portion of the implant. A close adaptation was seen at areas of the implant-bone interface. Secondary imaging demonstrated close cortical and

trabecular bone apposition to the Ti implants, as well as areas of intervening fibrous connective tissue.

Ravaglioli et al.[69] reported on the histology of failed retrieved implants in humans. Complete adhesion of bone to HA-coated implants occurred after 4-6 months and confirmed the close bonding and high biocompatibility of HA ceramic between implanted materials and bony tissue. The adhesions between bone and HA appeared contiguous and scattered with a large number of extremely calcified trabeculae forming a physical extension of the inorganic compound that comprises the implant. Mineralized tissue easily reached the recesses in the rough surface of the HA ceramic grains. In summary, the shape of newly formed bone adapts itself to the rough irregular surface of the HA-coated implant and is normal in appearance.

B. Clinical Expectations Concerning Tissue Regeneration

1. Guided tissue regeneration

Guided tissue regeneration (GTR), originally advocated as a technique for treatment of inflammatory periodontal disease,[28] uses a physical barrier to selectively inhibit epithelial downgrowth. This technique is based on different types of cells having different rates of migration into a wound area during healing. Nyman et al.[70] were the first to describe a membrane or barrier in periodontal healing studies. The filter served as a barrier preventing the root surface from being colonized by gingival cells. Secondly, it permitted selective repopulation of the root surface by PDL cells, which were assumed to have the potential to become cementoblasts.

Physical barriers like occlusive membranes can be interposed between the root surface and connective tissue of the periodontal flap. Membranes are available in either resorbable or non-resorbable forms. Examples of non-resorbable membranes are the commercially available Millipore filters or e-PTFE by Gore-Tex®. Resorbable membranes include those under the name Guidor and Resolut. In conventional periodontal therapy, root surfaces

treated with e-PTFE, have demonstrated the presence of twice as much new cementum, bone, and functional periodontal ligament (PDL) as compared to non-membrane controls.[71]

Nyman et al.[72] in a monkey study using Millipore filters obtained new cementum formation of 26-100% and new bone of 0-100% over surgically created root surface fenestrations. They demonstrating PDL cells possess the ability to reestablish connective tissue attachment when the epithelial cells are excluded. Numerous studies have looked at the amount of new connective tissue attachment gained with GTR techniques versus controls. Caton et al.[73] in a monkey model used Millipore filters over surgically created root surface fenestrations. They obtained 75.6% new cementum at experimental sites compared to 36.1% for sham operated controls and 86.1% new bone at experimental sites compared to 48.7% for sham operated controls. Gottlow et al.[74] in monkeys using e-PTFE over created dehiscences, obtained mean new attachment of 77% at membrane sites compared to 33% at non-membrane control sites. Aukhil et al.[75] in beagle dogs using Millipore filters reported 1.8 mm of new connective tissue attachment in horizontal defects compared to control sites with no membrane which gained 0.7 mm. New bone formation was determined to be 1.5 mm compared to the control sites of 0.4 mm. Magnusson et al.[76] using Millipore filters over a wide surgically created dehiscence obtained 2.9 mm of new connective tissue attachment at test sites compared to 0.1 mm in non-membrane control sites. They also found 1.1 mm of new bone compared to 0 mm at the control sites in their monkey model. Claffey et al.[77] using e-PTFE in beagle dogs with surgically created horizontal defects obtained 4.2 mm of new connective tissue attachment at experimental sites compared to 3.4 mm at the control sites with no membrane. The authors demonstrated 1.4 mm of new bone at test sites versus 1.0 mm for controls.

Human case reports have also shown good results with GTR concerning improvements in clinical attachment. Nyman et al.[70] using a Millipore filter in multiple wall defects obtained 56% new attachment. Gottlow et al.[78] using e-PTFE obtained 40% new attachment in class II and III furcations. Pontoriero et al.[79] using e-PTFE in similar

furcations obtained 67% new attachment versus 10% in non-membrane controls. Other studies by Becker *et al.*,[80,81] Caffesse *et al.*,[82] Lekovic *et al.*,[83] and Pontoriero *et al.*[84,85] have obtained similar positive results.

The principles of GTR are being applied to implants in both animal and human studies. The major difference between implants and teeth is a lack of pluripotential PDL cells around implants. The surrounding alveolar bone must supply the undifferentiated cells during healing.[10]

e-PTFE material is considered bioinert and somewhat bioactive in that osteoblasts can grow on this material and mineralization occurs against this substrate.[10] Dahlin *et al.*[86] has done many animal studies in this area and demonstrated GTR to be successful in rats. Osseous defects were placed in mandibles bilaterally and e-PTFE membranes were used to cover one side. Complete regeneration occurred on the test side in 3 weeks. In another study, Ti implants were placed in rabbit tibiae, with GTR used on the test side. In 6 weeks, test sites had healed almost entirely with new bone while the control showed little activity.

Zablotsky *et al.*[10] reported a dehiscence defect fill of 95.17% with HA-coated implants compared to 82.8% for grit blasted Ti in an e-PTFE GTR study with dogs. Controls treated by debridement only had a mean of 55% and 39% defect fill, respectively. In another e-PTFE study with dogs, Zablotsky *et al.*[10] noted the HA-coated implants had a significantly lower residual defect area at all levels of the healing site, 1.38 mm^2 versus 1.8 mm^2 for Ti.

Caudill and Meffert[61] used e-PTFE in dogs with circumferential defects around HA-coated implants and obtained improved bony remodeling compared to the non-membrane control. Becker *et al.*[63] used e-PTFE GTR in dogs to see if bone would cover exposed implant threads. For test sites, bone height gain was 1.37 mm while the non-membrane controls averaged 0.23 mm. In another Becker *et al.*[59] dog study, implants were placed in

immediate extraction sites with facial dehiscence defects. GTR using e-PTFE was incorporated and the amount of bone gain was 2.6 mm compared to controls of 1.0 mm.

2. Demineralized freeze-dried bone allografts

Freeze-dried bone allografts (FDBA) have been used in clinical orthopedic therapy since 1950. Their use in dentistry was further stimulated by the disadvantages of autogenous bone grafting noted in the early 1970's.[87] Autogenous bone, although ideal in concept, has limitations in its procurement by entailing more extensive surgical procedures and exhibiting unpredictable behavior following grafting.[88]

An allograft is defined as a graft taken from a donor of the same species but with different genes. In a fresh state, allografts can stimulate adverse immune reactions even if cross matching of blood type and human lymphocyte antigen (HLA) testing are done. Hurt reported in 1968,[89] that freeze-dried bone was successfully used to treat dog osseous defects. Urist hypothesized that a protein substrate existed in the bone matrix that would stimulate bone formation.[90]

Much research has been done to determine the efficacy of bone grafts and which form of allograft, either FDBA or DFDBA, produces better clinical results. Mellonig *et al.*[91] compared DFDBA with FDBA, autogenous osseous coagulum, and autogenous bone blend in guinea pig calvaria defects. The radionuclide Sr-85 was used as an indicator of new bone formation. The results showed DFDBA to have higher osteogenic potential than autogenous bone (osseous coagulum and bone blend), followed by FDBA. The authors concluded that DFDBA is osteoinductive while FDBA is osteoconductive, acting as a scaffold for the new host bone to regenerate. When allograft is demineralized, more osteogenic potential is realized because an extracellular matrix is uncovered,[7] labeled bone morphogenetic protein (BMP) by Urist *et al.*.[92] The demineralization process of cortical bone exposes the BMP, inducing undifferentiated host mesenchymal cells into bone

forming cells.[87] DFDBA is considered by many to be the allograft of choice in the treatment of periodontal osseous lesions.

Libin et al.[87] were the first to treat periodontal osseous defects in humans with DFDBA. Three sites responded with 4-10 mm of new bone. Werbitt[93] treated 20 intrabony defects in 6 patients with DFDBA. At 9 months, bone fill ranged from 75-95%. Quintero et al.[94] treated 27 intraosseous defects in a 9 patient study using DFDBA, obtaining osseous regeneration of 2.4 mm or 65%.

In a controlled human study by Mellonig,[87] 47 osseous defects were treated with and without DFDBA in an open flap procedure. Upon surgical reentry a mean bone fill of 2.6 mm (65% defect fill) was obtained with DFDBA compared to controls with 1.3 mm (38% defect fill). Bowers et al.[95] histologically compared 32 grafted and 25 nongrafted defects in nonsubmerged teeth in 12 patients. The amount of new bone with DFDBA was 1.75 mm while the nongrafted sites averaged 0.05 mm. They offered definitive histological evidence that new bone, cementum, and PDL were produced in DFDBA-treated osseous defects in humans.

DFDBA may also be used in combination with GTR techniques. Siebert et al.[96] have demonstrated in beagle dogs the usefulness of support materials under the e-PTFE membrane versus e-PTFE by itself. This study used alloplastic rather than allographic materials. Their results demonstrated that the use of a support structure under the e-PTFE would completely fill the space provided with bone.

Guillemin et al.[97] compared DFDBA and an e-PTFE membrane to a control site of DFDBA alone in bilateral intrabony defects. Experimental sites demonstrated a 70% bone fill along with a increase in recession, while control sites demonstrated a 58% bone fill and half of the amount of recession.

Anderegg et al.[98] used DFDBA and GTR in humans with Class II or III furcation invasions. Furcation defects showed greater horizontal and vertical bone fill with combination therapy than by GTR alone. Vertical measurements of 3.5 mm bone

formation were seen with a combination of DFDBA and GTR versus 1.7 mm for GTR alone. Horizontal open probing new attachment measurements demonstrated a 2.4 mm increase with DFDBA and GTR versus 1.0 mm with GTR only.

Controversy exists with regards to the use of DFDBA even though it has been used clinically for many years. The benefit of the allograft is its ease of availability compared to obtaining autogenous bone from other intra-oral sites. However, the benefit of the BMP has come under scrutiny since commercial bone banks do not verify the presence or quantity of BMP in their product.[99]

C. Guided Tissue Regeneration Around Implants.

1. Overview

Due to the long-term success of dental implant therapy, practitioners have become more comfortable in placing implants in less than ideal situations. Factors affecting implant positioning and stability are considered correctable with newer techniques, allowing implant therapy in patients that previously were not considered to be good implant candidates. Buser described 3 points of view that may require guided bone regeneration if the local bony architecture is not present. These are the orofacial direction, the vertical direction, and the implant axis.[34]

Case reports by Sendax described the use of DFDBA around implants to "augment minimal crestal bone and downgrade the risk of subsequent bone die-back and related pocketing problems."[100] In a case report by Yukna[101] concerning implants immediately placed after tooth extraction, he commented that freeze-dried bone or another particulate alloplastic graft would be of "use" in filling the spaces around implants that are almost always present. Zablotsky felt there is potential for the use of GTR and DFDBA combinations around implants, but it has not been confirmed histologically.[28]

Bony dehiscences on the facial and/or lingual aspects of the edentulous ridge are complications of cylindrical endosseous implant placement.[10] Bony defects or anatomical problems may be classified as summarized by Zablotsky:[28]

Dehiscence. A dipping of the facial or lingual crestal bone margins exposing the implant; may be combined with vertical proximal or moat defects. This defect may be narrow or wide and extend to the apical extent of the fixture. Dehiscences are often associated with implant placement in very narrow ridges.

Fenestration. A perforation in the facial or lingual alveolar cortical plate which is not in communication with the crestal marginal bone. There may be an accompanying dehiscence defect. Areas with typical bony concavities have been associated with fenestration defects; these may turn into a dehiscence if the marginal bone isthmus is lost.

Horizontal Bony Defects. A uniform absence of proximal or circumferential osseous support when associated with facial and lingual dehiscences.

Vertical Bony Defects. A proximal bony defect which extends apically.

Periapical Defect. When the apical portion of the implant either facially or lingually is independent of marginal bony topography. Examples are placement into the maxillary sinus, the mandibular canal, the inferior border of the mandible, or into concavities.

2. Guided bone regeneration

One of the techniques for improving bone height or insufficient crest width is guided bone regeneration (GBR). This label, discussed by Buser, refers more to the goal of membrane application around implants than does the term guided tissue regeneration.[65,102] This technique utilizes barrier membranes to improve bone volume by protecting against an invasion by nonosteogenic, competing tissues. This technique was first reported in the late 1950's and early 1960's by Bassett *et al.* and Boyne *et al.* who examined the healing of cortical defects in long bones and osseous facial reconstruction. This early work was done with Millipore filters, establishing an environment of osteogenesis. As previously

discussed, this methodology was tested in the regeneration of periodontal tissues in the early 1980's. The concept involves a temporary device, such as a barrier, to provide a space in which the body can use its' natural healing ability to regenerate lost and absent tissue.

Early work with GBR around implants was done in animals using long bones. Dahlin et al.[86] placed implants in rabbit tibiae and left 3 to 4 threads exposed. Half of the implants were covered with an e-PTFE membrane, thereby creating a space. New bone formation was found in the space with a mean fill of 99.5%. This growth of bone was significantly greater than that seen at the non-membrane controls. Osseointegration was also observed against the Ti surface in the new bone regions.

Becker et al.[63] in a similar study in dogs demonstrated that threads above the crest of bone treated with e-PTFE membranes clearly formed new bone. Using HA-coated implants in dogs with facial dehiscence defects, Zablotsky et al.[10] found enhanced bone regeneration using both Ti (mean 82.8%) and HA-coated (mean 95.2%) implants compared to non-membrane controls.

In 1994, Schenk et al.[103] used e-PTFE in foxhound dogs to demonstrate the healing in surgically created defects in edentulous areas 8 mm deep and 12 to 15 mm long. Experimental sites were filled with intravenous blood to ensure clot formation under the membrane. Contralateral control sites received neither the membrane nor intravenous blood. Dogs were allowed to heal for 2 and 4 months prior to sacrifice. At 2 months, controls consistently healed at the margins of the defect with little bony advancement into the defect. Clinically, the ridge demonstrated a deep indentation. At 2 months, remnants of the clot could still be observed in the middle of the experimental defects. It was completely penetrated by blood vessels and granulation tissue. Bone formation appeared to have begun at the margins of the defect, initially covering the marrow openings, later spreading into the defect. The membrane appeared to be separated from the newly formed bone by a layer of connective tissue interposed between itself and the defect. From the

surgical defect walls, woven bone sprouted out in the shape of thin bifurcation plates. These trabeculae progressed between blood vessels, surrounding them prior to fusing, creating an intertrabecular space. Trabeculae began as osteoid prior to the start of mineralization in the center. This primary scaffold or primary spongework is a form of intramembranous ossification of directly formed bone and does not involve a cartilaginous precursor. This primary spongework was different from adult spongiosa in that the porosity was less than 50% compared to 70-80%, the mean trabecular diameter was 60 μm compared to 200 μm, and the mean width of pore intertrabecular spaces ranged from 100 to 200 μm compared to 500 μm. The intertrabecular spaces were filled with large, thin-walled blood vessels.

In the third and fourth month, a cortical layer formed and regular spongiosa and marrow spaces developed. Maturation continued with the development of parallel-fibered bone, finally maturing when intertrabecular spaces appearing as regular cortical canals with surrounding concentric lamellae. Secondary spongiosa began in the coronal region by expansion of the marrow space as the primary spongework resorbed. Spared trabeculae remodeled, while the remnants of woven and parallel-fibered bone were replaced by packets of lamellar bone. In addition, the cortical bone was also remodeled by haversian system development.

The connective tissue below the membrane decreased in thickness between the 2 and 4 month time frame, probably by an increase in the periosteal side bone apposition and the stiffness of the membrane. In places where the membrane was in intimate contact with the bone surface, the bone grew into the pores and interstices of the membrane. This reinforces the idea that the e-PTFE is both bioinert and perhaps osteoconductive.

Dahlin *et al.*[104] have published results of 10 fixtures in 6 patients using e-PTFE membranes over implants with exposed threads at the time of placement. Upon membrane removal at 6 months, between 0.5 and 3.0 mm of new bone was gained. The authors felt the membrane technique was a useful tool and the newly formed bone seemed able to bear

the stress when loaded with the final implant restoration. In a multicenter study with e-PTFE, Dahlin et al.[105] reported on 55 Brånemark implants with fenestrations or dehiscences at placement that were treated with guided bone regeneration. Mean defect height was 4.7 mm at placement and was reduced to 1.1 mm in 3 to 4 months in the maxilla and 5 to 6 months in the mandible. These procedures reduced the need for augmentation prior to implant placement. Nyman et al.[106] used e-PTFE in 2 patients, one with exposed threads after implant placement and the other with an inadequate ridge for implant placement. Both resulted in adequate bone formation to improve the prognosis for the patient.

Jovanovic et al.[107] examined 19 Ti implants in humans with exposed threads that were treated with e-PTFE membranes. Range of dehiscence defects was 2.0 to 9.0 mm. Therapy resulted in 28.4% to 100% defect fill (mean 89.6%) over 4.5 to 6 months.

Buser recommended the use of membrane fixation to greatly improve the predictability of GBR. Such factors as membrane micromovement may facilitate the formation of fibrous tissue, and loss of the close adaptation of the membrane to the bone surface, allowing an influx of soft tissue cells. To date, the length of time for healing under a membrane is patient and site dependent. The recommended minimum time is 6 to 9 months for large defects.[108,109]

Buser et al.[110] have recently shown that bone regenerated through GBR techniques in dogs is able to physiologically respond to staged implant procedures similarly to non-regenerated bone.

3. Guided bone graft augmentation

GBR has been proven clinically; however, occasionally the volume of the defect to be regenerated is beyond the capability of GBR using membrane therapy alone. In these cases, allografts or autografts may need to be used with barrier membranes. This technique is described by Buser as guided bone graft augmentation (GBGA). He states that bone

volume expansions beyond a factor of 10 exceeds the capacity of GBR alone. GBGA implies the barrier helps maintain and preserve the bone graft itself. This procedure is recommended for sinus lifts, total lateral alveolar augmentation with or without sinus lift, total vertical alveolar augmentation, and nasal floor mucosal lift. The use of membranes to protect cancellous bone grafts is important since this material is susceptible to early resorption by compressive or tensile loading or fibrous ingrowth. Coverage with a membrane maintained 100% of the bone while sites without membranes lost 50% or more of the bone graft.[111]

Nevins and Mellonig[112] used guided bone regeneration and freeze-dried bone allograft in humans to reconstruct a damaged alveolus after removing a failing implant, for an absence of buccal plate after a central incisor was extracted, and to restore a posterior ridge after extraction of teeth with severe adult periodontitis. All areas were allowed to heal for 5 to 6 months after which implants were placed in a conventional two stage approach. After treatment with their techniques, esthetic and functionally positioned implants were placed in these newly regenerated alveolar ridges.

Becker *et al.*[113] examined the combination of DFDBA and e-PTFE membranes as part of a study looking at bone regeneration around Brånemark implants in dogs with dehiscence defects. Their results after 12 weeks of healing revealed that guided bone regeneration was more successful with autologous bone and membrane (95% defect fill) or membrane alone (80% defect fill) than with DFDBA and membrane (75% defect fill).

Although case reports have indicated clinical success in implant thread coverage, there are currently no data to indicate DFDBA has any osteoinductive potential around implants nor that it adds to the loading capability.[114] Becker *et al.*[99] stated there is no evidence that the use DFDBA around dental implants induces bone formation. Becker *et al.*[60] used human DFDB xenografts in dogs at implant dehiscence sites along with e-PTFE membranes. Controls were similar sites without the use of graft material. They found less than desirable results with the allograft as compared to controls. Concerning the use of

xenografts, Sampath and Reddi[115] examined the homology of BMP from human, monkey, bovine, and rat extracellular matrix. They found xenographic use of bone matrix produced only weak or no bone differentiation in ectopic sites. This suggests that extracellular matrix-induced bone differentiation is species specific. When the BMP was extracted from the matrix and reconstituted with inactive rat residue (insoluble demineralized bone matrix remaining after extraction), similar results were achieved. However, when these same protein extracts were processed through gel filtration and only proteins less than 50,000 daltons were reconstituted with inactive rat residue, bone induction occurred by all species. Therefore, although BMPs are homologous between species, xenografts are prone to failure due to immunogenic or inhibitory components present in the extracellular bone matrix.

4. Implant placement in immediate extraction sites

Successful placement of implants into fresh extractions sites has been reported by several investigators.[28,47] This may allow preservation of the ridge by preventing the resorption buccolingually and apicocoronally that occurs during the first 6 months to 2 years after extraction, prior to implant placement.[108] Additionally, by decreasing the restorative interval between time of extraction and final restorative placement, the psychological aspects of loosing a tooth may be minimized. Indications for immediate implants may include root fractures, failed endodontic therapy, unrestorable carious lesions, poor crown to root ratio, and advanced periodontitis.[114]

Alveolar defects around implants present a therapeutic challenge. Using monkeys, Warrer *et al.*[58] extracted maxillary second molars and placed screw-type implants. e-PTFE membranes were placed to cover only half of the implant and surrounding crater. Non-membrane portions of the implants presented with soft tissue after 3 months of healing while the membrane covered portions of the implants revealed osseointegration to the top of the implant.

Gotfredsen et al.[116] using porous HA in bony defects in monkeys created 4 test groups and allowed them to heal for 12 weeks. All peri-implant bone defects treated with a combination of porous HA and membranes or with membranes alone completely filled with bone. Control defects and those treated with porous HA alone demonstrated new bone formation only at the bottom of the defects.

Knox et al.[15] studied in dogs the healing response to circumferential bony defects (0 to 2 mm radius) created prior to implant placement. The study suggested that predictable bridging and defect resolution occurred when the alveolar defect was between 0.5 and 1.0 mm from bone to implant. The authors speculated that the use of a membrane with or without bone grafting material may achieve better results.

Studies by Denissen et al.[11] using dogs and HA-coated implants demonstrated bone was deposited in extraction sockets in direct contact with the HA coating. The bone was of the lamellar type and was mostly laid down as secondary osteons.

Becker et al.[59] placed Brånemark implants in simulated extraction sites in dogs. Healing was allowed for 18 weeks prior to clinical and histologic assessment. Non-membrane controls only gained an average of 1.0 mm of bone while the experimental sites gained an average of 2.6 mm with e-PTFE membranes. Nearly 100% coverage by bone was seen on the previously exposed implant threads at experimental sites. Caudill and Meffert[61] found similar results in the same animal model.

In an effort to prove the benefit of GBR, Lekholm et al.[62] removed membranes at different intervals during the healing phase after implants were placed in immediate extraction sites in dogs and found that membranes retained for 16 weeks had 100% new bone formation over previously exposed threads. However, if the membrane was removed at an early point, only 2.0 mm of average bone growth could be found, compared to 5.2 mm for the membrane retained sites. If the membrane and granulation tissue were removed at an early time point, even less new bone was found (1.0 mm). Buser agreed that better

results are found with longer membrane retention times and stressed the importance of maintaining barrier stability and mucosal flap coverage for the entire healing period.[114]

Lazzara[117] is credited with the first reported use of GBR with implants in immediate extraction sites. Human case reports have shown a benefit to the use of e-PTFE membranes in the immediate placement of endosseous implants in extraction sites.[4,118] Dahlin et al.[104] placed implants in less than desirable ridge areas and used GBR to gain bone on the exposed threads. Bone gain ranged between 0.5 and 3.0 mm. Becker et al.[47,119] have demonstrated the successful use of e-PTFE with implants placed into extraction sockets in case reports and multicenter studies. Sendax[100] has used GBR around implants wherever intrabony defects were present to enhance the prognosis of fill.

A number of case reports have been published for implants placed in extraction sites. Becker and Becker,[47] and Lazzara[117] used guided tissue regeneration; Block and Kent[120] used non-resorbable HA; while Ashman[121] used synthetic bone polymer. Tolman and Keller[122] report placing 303 Brånemark implants in 61 patients immediately after extraction using only alveoloplasty and primary closure. In their study, only 2 implants were lost due to infection in a maximum of 6 years follow-up. Augthin et al.[123] placed 20 Brånemark implants in immediate extraction sites and used e-PTFE membranes to resolve thread exposure. Biopsies were taken from the new bone surface at the time of abutment connection. Histology revealed a combination of fibrous healing with various stages of maturing bone tissue.

Landberg et al.[46] placed a variety of implants (Brånemark, Integral, and Screw-Vent) in immediate extraction sockets in 22 patients using DFDBA and e-PTFE membranes to repair exposed threads. When the membrane remained covered during the 4 to 6 month healing prior to abutment connection, complete bone regeneration occurred. Sites with membrane exposure only regenerated 50% of the original defect. Biopsies of non-supporting regenerated bone were collected. The specimens contained both particles of devitalized bone with empty osteocytic lacunae and large areas of vital bone tissue.

The results of a prospective multi-center study published by Becker *et al.*[119] using e-PTFE membranes at immediate implant sites are encouraging, with a short-term implant survival rate of 93.9% and 4.6 mm of new bone for membrane retained sites. Another report by this author supplemented membrane therapy with autogenous bone in humans.[48] Unfortunately, none of these human case reports and clinical trials can report the actual degree of histologic osseointegration.

D. Subtraction Radiography/Computer-Assisted Densitometric Image Analysis

1. Subtraction radiography

Radiographs are basic to dental diagnosis, treatment planning, and evaluation of therapy. However, in implant therapy, the gold standard of histology, is difficult to obtain. Therefore, clinicians must rely on radiographic interpretation, presence or absence of mobility, and clinical assessment of alveolar regeneration around the fixture to evaluate implant stability. To visualize a change on a radiographic image, 30 to 60% of the mineral content of the bone has to be lost.[124-127] However, subtraction radiography may reveal changes in mineral content in specimens as low as 5%. This has been supported by Ortman *et al.* using ^{125}I absorptionometry.[128] Furthermore, an examiner's ability to identify bony lesions 0.5 mm in depth was near perfect with subtraction radiography; however, with conventional techniques similar accuracy was not achieved until the lesion was 3 times as deep.[129] Subtraction radiography increases diagnostic accuracy compared to conventional radiographic interpretation. Many authors acknowledge its ability to eliminate disturbing image noise, thereby facilitating the detection and perception of significant diagnostic information.[130]

Subtraction radiography was used in clinical practice as early as 1935 according to a review paper by Brägger.[130] More modern adaptation of this technique was introduced by Klein in 1967 with the application of television and electronic engineering, producing a television subtraction read-out. By his method, a negative signal of the original radiograph

was paired with a positive signal of the subsequent film. In 1976, Kasser and Klein were able to demonstrate with television subtraction a developing periapical lesion 7 to 42 days earlier than conventional methods.

Technology continued to advance when video and computer interface came of age. Early work with digital formatting of dental radiographs was described by Ando in 1969. Using a microphotometer, for each of the 5400 to 5600 picture points scanned, a grey-level between 0 and 255 was determined. Mathematical processing followed by image printing allowed the visualization of differences in relative densities between 2 radiographs. In 1987, Okano *et al.*, using a similar technique followed 15 interdental crest sites in 5 patients after initial therapy and analyzed density changes at 1, 3, and 6 months. They detected changes of 0.04, 0.07, and 0.09 in optical density, respectively, in contrast with a 0.7 background density.

While Ando and Okano *et al.* worked with the microphotometer, several groups developed the use of video cameras for viewing radiographs. They placed baseline radiographs over a light source and analyzed the transmitted light intensity at each picture element or pixel by a video camera. This signal was converted into grey-level values between 0 and 255. Since negative values could not be represented on the image processor, the value of 128 is added to each pixel and represents the mean grey-value (i.e. one half of the grey-level value range of 0-255). The digitized image was then stored in a computer for mathematical manipulation and was presented on a monitor screen as a positive image. A subsequent radiograph was presented as a negative image superimposed on the same monitor screen. The 2 images were then aligned, after which differences in grey-levels were calculated and displayed as either darker or brighter areas. Bethman *et al.* demonstrated the detection of loss of bone in a case of acute osteomyelitis as early as 5 days after exacerbation. Using conventional methods, these changes were not apparent. These same authors also introduced the concept of using an aluminum step wedge to allow quantitation of mineral content.

In the early 1980s, Groendahl *et al.* added the concept of determining the median grey-level range of the background as previously discussed. Contrast correction methods were later developed by Rüttimann using the cumulative sum of the grey-levels in the histograms. With this methodology, closer matching of the grey-levels in baseline and follow-up images was obtainable. In 1984, Groendahl *et al.* found that artifacts were too high in radiographic pairs for subtraction that differed in angulation more than ± 6 degrees. They determined diagnostic accuracy for lesions detectable with subtraction radiography increased if the error in angulation was less than ± 3°. To obtain this consistency in angulation or repeatable exposure geometry, the use of a film alignment device is required. Early work used custom bite blocks or stents that proved tedious and time consuming to construct. Problems with these devices included distortion of the devices over time and migration of periodontally compromised teeth resulting in an ill-fitting stent. Jeffcoat *et al.*[131] in 1987, introduced the use of a cephalostat, improving the repeatability over custom stents. Disparity in angulation using the cephalostat was 0.33 ± 0.1 degrees. A third option for standardizing these radiographs is real-time video. This method utilizes a stored video image of the face allowing the operator to align the subsequent exposures with the first by comparing the current position of the face with the stored image. The subject is aligned when the monitor has a neutral grey appearance. This method has demonstrated an accuracy for anterior teeth of 0.31 degrees.[124]

Subtraction radiography is only a qualitative tool, reporting results as loss, no change, or gain in alveolar bone density. However, in 1985 Rüttimann began experimentation using a continuous wedge of bone of known dimensions as a comparison in the radiograph to determine volumetric measurements. This was placed apical to root apices and therefore presented as a linear grey scale wedge on subtracted images. This technique proved to be within 10% agreement with actual volumetric measurements.

Other image processing modifications have included removal of the lowest and highest grey-levels and expansion of the remaining grey-levels over the 0 to 255 value range to

enhance the subtraction images.[132] Brägger *et al.* have also attempted coloration of the density changes displayed in the subtraction image; however, the benefits of this technique need to be investigated.

2. Computer-Assisted Densitometric Image Analysis (CADIA)

Brägger *et al.*[132,133] in 1987 and 1988 tested the capability of a computer-assisted densitometric image analysis method for quantitative density changes. They compared CADIA to visual interpretation of digital subtraction images and conventional radiographic interpretation. Their results revealed CADIA was the most sensitive of the 3 tested methods for detecting surgically induced bone loss.

The methodology for CADIA is a continuation of subtraction radiography previously discussed; however, specific selected areas can be quantified for density changes and a numeric value generated. Another feature of this system is an algorithmic correction for differences in density between initial and subsequent films. These differences may stem from different exposure and/or developing conditions. Contrast changes are inherent in conventional radiography from changes in developing time, temperature of the chemicals, age of the chemicals, and even differences in processors. With the advent of this algorithm, grey-levels were matched between radiographs and either linear compression or expansion and shifting corrected any differences.

Areas of pixel interest (also known as areas of interest, windows of interest, or regions of interest) are selected for quantitative information. These areas are defined by drawing a rectangle at the area of interest and the mean and standard deviation of the grey-level histogram is calculated for each 2 x 2 pixel area and compared by the computer. The values in the subtracted image are the difference between the values of the baseline and subsequent radiograph. Positive values represent an increasing density while negative values represent a decrease in density. In routine CADIA procedures, a threshold is selected to remove the effect of system noise on the CADIA values. This threshold is measured from the

subtraction image by calculating the average pixel grey value and the standard deviation in areas that are not expected to change. The threshold is set to 2 times the standard deviation thereby reducing the chance of measuring a false positive reading to 5%.[134] For example, if the measured background noise level (standard deviation) in the image is 5 grey values, the threshold is set to 10, and any values between minus 10 and plus 10 are excluded from the calculation of the CADIA value. The difference between means of pixel changes for the baseline and subsequent film are reported as positive for density increase and negative for density loss. CADIA values or overall density changes in the areas of pixel interest are calculated by multiplying the area of change by the density difference.[135]

Brägger et al.[132] in 1988 further showed by atomic absorption spectroscopy that the actual calcium loss in bone specimens was highly significantly correlated to the changes assessed by CADIA. In this same report, Brägger et al. reported a clinical test of surgically-induced bone loss associated with crown lengthening procedures, and found that CADIA was able to detect this bone loss with a sensitivity of 82%, a specificity of 88%, and a diagnostic accuracy of 87%.

E. Summary

Researchers have proven in animal studies that bone osseointegrates with Ti implants and biointegrates with HA-coated implants. This is demonstrated at both the light and electron microscopic levels. Many clinical case reports have demonstrated the dependability of these treatment modalities. However, long-term function, mobility, and status of the supporting tissues can be demonstrated only in clinical studies.

Much research has been done in the area of dental implants concerning healing in both animals and humans. Investigators have created or selected ideal environments for implant placement in most cases. However, conditions are often less than ideal, necessitating the use of augmentation materials such as e-PTFE membranes and DFDBA.

Reports in the literature by Becker and Becker,[47] Dahlin *et al.*,[104] Lazzara,[117] Sendax,[100] and Nyman *et al.*[118] have used GBR around implants in humans with clinical success. Likewise, Yukna suggests using GBR in immediate extraction sites.[5] However, only in limited circumstances can the histology of the area be examined to demonstrate the response at the cellular level. Arvidson commented that animal studies are the only acceptable way to examine tissue at the cellular level.[19] Zablotsky noted that the reports of GBR with implants have not been substantiated by histologic studies.[28]

DFDBA has been proven as a valuable adjunct in treating intrabony defects around teeth. Case reports have demonstrated clinical success around implants with either autologous, allographic, or alloplastic materials.[47,100,101,112,121] Shanaman[137] treated clinical implant cases with e-PTFE along with DFDBA or FDBA or a combination of both in areas where space-maintenance was desired. It is unknown at the histologic level whether these techniques are healing with the same degree of consistency or type of repair that is seen with the traditional bone-implant interface. However, it has recently been established that bone regenerated in membrane-protected defects is able to physiologically respond to implant procedures similarly to non-regenerated bone.[110]

Using both modalities- GBR to block faster growing epithelium and connective tissue together with DFDBA to fill intrabony, fenestration, and dehiscence defects- one may potentiate the short term healing and long term prognosis of both HA-coated and Ti implants in less than ideal areas. Once the healing process with these augmentation materials associated with HA-coated and Ti implants is understood, it will be easier to select the type of implant and predict the healing that occurs with immediate implant placement in extraction sites.

The question exists as to what degree bone regeneration is achieved in areas where an immediately placed implant is not in intimate contact with the bony walls of the extraction site. It is imperative that osseointegration be verified in a standardized manner with properly controlled studies where histology can be obtained. The purpose of this study was to investigate radiographic density of healing through CADIA and the quality and quantity of

osseointegration through histology for two of the major implant types, commercially pure titanium (Ti) screws and double plasma sprayed TPS/HA-coated root-form cylinders, when guided bone regeneration is required.

III. MATERIALS AND METHODS

A. Animal Population and Management

A total of 10 healthy, heart worm-free, 1-5 year old mongrel dogs were obtained by the Clinical Investigation Directorate (CID), Lackland Air Force Base, Texas. The animals were placed in quarantine for 14 days upon arrival to confirm systemic health. Quarantine is defined by CID as a separate set of runs at the kennel site (kennel site defined as a separate facility 1/4 of a mile from the main CID facility) that is physically separated from the remaining animal population on the site. The dogs were sedated with 3.0 cc of Ketamine-Ace (drawn from a mixture of 1000 mg ketamine HCl [Fort Dodge Laboratories, Fort Dodge, IA]) and 20 mg acepromazine maleate (Vedco, Inc., St. Joseph, MO) during the first week after arrival. A physical exam was accomplished by one of the staff veterinarians, along with blood samples for a complete blood count (CBC) and Hitachi battery. A Hitachi battery includes profiles on sodium, potassium, chloride, carbon dioxide, blood urea nitrogen (BUN), glucose, calcium, creatinine, phosphorous, total bilirubin, aspartate aminotransferase (AST), alkaline phosphatase, lactic dehydrogenase (LDH), total protein, alanine aminotransferase (ALT), and cholesterol. A chart was created for each animal, noting their general condition along with any specific markings, weight, and eating habits to date. Each dog was subsequently tattooed on the inner surface of the right ear using Animal Tattoo Ink (Ketchum Mfg, Ottawa, Canada) with their 4 digit CID issued number.

After completion of the physical exam, 3 separate pieces of Boxing Wax #00816 (Hygienic Corporation, Akron, OH) were folded over the mandibular teeth to form a crude outline of the mandible. The intent was to reproduce the basic size and shape of the mandible. This would be used to create a custom oversized alginate impression tray since stock canine trays were not available. The wax was removed from the mouth and stabilized on the external surface using wooden sticks (anterior and posterior) with a standard hot glue gun. A toe tag was attached to

34

each impression for identification. Subsequently, lab values for each dog were evaluated by the veterinarian to complete the examination process. All dogs were given a clean bill of health and cleared for treatment. All animals were placed on a hard chow diet until the time of extractions, after which the diet would remain a dental diet (hard chow softened in water prior to serving or canned food if an appetite problem developed).

The boxing wax impressions were taken to the dental laboratory after disinfection with Alcide DL (Alcide Corp., Redmond, WA) and poured with yellow dental stone. After the initial pour, a second pour was accomplished to create a base. For fabrication of the custom impression trays, an additional 2 layers of boxing wax were added to the 1-3 layer thick boxing wax already on the cast from the clinical impression. A total of 3-5 layers of boxing wax now existed on the cast. The cast and boxing wax were well lubricated with White Petroleum Jelly (Linder Co, Inc., Englewood Cliffs, NJ) and blue Triad VLC Custom Tray Material #95752 (Dentsply International Inc., York, PA) was applied with an anterior extension for a handle. It was not possible for these grossly oversized sized casts to fit into the Triad 2000 Polymerizing Unit (Dentsply International Inc., York, PA) and still allow rotation for optimum curing. The trays were placed in a sunny window to allow a slower complete polymerization over a 24 hour period. The trays were subsequently separated from the casts and trimmed, grossly polished, and labeled with the unique 4 digit CID number for each animal.

B. Phase I

1. Extractions

After completion of the 14 day quarantine and review/clearance of all lab values, the dogs were brought into the main CID facility for lateral skull radiographs. Each animal was sedated with 4-6 mg/kg propofol (Diprivan, Stuart Pharmaceuticals, Wilmington, DE) in the Radiology Suite. Once sedated, the animal was placed on the appropriate side without a bite block and its head rotated 25 degrees off the horizontal plane and stabilized by an aproned technician while a 24 x 30 cm Kodak Diagnostic Film T-MAT 170-9039

(Eastman Kodak, Rochester, NY) was exposed at 64 kVp, 6.4 mAs, and 500 mA on the Sentry Three Medical X-Ray Unit (General Electric Medical Systems, Milwaukee, WI). There was adequate time using the Kodak RP X-OMAT Processor Model M6B (Eastman Kodak, Rochester, NY) available at CID to review the film prior to the dog completely waking up. No pathology or aberrant tooth morphology was identified which would contraindicate the use of any of these dogs in the study. General structures of the mandible were observed along with root length, curvature, dilacerations, and relationship of teeth and alveolar ridge to the mandibular canal. Mandibular premolars 1-4 and first molars were planned for extraction.

On the day of all surgical procedures, the animals were given nothing by mouth (*n.p.o.*) and were transported from the kennel to a smaller run inside the CID facility. In the presurgical/anesthesia holding room, each animal was given sodium pentothol (Abbott Laboratories, Chicago, IL) 12 mg/kg IV as an inductive drug, prior to endotrachial intubation. After successful intubation, the tube was secured to the maxilla. The animals were anesthetized with Isoflurane (Anquest, Madison, WI) and maintained with a 1-1.5% dose. Electrocardiogram (ECG) Electrodes (Medtronic Andover Medical, Haverhill, MA) were applied to the appropriate limbs after shaving with an electric hair clipper to provide maximum contact. Electrocautery was not planned in any of the surgeries and therefore additional shaving for the pad was omitted. Ilotycin Opthalmic Ointment (Dista Product Co., Indianapolis, IN) was placed in the eyes.

While in the holding area, alginate impressions were made by mixing 84 grams Jeltrate Plus Type II-Regular Set Alginate (L. D. Caulk , Milford, DE) and 204 cc of cool tap water. The trays were painted with Hold Impression Tray Adhesive #11460 (Teledyne Getz, USA) at least 15 minutes prior to use. Through trial and error it was determined that the dog's natural secretions produced the best results, i.e. no lubricant or excess drying with gauze was needed for an excellent impression. In addition, painting the occlusal surfaces with an alginate moistened finger provided no benefit. The impression was then

made and hand carried to the dental laboratory after rinsing and decontamination with Alcide DL. Pouring of the impression was accomplished in less than 10 minutes with Die Keen Stone #46598 (Miles Dental Products, South Bend, IN).

Animals were then transported by gurney to the operating room (OR), where appropriate monitors (ECG, CO_2, O_2, temperature probe, and blood pressure) were connected to insure safe anesthesia and an Anesthesia Log Form (Standard Form 516) was completed for each surgery. The dog's mouth and external oral regions were prepped with T-Scrub Providone-Iodine Cleansing Solution (Thatcher Co., Salt Lake City, UT), then followed with Betadine Solution as paint (Purdue Frederick Co., Norwalk, CT). The operating field was defined with towels, and the animal was draped. The extraction surgeries were considered clean and personnel were not gowned but did wear surgical scrubs and sterile gloves. Local vasoconstriction was accomplished by infiltration with 72 mg of lidocaine HCl containing 36 μg of epinephrine (Henry Schein, Port Washington, NY) along the lingual and buccal vestibule. Facial and lingual sulcular incisions were made from the mesial of the first premolar to the mid facial and lingual of the second molar. A mucogingival flap was elevated on the facial while only slight reflection was accomplished on the lingual. A #702 surgical length bur (IDE Interstate, Amityville, NY) on a Hall Micro-Aire 100 Drill #5053-09 (Zimmer, Warsaw, IN) was used to section mandibular premolars 2-4 and the first molars through the furcation to the cusp tip. A #301 elevator (Hu-Friedy, Chicago, IL) was used to gently luxate the teeth with a deep purchase in the furcation area. A #151 forcep (Hu-Friedy, Chicago, IL) with rotation only was used to extract the 4 premolars. Attempts to roll the tooth or excessive buccolingual movement almost always resulted in fracture of the tooth at the alveolar crest. If a root tip needed to be retrieved, a #79S or 80S root tip pick (Hu-Friedy, Chicago, IL) was used. Occasionally, the Hall Micro-Aire 100 Drill was used to remove the root. While the alveolar ridge was surgically exposed, measurements of width and length were recorded. No alveoloplasty was attempted and the sockets were well irrigated prior to flap coaptation

with #3-O Mild Chromic Gut Suture with a CE-4 needle (Davis and Geck, Willowdale, Ontario, Canada). Primary closure was accomplished using a continuous locking suture. The dog was then turned and the procedure was repeated on the contralateral side. One gram of chloromycetin sodium succinate (Chloramphenical, Parke-Davis, Morris Plains, N.J.) was administered intravenously (I.V.) during surgery, followed by 500 mg 3 times daily (*t.i.d.*) by mouth (*p.o.*) for 6 days.

Post-surgically the dogs were moved via gurney to the recovery area and extubated when signs of adequate recovery were observed. Post-surgical analgesia included 0.3 mg/kg intramuscularly (IM) of buprenorphrine hydrochloride (Buprenex, Norwich Eaton Pharmaceuticals, Inc., Norwich, N.Y.) for discomfort. Post-operative analgesia was obtained using 0.3 mg of buprenorphrine hydrochloride t.i.d. x 4 days IM. Animals remained in the main facility for the next 7 days and were then transported to the kennel area. Since gut sutures were used, no post-operative treatment appointments were scheduled unless recommended by the veterinarian. The animals were allowed to heal for 3 months prior to implant placement. (Figure 1)

2. Radiographic stent fabrication

The presurgical alginate impressions were made with the intent of fabricating custom trays for accurate impressions for fixed prosthodontic appliances. The design would have protected the implant areas and served as guides for custom radiographs. Each dentulous cast was originally treatment planned for a fixed partial denture. Unfortunately, the span remaining after the extraction of 5 teeth in each side was too long and the second molars were quite variable in size and anatomy precluding adequate retention of the planned appliance. The emphasis thus shifted to the design of a removable device that would only be used for radiographs.

Approximately 2 weeks prior to the implant surgery, each dog was sedated with 4-6 mg/kg propofol and another mandibular full arch alginate impression was made with the

Figure 1.   Time Line for Surgical Design of the Study.

Day 0   3 Months   7 Months

|<------------- 3 mos ------------->|<--------------- 4 mos --------------->|

Stage 1   **Stage 2**   **Stage 3**
Mandibular   Implants   Sacrifice
Premolars &   Placed
First Molar
Removed
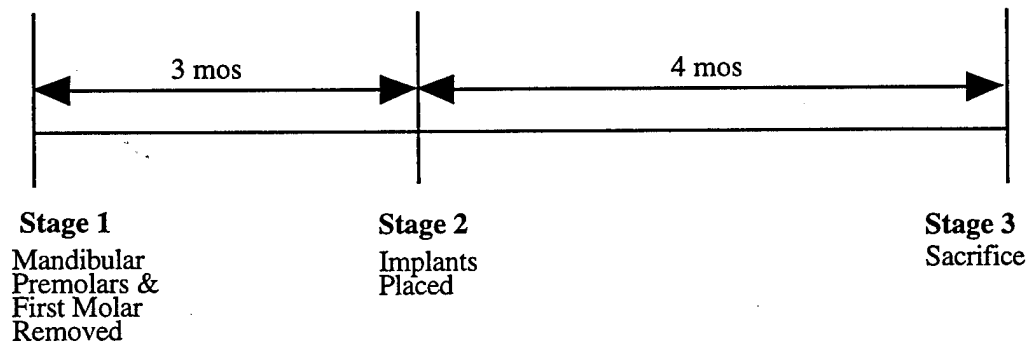
original custom alginate tray. This impression of the edentulous ridge and adjacent teeth was used as a master impression for the fabrication of a removable radiographic device. At this time all ridges were completely closed with no evidence of any post-operative complications.

Two prototype stents were made to test the feasibility of using #3 film (Kodak Film #129-6771, Eastman Kodak Company, Rochester, NY) to capture all 3 implants in 1 exposure versus having to use 2 #2 films (Kodak Film #165-8210, Eastman Kodak Company, Rochester, NY). Using #2 film had its advantages in that the film is double packed and plastic coated preventing the possibility of moisture contamination by saliva. However, this would mandate the need for 2 custom radiographic stents for each dog, i.e. one for anterior and one for posterior views. The total minimum dimension of the implant sites was 45 mm which exceeded the width of one #2 film at 41 mm. The #3 film was 54 mm wide and appeared to have adequate height at 27 mm to include bone beyond the apical end of the 10 mm implants. A trial run with both implants was conducted using an Oralix 70 (70 kVp/7 mA) Mobile X-Ray Unit (Philips Medical Systems, Inc. Shelton, CO). Automatic settings were selected using Film Type = 1, Technic = paralleling, Size = medium, Mandibular = bicuspid; based on the 20 cm focus-to-film distance. The #3 film was determined to be adequate for this study.

The final radiographic stent was fabricated by using 2 rows of Utility Wax Strips (Hygenic Corporation, Akron, OH) to outline the periphery of the proposed stent and covering all of the facial tooth surfaces except for the incisal 2 mm of the canine and incisors. The lingual aspect of the stent was designed similar to a removable partial denture with a lingual apron. Distal to the second molar, rope wax was extended only to the distal cusp tips. The second molar was relieved circumferentially in the gingival region and in any deep fissures or pits in the occlusal surface. Additional wax was flowed into all gingival sulci as blockout and any sharp anatomical features were alleviated. Two layers of Tru Wax Baseplate Wax #7709002 (Dentsply International Inc., York, PA) were applied from

the mesial of the second molar to the distal of the canine. In addition, a single later of base plate wax was placed over the lingual attached gingiva and mucosa of the incisors. This was done to avoid impingement of the tissues and provide a stent which was fully tooth born and would not be affected by tissue changes over the healing period after implant placement.

An initial layer of Orthodontic Resin #651006 (L. D. Caulk, Milford, DE) with Pink Orthodontic Resin Liquid #551025 (L. D. Caulk, Milford, DE) was sprinkled on the second molar areas and the canines first to avoid excessive shrinkage. A thin layer of resin was sprinkled in the edentulous areas prior to placement of a XCP Posterior Bite Block #54-0862 (Rinn Corporation, Elgin, IL) assuring that a #3 film would include the mesial of the second molar. Once the bite block was positioned, it was incorporated into the stent with at least 5 mm of resin. A final sprinkle of resin connected all the regions together. Special care was taken not to get resin in the holes where the Rinn positioning rod attached. The stent was allowed to cure for 24 hours in a humidor prior to separation. After separation the wax spacers and peripheral border wax were removed with a Portable Steamer #017 100 (Belle de St. Clair, Chatsworth, CA) and the edges were trimmed on a Red Wing Lathe (Handler Manufacturing Co., Westfield, NJ) using a tapered Dedeco Lab Carbide Bur #84-T (IDE Interstate, Amityville, NY). Each dog's 4 digit CID number was incorporated into the lingual area of the stent by adding additional resin over an identification number tag. Stents were pumice polished and placed in denture bags with a moistened cotton roll. (Plate 1)

For initial radiographic examination, the dogs were sedated with propofol and periapical films were taken with #3 film. Once the radiographic stent was in position, the dog's mouth was closed causing the maxillary first molar to occlude on the stent and stabilize it. Using lead lined gloves and an apron, the operator was able to make final position adjustments by moving the animal's snout to line up the Indicator Arm #54-0858 and Aiming Ring #54-0860 (Rinn Corporation, Eglin, IL) with the mobile dental X-Ray

42

Plate 1.   Custom Made Radiographic Stent Fabricated for each Animal with Attached
             Alignment Device Used for Standardized Radiographs.
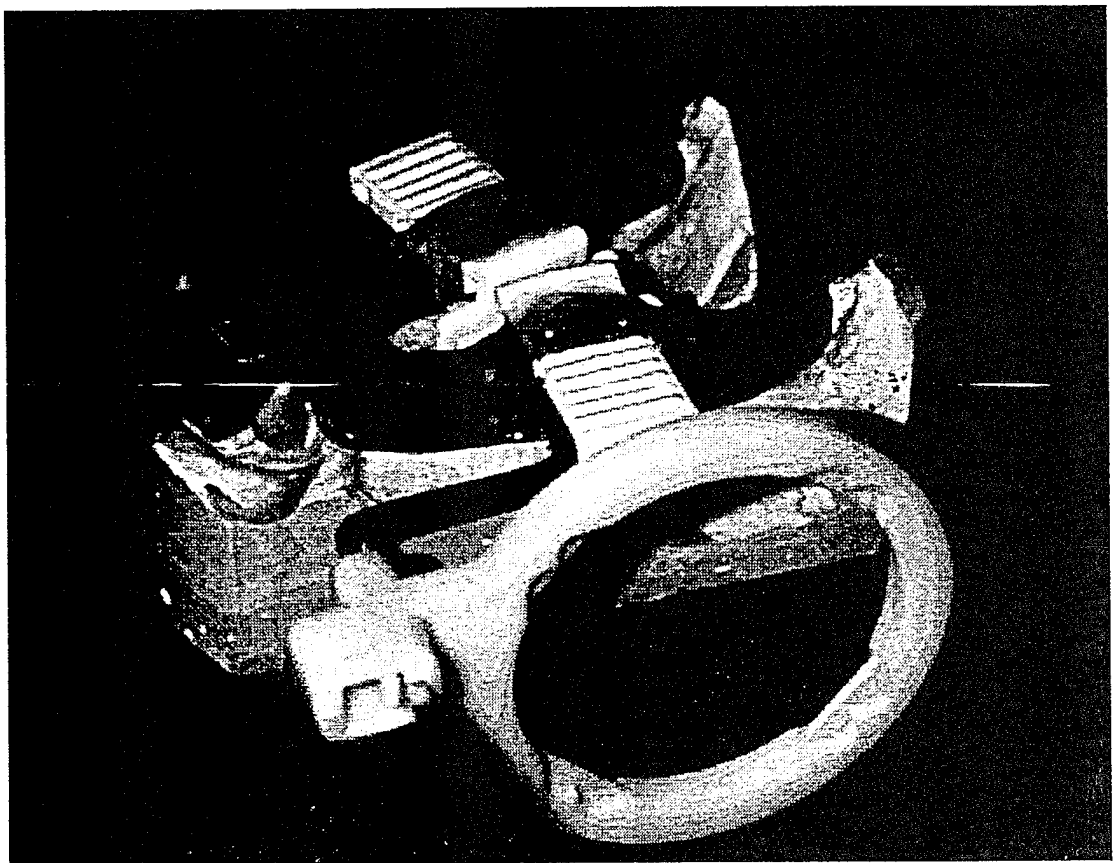
unit. A device using Velcro® was contemplated to keep the dog's mouth closed during radiographs but was determined not to be needed with the use of the lead lined gloves. Exposed radiographs were dried with paper towels and processed (Automatic Processor, Allied AP201, CPAC, Inc., Leicester, NY). Duplicates of the films (X-Omat Duplicating Film #121-5821, Eastman Kodak Company, Rochester, NY) were made immediately for archival purposes, since the #3 film is only available in a single pack.

3. Surgical defect creation

The original protocol called for an implant manufacturer to fabricate a custom trephine to create the surgical defects. However, this service was not available and a substitute needed to be devised. The Ti implants were 3.75 mm in diameter and the HA-coated implants were 3.3 mm. Using a drill that created a defect 3 mm larger than the implants would require 2 different sizes, i.e. 9.75 mm and 9.3 mm. These values when compared to a 9.525 mm (3/8") defect drill yielded a 2.89 mm residual defect for the Ti implant and a 3.11 mm residual defect for the HA-coated implant. This created an average defect of 3.0 mm. Several styles of commercially available drill bits in this size range were considered. Originally, a 9.525 mm Long Twist Drill #1291-06 (Zimmer, Warsaw, IN) used for preparation of acetabular cement anchor holes during hip replacement was contemplated. However, at a trial run with a necropsy specimen, the angle of the tip created a 2 mm slope from the parallel edge of the defect to the tip. This was unacceptable since the protocol called for a parallel 5 mm defect with a flat floor. This particular drill would have removed a total of 7 mm at the apical aspect of the defect and voided the intended design.

Several commercially available non-surgical steel drill bits were considered. A pilot point proved to be necessary with the necropsy specimen and therefore would need to be of a specific size, i.e. less than the final drill size used in the implant preparation. Several manufacturers market a 9.525 mm (3/8") drill bit with pilot points. However, only the Bosch T4009 3/8" Brad Point Drill Bit (Bosch, New Bern, Germany) had a tapered pilot

point with a base less than 3.0 mm. Additionally, a reduced 6.4 mm (1/4") shank was needed to fit in the Hall Series 3 Drill/Reamer #5044-01 (Zimmer, Warsaw, IN) to the 1/4" Jacobs Chuck Adapter #5044-09 (Zimmer, Warsaw, IN).

The total length of the drill bit selected was 90 mm. Only 5 mm of cutting length was required to create the alveolar defects and since the drill bit needed to be stabilized near its' terminal end while in use, the flutes of the bit were covered with blue Triad VLC Custom Tray Material #95752 (Dentsply International Inc., York, PA) from 1" above the cutting edge tip all the way to the reduction portion of the shaft. To maintain cutting efficiency over the course of the study, 5 drill bits were prepared in this manner so that only 12 defects would be prepared per drill bit. Each drill was placed in a conventional dental lathe. A Royal Hand Engine #C-321 (Royal Mfg. Co, LTD., Japan) with a tapered Dedeco Lab Carbide Bur #84-T (IDE Interstate, Amityville, NY) was then used while the drill bit was rotating at high speed, acting as a lathe making the acrylic jacket perfectly round. Traditional pumice polishing of the acrylic provided a smooth surface needed to stabilize the drill during intraoral use. Since these were made of carbon steel and not surgical stainless steel, ethylene oxide sterilization would be necessary, requiring a 2 day turn around time. Having multiple drills also provided a safety factor in case one of the drills became contaminated during the procedure and another was needed. Flash sterilization was not considered an option with the potential for rusting. After use, each drill bit was individually prepared for gas sterilization. (Plate 2)

C. Phase II

1. Implant placement

Surgical assignments were derived by random drawing of the dogs' CID numbers (within their respective groups of 5 based on arrival/extraction dates). These 2 schedules were combined into a master list of 10. The order of surgery was dog 1045, 1136, 1127, 0870, 1125, 1479, 1647, 1700, 1496, and 1702. Next, the side of the arch to receive Ti

45

Plate 2.

A.   Modified 9.525 mm Brad Tip Drill Bit Used to Surgically Creat Defects
             Compared with a UNC-15 Periodontal Probe. (Magnification 0.75x)

B.   Close-up of Brad Tip Drill Bit Used to Surgically Creat Defects. (Magnification
             4.7x)
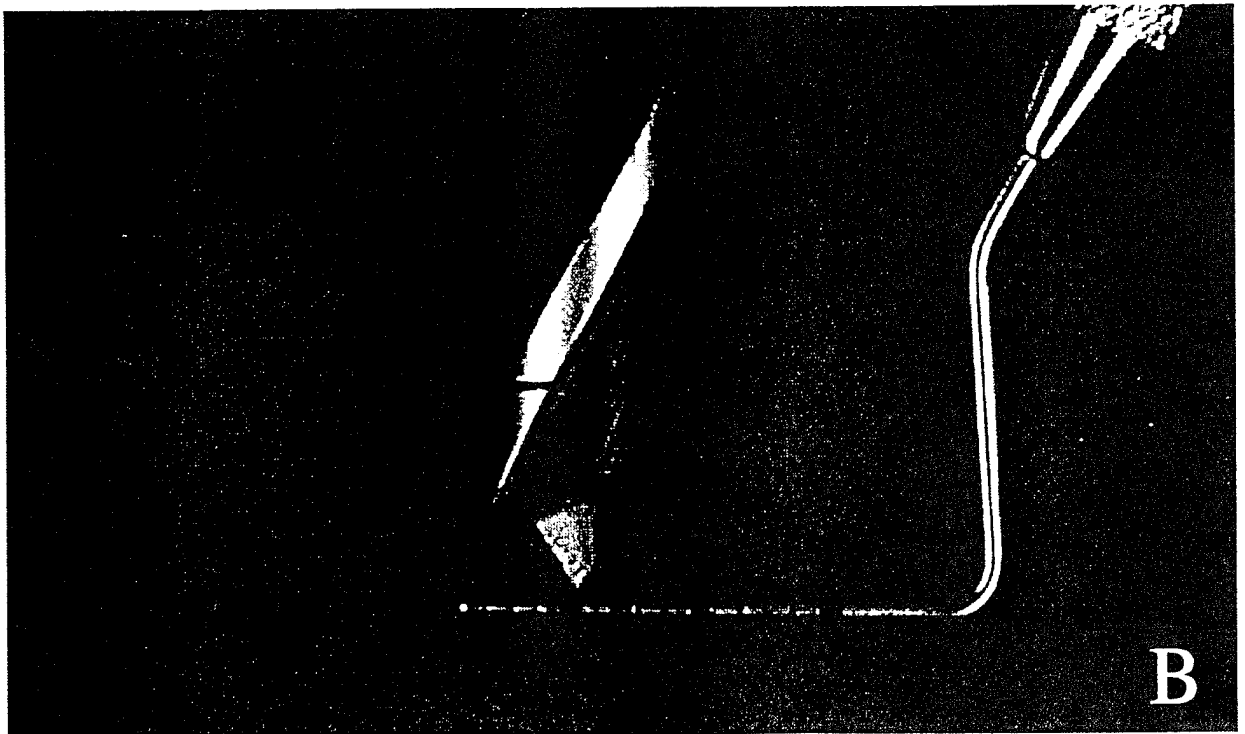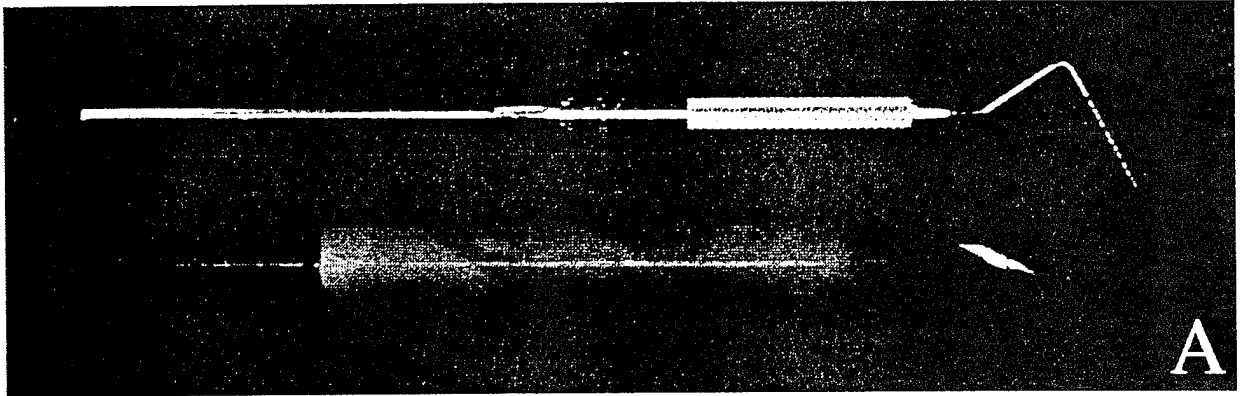
implants was determined by coin flip. The Ti implants were then alternated side to side through the remainder of the animals. The control was selected as consistently being the center implant. This was based on the desire to avoid placement of e-PTFE membranes on 2 immediately adjacent implants, insuring adequate blood supply around the periphery of the membrane. Another coin toss was used to determine which of the non-control sites would receive DFDBA, which was then alternated from anterior to posterior location through the remainder of the animals. The DFDBA site was consistently the same on the left and right sides of each animal. (Plate 3)

Following a post-extraction healing period of 3 months, the animals were treated in their previously determined order under general anesthesia for alveolar defect preparation and implant placement. A crestal incision was made, followed by full thickness facial and lingual flap reflection. The bucco-lingual ridge dimension was measured approximately 5 mm below the height of the ridge with a Boley gauge #68-694 (IDE Interstate, Amityville, NY). A large barrel Dedeco Lab Carbide Bur #88-A (IDE Interstate, Amityville, NY) in the Hall Micro-Aire Handpiece with the incoming pressure reduced to 40 pounds was used for slight alveoloplasty under sterile saline irrigation if the ridge presented with a rough surface from the extraction healing. This would be no more than 1 or 2 mm in apico-coronal height and was not an attempt to create an ideal ridge form or width as one might do in traditional implant placement, i.e. no intentional height reduction was accomplished. The distal defect was always prepared first beginning 5 mm anterior to the second molar or slightly anterior to this if the center of the first molar extraction site proved to have a more even alveolar topography. Once the site was selected, the 2 mm Round Marking Bur #RMB (Sterngold-ImplaMed, Sunrise, FL) was used to make a pilot hole at 1100 revolutions per minute (RPM) using the 1:16 Reduction Handpiece #AHP-62 of the Aseptico Duotron #AEU-217 (Aseptico, Kirkland, WA). Using the 9.525 mm drill in the Hall Series 3 Drill/Reamer with the incoming pressure reduced to 25 pounds, a 5 mm deep defect was created in the ridge. Copious irrigation was used with the drill turning at 60

Plate 3.   Diagrammatic Representation of Defect Location and Distribution of Implant Types. One Quadrant Received 3 Ti Implants While the Contralateral Quadrant Received 3 HA-coated Implants. Center Implants Were the Control. Anterior and Posterior Implants Were Either DFDBA/e-PTFE or e-PTFE Alone.

HA-Coated Cylinder

Defect

Ti Screw
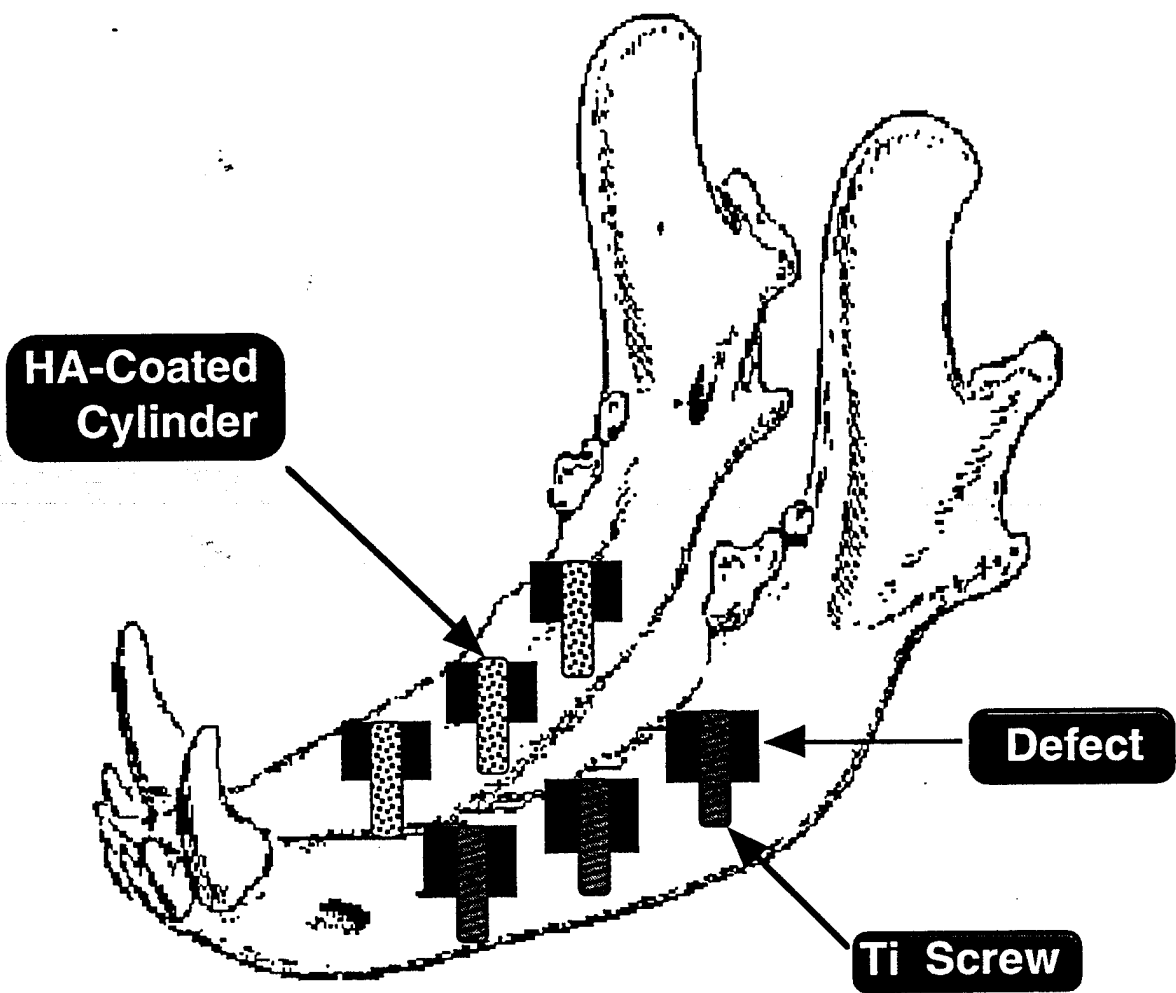
RPM. By lowering the incoming nitrogen pressure, the drill would bind and stop if the flutes caught the facial or lingual walls during site preparation. At normal operating air pressure the drill would not bind if the flutes caught and would damage the facial or lingual plate. Slow and steady light pressure was required to create a uniform defect. Excessive pressure would cause the drill to take too large a bite and change its direction. If fenestration did occur during the defect preparation, it was noted and any gross osseous roughness or bony projections were removed with an Ochsenbein chisel #1 (Hu-Friedy, Chicago, IL).

The 9.525 mm drill's pilot point created a 2.7 mm diameter hole which was used as a pilot for the 2.0 mm Internally Cooled Drill #ICD2 (Sterngold-ImplaMed, Sunrise, FL) using the 1:16 Reduction Handpiece at 1100 RPM. Even though higher speed could be safely tolerated, it was easier to control the handpiece at 1100 RPM. The 2.0 mm drill was taken to a depth of 10 mm measured from the height of the alveolar ridge on either side of the defect. A final step for the Ti implants and an interim step for the HA-coated implants included the 3.0 mm Internally Cooled Drill #ICD3.0 (Sterngold-ImplaMed, Sunrise, FL), also taken to 10 mm in depth. The 3.3 mm Internally Cooled Drill #ICRTD3.3 (Sterngold-ImplaMed, Sunrise, FL) was used to prepare the final size for the HA-coated implant sites. The Ti sites were not tapped unless the implant would not engage the osteotomy site.

Moving 10 mm anterior from the most mesial edge of the previous defect, a new pilot hole was created and the procedure was repeated. Again, slight adjustment anteriorly was tolerated if a more ideal defect site would have been accommodated. For the final implant location, special care was taken to avoid the mental foramen. This resulted in several animals having their most anterior implant placed considerably more mesial than originally planned. One animal actually had 2 mental foramina on one side and required the implant site to be placed between the two. Copious irrigation was done to remove any debris in the preparation sites and under the flaps prior to fixture placement.

Titanium Standard Screw 10 x 3.75 mm Implants #S10X3.75 (Sterngold-ImplaMed, Sunrise, FL) were used in all Ti sites. These were placed at 16 RPM using the 1:256 Reduction Handpiece #AHP-60 (Aseptico Inc., Woodinville, WA) and an Implant Mount Attachment #IMA (Sterngold-ImplaMed, Sunrise, FL). Combination Hydroxyapatite-Titanium Plasma Sprayed 10 x 3.3 mm Cylindrical Implants #HCH10X3.3 (Sterngold-ImplaMed, Sunrise, FL) were used in all HA-coated sites. These were placed with straight vertical finger pressure until firmly in place. Occasionally the Cylinder Seating Tool #CST (Sterngold-ImplaMed, Sunrise, FL) was needed. (Figure 2)

Implants were placed sequentially starting with the distal site. Once the implants were placed, minimal suction was done in the defect sites to promote good clot formation. Internal Hex Cover Screws (low profile) #CS002 (Sterngold-ImplaMed, Sunrise, FL) were placed and tightened. Using a periodontal probe (#PCPUNC15, Hu-Friedy, Chicago, IL), the distance from the top of the implant cover screw to the bottom of the defect was measured on both the mesial and distal to the nearest 0.5 mm. Measurements ideally would be 6 mm, incorporating 1 mm for the cover screw and 5 mm for the exposed implant. The width of the superior portion of the defect was also measured and should have been approximately 10 mm mid-defect in an anterior/posterior direction. The final measurement was the distance from the edge of the cover screw to the defect wall in both a mesial and distal direction. This measurement took into consideration any deviation of the drill during defect creation or implant preparation. Notations were made about any fenestrations, angulation, bone quality, or positioning problems of the defect site or implant. (Plate 4)

One or two 0.5 cc bottles of 90-500 μm canine DFDB (Dr. Ann Prewett, Osteotech, Inc., NJ), depending on the amount of fenestration and width of the ridge, were reconstituted in a sterile dappen dish and saturated with saline during the implant placement. The material was transferred to the selected DFDBA defect site with a #7 wax spatula (Premier, Norristown, PA) while taking care not to touch the implant. The DFDBA

Figure 2.   Diagrammatic Representation of Implant and Defect Relationships From Occlusal and Buccolingual View.

This figure page will be a line drawing of the implant and defect relationships with measurements. There was a problem in printing for this review.

51

Plate 4.   Clinical Representation of Implant Placement in Surgically Created Defects.
              Defects Measured 9.525 mm in Circumference and 5 mm in Depth. Three 10
              mm Long HA-coated Implants Are Shown after Placement in the Left
              Mandibular Quadrant. Right Quadrant in This Animal Received 3 Ti Implants.
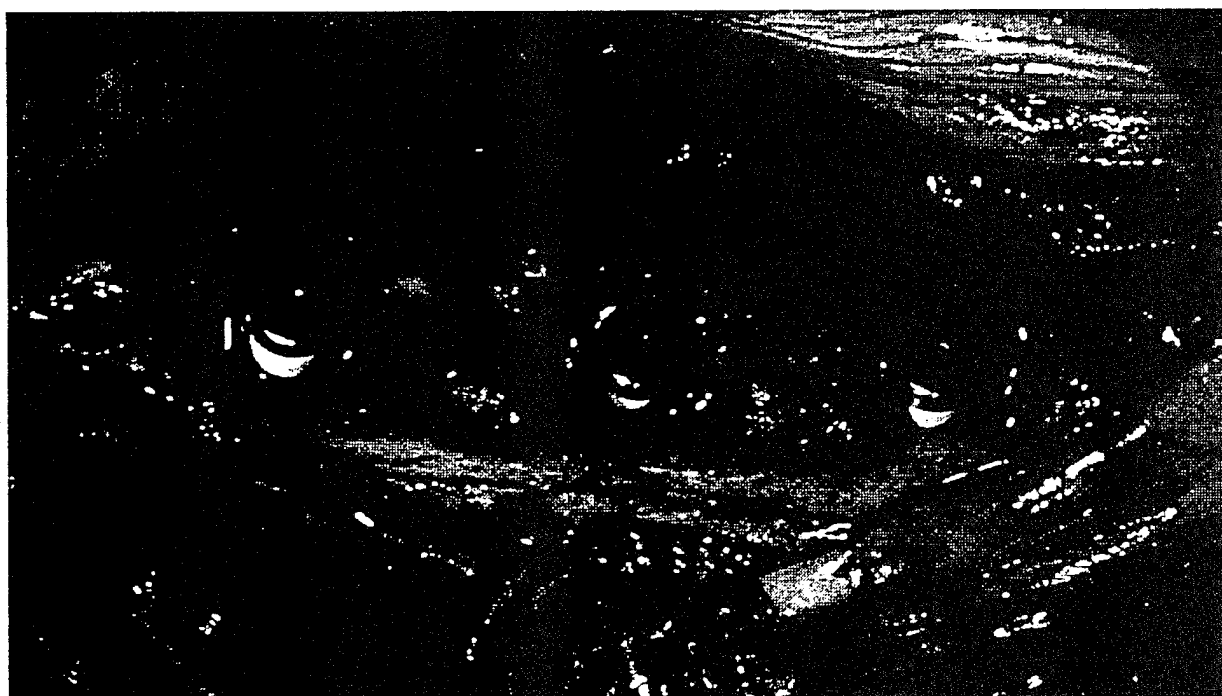
was processed and packaged at the Osteotech facility using widely accepted procedures for bone banking as reported by Mellonig and Prewett in 1992.[138] The material was harvested from cortical plates of long bones of dogs and were cleaned, ground to a course particulate, washed and defatted with 70% ethanol. The material was then freeze-dried in a vacuum. After drying, the bone particles were further ground and sieved to yield a particulate graft in the range of 90-500 μm. The material was then treated with 0.6 N HCl and a virucidal agent (Permein) which was a combination of ethanol and non-ionic detergent. The material was subsequently washed, freeze-dried and vacuum sealed in glass containers containing 0.5 cc of DFDBA. The defect was packed to the height of the cover screw and condensed with a 2 x 2 gauze sponge (Kendall Healthcare Products, Mansfield, MA) rolled on the end of a hemostat. In areas of facial or lingual fenestration, the original contour of the alveolar ridge was replicated. (Plate 5 A)

An Oval-4 GTAM #OV4AS (W.L. Gore & Assoc., Inc., Flagstaff, AZ) membrane was gently curled around a sterile mirror handle prior to placement. The GTAM was placed over the defect/DFDBA/implant without any need for trimming. No fixation pins or other special retaining devices were used. A single interrupted suture using an e-PTFE nonresorbable monofilament suture (Gore-Tex® Suture #P5K17 with CV-5 needle, W. L. Gore and Associates, Flagstaff, AZ) was placed in facial and lingual flaps over the center of the cover screw and tied with enough tension to evert the flap edges. Both membranes were secured in this fashion prior to closing the entire flap with interrupted sutures. (Plate 5 B)

Once the GTAM was in place, interrupted CV-5 Gore-Tex Suture was placed, starting in the posterior and working anteriorly. Sutures were placed 2 mm apart and penetrated the mucogingival junction on the facial with an adequate bite on the lingual to prevent tearing. Usually, the surgical sites required at least 20 sutures. After insuring adequate hemostasis, the throat pack was removed and the animal was released to the anesthetist. Clinical photographs were taken at multiple time points during surgery.

53

Plate 5

A.   Implant Site after Placement of DFDBA into Defect Prior to Coverage with an e-PTFE Membrane.

B.   Implant Sites after Placement of Two e-PTFE Membranes Prior to Flap Closure. The Center Site Consistently Served as the Control.
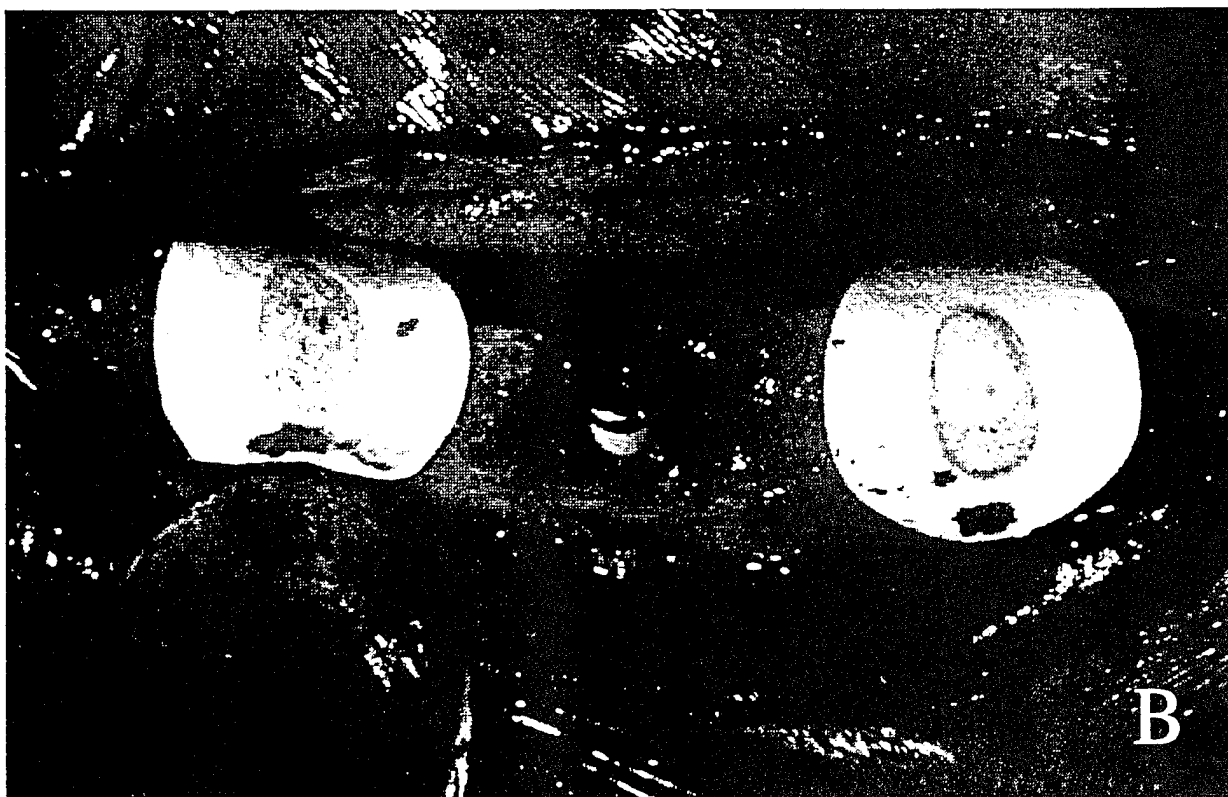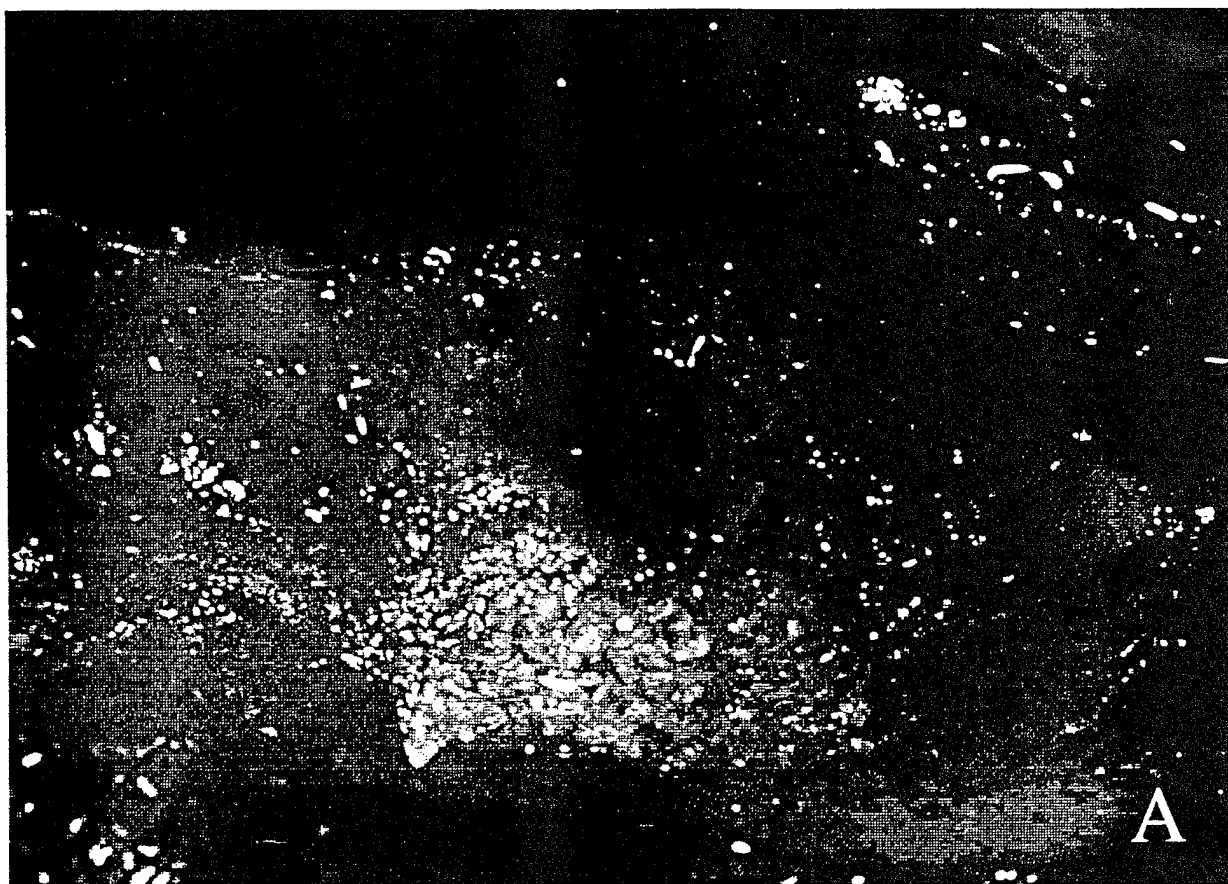
2. Post-surgical treatment and fluorescent labeling

During post-surgical recovery, chloramphenical and buprenorphrine hydrochloride were given as previously described. Oral hygiene was accomplished by swabbing the surgical areas with 0.12% Chlorhexidine Gluconate (Peridex, Proctor and Gamble, Cincinnati, OH) 5 days a week until complete tissue healing had occurred. This schedule was modified as needed, depending on the post-surgical response and/or complications noted.

All animals were seen at 7 days after surgery for post-operative treatment (POT) to include examination of the surgical sites, Peridex application, and standardized post-implant placement radiographs. Dogs were sedated with propofol and intraoral photos were taken of each mandibular quadrant. All surgical sites were healing well at 1 week with slight generalized edema and erythema in the suture areas. All implant sites were closed and there were no exposures of e-PTFE membranes. Animals were eating well and were moved to the kennel area until their next POT.

Tetracycline (TCN) labeling for reflective fluorescence was also accomplished at the 7 day POT session. Two versions of TCN administration were used. The first group of 5 dogs received a tablet of Achromycin V (Lederle Laboratories Division, Pearl River, NY) 750 mg PO each day for 3 days. This method is easy to accomplish by rolling the tablets in cheese or meat as a treat for the dogs and was a pharmacy item at CID. This method of administration has been used by several animal researchers in the area with success. However, concerns for inadequate or erratic systemic absorption were also considered.

As a comparison, a more traditional TCN administrative route was used on the second group of 5 dogs. For many years, Achromycin IM (Lederle Labs, Pearl River, NY) was the drug of choice in research circles; unfortunately, its production was discontinued by Lederle Labs. The formula was obtained from Lederle's medical advisory department. This injectable form was prepared at CID by combining Tetracycline Hydrochloride Crystalline #T3383 250 mg (Sigma Chemical Company, St. Louis, MO), Magnesium

Chloride #M8266 46 mg (Sigma Chemical Company, St. Louis, MO), Ascorbic Acid #A1417 275 mg (Sigma Chemical Company, St. Louis, MO), and Procaine HCl 40 mg (Winthrope Pharmaceuticals, New York, NY). This was mixed with 2 ml of sterile water creating 2 ml of the previously marketed drug called Achromycin. This Achromycin equivalent was administered once in a rear thigh muscle in 5 dogs at 11.4 mg/kg. No animal showed signs of post-injection sequelae.

A second POT was performed at 14 days to remove the sutures. As before, propofol was used and intraoral photos were taken. Peridex was applied before and after suture removal. Surgical sites were closed; however, there was an increase in erythema around the sutures at this visit. A biweekly POT schedule was followed after this point. Modifications of the 2 weeks occurred on an individual basis as needed for implant and membrane exposures. Membrane exposures were handled by trimming the material with scissors as close to the remaining attached margin as possible and sites were maintained with the daily application of Peridex. Implant exposures were handled similarly. No additional surgical treatment or systemic antibiotic therapy was administered.

At the 15 week visit, the animals were induced with propofol and placed under light general anesthesia. Standardized radiographs were taken with the previously described radiographic technique. Two films were taken in succession to be used as a quantitation of the reproducibility of the radiographic stent. Radiographs were developed as previously described and no attempt was made to identify which radiograph was taken first. Prior to the radiographs, POT procedures were accomplished. Xylenol Orange (Fisher Scientific, Fair Lawn, NJ,) was prepared at CID to 20 mg/kg. This solution was administered at this time using a FLO-GARD 6200 micropump (Travenol, Deerfield, IL) with a 20 gauge Quik-Cath Catheter #2n-1115 (IDE Interstate, Amityville, NY) in the cephalic vein of all dogs. Solution was administered at a rate of 50 ml/hr. The dogs' mucosa and skin took on a purplish hue as the drug was administered. The dogs tolerated the procedure well and excreted the product through their urine over the next 6-8 hours.

D. Stage III

1. Clinical exam and sacrifice

At 16 weeks post-implant placement, the animals were anesthetized as previously described. Four dogs were selected to have clinical evaluation of implant healing prior to sacrifice. Dogs 1127, 1136, 1496, and 1702 were taken to the operating room and a midcrestal incision was made followed by elevation of buccal and lingual mucoperiosteal flaps. Clinical photos before and after membrane removal along measurements of ridge width were made. A carotid cut-down was accomplished on all dogs, while under general anesthesia, to isolate vessels for head perfusion with Buffered Formalde-Fresh Low Odor 10% Formalin (Fisher Scientific, Fair Lawn, NJ). The animals were euthanized while under general anesthesia with 10% potassium chloride (H. R. Cenci Lab, Inc., Brooklyn, NY). Each dog was transferred to a necropsy room where the mandible was sectioned in the ramus region and at the symphysis. Each half mandible was placed in an appropriately labeled jar containing Formalin Solution, 10% buffered, pH 7.0 (Stat Lab Medical Products, Inc., Dallas, TX) until further processing. The remains of the animals were disposed of according to CID protocol.

E. Radiographic Analysis

1. Analysis system

Standardized radiographs were analyzed at the University of Texas Health Science Center at San Antonio, Department of Dental Diagnostic Science, Longitudinal Radiographic Assessment (LRA) Facility. The image analysis system was composed of an Intel 80486 AT/bus personal computer (Lane i486/33, Lane Systems, San Antonio, TX) with a serial trackball, an external 940 megabyte (MB) optical disk drive (Panasonic LF-7010, Matsushita Electric Industrial Co., Kadoma, Osaka, Japan), a NEC 4FG color monitor (NEC Technology, Inc., Tokyo, Japan), and a 16" non-interlaced high resolution color monitor (Mitsubishi Diamond Scan, HC 3925 ATK; Mitsubishi Electric Corp.,

Nagasagi, Japan). The specimens were placed on a light field stage and imaged with a high resolution CCD camera (MTI Series, Dage/MTI Inc., Michigan City, IN). An 8 bit analog-to-digital conversion of the video signal was performed with a VFG-100-AT frame grabber board (Imaging Technologies, Inc., Woburn, MA).

The software is based on MS-DOS v5.0 and Microsoft Windows v3.0 (Microsoft Corp., USA) operating system environment. The basic database structure utilized Novell Btrieve and ran on a Novell Netware 386 network. The software package named CARE© (Computer Aided Radiographic Evaluation)[139] was developed on site and incorporates real-time subtraction capabilities and is based on a modification of the RadWorks© program for direct digital radiography.[140]

The video camera measured the light passing through the baseline radiograph positioned on the radiographic viewer. Each image was digitized into a 640 x 480 picture elements (pixels) image and converted to grey levels with values of 0 to 255. The image processor and computer provided storage and mathematical manipulation of the images. Images were saved to the 940 MB optical disk and recalled when needed for analysis. Images could also be displayed and viewed on the monitor. The follow-up radiographic image (i.e. recall #1 or #2) was digitized after it was aligned with the baseline digitized image using a real-time subtraction method on the 16 inch monitor. The microcaliper driven table held the radiograph and allowed precise movement and alignment with the original radiograph. Each superimposed image was saved as recall #1 and the same procedure was accomplished for the successive film (defined as recall #2). Background noise level in the subtraction images was established by calculating the standard deviation of pixel values observed in a non-treatment Area-of-Interest (AOI) in the body of the mandible between the mandibular canal and the center implant. These values resulted in an average standard deviation of 5.057 grey values from the 20 sets of radiographs. For the CADIA system used at the LRA facility, values between 5 and 8 are considered excellent. Significant density change ($\pm$ 2 standard deviations = 95% confidence interval) was chosen

as 10 by doubling the standard deviation.[134] This was used to exclude 95% of the differences due to normal image variation (noise) in the system. Therefore, only those 2 x 2 pixel areas which changed more than 10 grey levels were recorded.

Decreases in radiographic density were represented by negative values while increases were represented by positive values. Additionally, the size of the area affected by change was recorded in square mm. Pixel size was determined by calibrating the image to the known size of the implants. The area in which density changes were noted was multiplied by the difference between the means of the grey level averages, giving the CADIA value.

2. CADIA

Before CADIA analysis, a non-parametric histogram matching program was used to adjust for differences in overall grey tone levels between images.[141] Six AOIs were selected for each implant using a preformated 32 x 32 pixel box, each representing 2.25 mm^2 of area. Boxes were stacked on the mesial and distal aspects of the implant at least 0.2 mm away from the implant surface so no interference would be registered by any misalignment of the implant during superimposition. Boxes were positioned to maintain a consistent AOI size and location between the two implant types. Boxes 1 and 2 were at a crestal defect location, 3 and 4 were a mid-defect location, while 5 and 6 were at an apical defect location. (Plate 6 A) If increases and decreases representing positive or negative density change occurred at the same time in an AOI, a summation of the changes were calculated as a measure for the net density change. Changes in osseous density between the 1 week post-implant placement image and the 3.5 month follow-up image were then calculated. These were quantitatively expressed as the CADIA values representing average density increases and decreases multiplied by the area of the given AOI. This was also done with each of the retake follow-up radiographs.

Plate 6.

A.   Radiograph Demonstrating Positioning of Areas of Interest in the Surgically Created Defect for CADIA Evaluation. (Magnification 7.8x)

B.   Subtraction Radiography Demonstrating Density Loss (darker areas) and Density Gain (lighter areas) after 4 Months of Healing. The Left Implant Represents an e-PTFE Site, the Center a Control Site, and the Right a DFDBA/e-PTFE Site. The Gain in Density at the DFDBA/e-PTFE Site is Apparent Along with the Loss of Alveolar Ridge at the Control Site. (Magnification 5x)

A

B
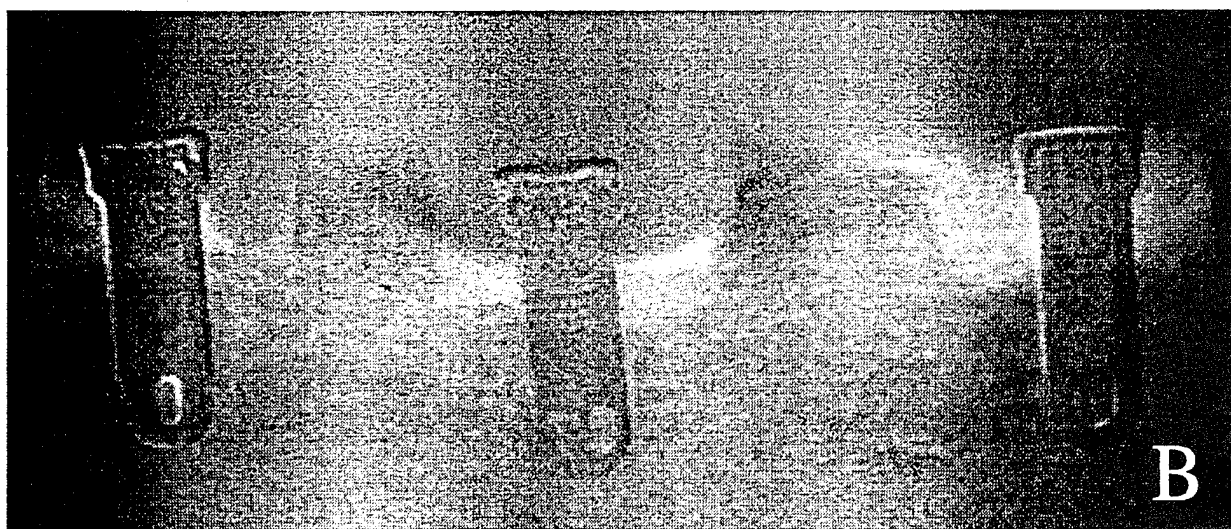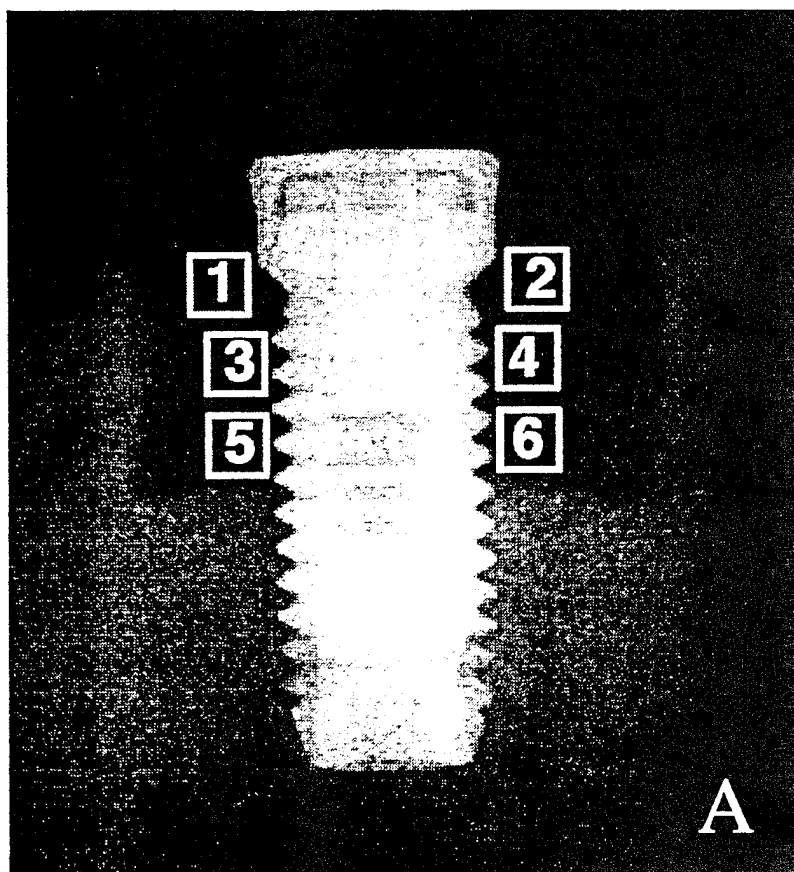
3. Subtraction radiography

The same images stored digitally for CADIA could be called up for Subtraction Radiography. This software (part of CARE©) produced a visual image of the changes in radiographic density by superimposing the 2 images. Any loss in bone density was depicted as a dark grey area while gains in bone density appeared as light grey. The resultant image could be downloaded and printed as a visual aid. (Plate 6 B)

4. Clinical interpretation of radiographs

Pre-sacrifice radiographs were examined on a radiographic view box #380430 (IDE Interstate, Amityville, NY) using a standard hand held magnifying glass. Radiographs were subjectively examined for defect fill based on the amount of fill from the depth of the defect to the cover screw on the implant. For non-control sites, the defect fill was evaluated compared to the final regenerated height as greater then or equal to the cover screw, equal to the fixture table, or less than the fixture table. Apparent changes in radiographic density of the defect compared to the surrounding alveolus was also determined for treatments and implant type. Ratings of greater than the surrounding alveolar density, less than the surrounding alveolar density, and equal to the alveolar density were assigned. Finally, implants with vertical peri-implant radiolucencies in the defect region were identified by treatment and implant type.

F. Histology

1. Specimen preparation

Block sections of the mandible halves were made using an Exakt Cutting-Grinding System (Exakt Medical Instruments, Inc., Oklahoma City, OK). Prior to sectioning, straight pins were used to approximate the implant and defect area. Occlusal films #4 (Kodak Film #166-6122, Eastman Kodak Company, Rochester, NY) were used to radiograph each half mandible to determine the implant location prior to buccolingual

sectioning. Sections through the mandible were 15 to 20 mm apart to include the implant and the surrounding defect area. Individual implants with surrounding bone were transferred to labeled bottles of formalin by location and dog number. Each specimen was then radiographed in the mesial-distal direction to determine the implant's orientation relative to the lingual surface of the mandible. If the implant was not parallel to the lingual plate of the mandible, the specimen was returned to the Exakt Cutting machine and a slice was made on the lingual surface to create parallelism with the implant to facilitate embedding and sectioning. Block specimens were returned to their individual specimen jars containing formalin.

Specimens were transported to the Histology Laboratory, Department of Periodontics, University of Texas Health Science Center at San Antonio (UTHSC-SA) for histologic preparation. After fixation (minimum of 72 hours), specimens were dehydrated through graded alcohols (Dehydrated Absolute Alcohol- 200 Proof, McCormick Distilling Co., Inc., Weston, MI) of 70% for 24 hours, 95% for 24 hours, 100% for 24 hours, followed by a solution change of 100% alcohol for an additional 24 hours. The next processing step involved 48 hours in 100% Xylenes GR (EM Science, Gibbstown, NJ) since the plastic for embedding is not compatible with alcohol. The solutions were changed on a 24 hour basis, gradually increasing the Osteo-Bed Bone Embedding Media (Polysciences, Inc. Warrington, PA) concentration to 100% (Appendix A). All of these procedures took place at room temperature. The final infiltration and embedding took place by the addition of Benzoyl Peroxide (Polysciences, Inc. Warrington, PA) to the Osteo-Bed Resin.

Embedding was done in catalyzed resin III (Appendix A). A 2 oz Qorpak™ Bottle #B7465-40 (Baxter Scientific Products, McGaw Park, IL) was filled to 20% of its volume and the specimen was oriented with the flat lingual surface down. Additional resin was added to cover the specimen and fill the jar to 80% of its' maximum volume. The jars were not opened or disturbed after embedding for 48 hours to avoid bubble formation during polymerization. After polymerization, the jars were briefly placed in the freezer to chill for

10 minutes. Jars were then wrapped in a cloth towel and struck with a hammer to break the glass. The unpolymerized superficial layer of resin was trimmed on the Leica 1600 Saw Microtome (Ernst Leitz Wetzlar GmbH, Wetzlar, Germany) and the specimens were mounted for final sectioning on an EBH-2 Block Holder #15899 (Polysciences, Inc., Warrington, PA) with Permabond Industrial Grade 910 Adhesive (Electron Microscopy Services, Ft. Washington, PA). Mesiodistal sections 15-20 μm in thickness were prepared using a Leica 1600 Saw Microtome. Two sections were obtained from each specimen, separated by the blade thickness of approximately 300 μm.

2. Reflective epifluorescence

Prior to staining, all sections were examined using reflective epifluorescence to observe both the TCN and xylenol orange labeling. An Olympus BH-2 Microscope scope equipped with a Reflected Light Fluorescence Attachment BH2-RFL and a 100 watt Mercury Burner HBO100W/2 (Olympus Optical Co., LTD., Tokyo, Japan) was used. To observe tetracycline, a violet excitation filter for 405 nm and 435 nm #V(BP-405) was used with a V(DM-455) dichroic mirror containing a Y-455 barrier filter. To observe xylenol orange, a green excitation filter for 545 nm #G(BP-545) was used with a G(DM-580) dichroic mirror containing a O-590 barrier filter. Objectives used included SPlanFL1 (1x), SPlanFL2 (2x), SPlanApo4 (4x), and DPlan10UV (10x). The specimens were examined and photomicrographs taken using the Olympus Automatic Photomicrographic System PM-10ADS incorporating a NFK2.5xLD multiplier resulting in a 2.5x magnification for photography. Using Kodak Ektachrome 400 film, photomicrographs were taken of the entire implant at 1x, the implant defect area at 20x, the entire circumference of the implant in a clock-wise direction at 40x, and any special areas of interest at 100x. The final photomicrograph magnification was 2.5x, 50x, 100x, and 250x respectively.

3. Staining for light microscopy

Sections were deplasticized and hydrated to water by using Osteo-Bed Solvent Solution (Polysciences, Inc., Warrington, PA) prior to staining. Sections were washed with 2 changes of 3 minutes each of the Osteo-Bed Solvent Solution followed by 5 minutes each in 70% and 40% ethanol before specimens contacted water. Paragon stain and Alizarin Red stain (Appendix B) were applied to one section from each implant after random selection. The remaining section was stained with Masson-Trichrome-Goldner Stain (Appendix C). Alizarin Red stains mineralized structures and appears red while the Paragon stains non-mineralized structures such as connective tissue pink. Masson-Trichrome-Goldner stains mineralized structures aqua and non-mineralized structures golden brown. Differences between mineralized and non-mineralized structures were well delineated with the latter stain; therefore, only the Masson-Trichrome-Goldner stained sections were histomorphometrically analyzed.

4. Histomorphometry system

Histomorphometry was accomplished to determine osseointegration, trabeculation, and residual DFDBA particles at CID using a Vanox AHB S3 Research Photomicrographic Microscope System (Olympus Corporation, Lake Success, NY) equipped with an SPlanApo4 objective and an attached Sony Color Video Camera and Control Unit DXC-750MD (Sony Corp., Japan). The video signal was digitized with an Imascan RGB Frame Grabber and Super VGA Display Controller (Imagraph, Chelmsford, MA) in a Hewlett-Packard Vectra Xu personal computer (Hewlett-Packard, Villefontaine, France) with a 90 MHz Intel Pentium chip, 16 MB of RAM (Random Access Memory), and a 500 MB hard drive. The software is based on MS-DOS v6.2 and Microsoft Windows v3.1 (Microsoft Corp., USA) operating system environment. Images were analyzed using Image Pro Plus for Windows v1.2 (Media Cybernetics, Silver Springs, MD) on a NEC Mulitsync XE 21 Monitor (NEC Technologies, Wood Dale, IL) at 30x magnification.

Histomorphic data were automatically exported to a Microsoft Excel v5.0 (Microsoft Corporation, USA) spreadsheet. Completed spreadsheets were printed on a Hewlett-Packard LaserJet 4 Plus printer (Hewlett-Packard, Boise, ID).

5. Histomorphometry

The apical extent and lateral border of the defect region were identified and outlined using reversal or cement lines as a histologic determinate. Additionally, defect borders were verified through external thread count, trabecular patterns, or internal anatomy of the implant using photomicrographs of reflective epifluorescence. The implant was then divided into 6 sections starting in the defect region at the implant collar on the mesial surface of the implant and working apically around the apex of the implant until the distal junction of the collar was reached. Each section of the implant was digitized and saved as an independent file for later recall. Measurements for osseointegration, trabeculation, and residual DFDBA were completed for both the mesial and distal surfaces of the implant; however for the non-defect region only one measurement was determined for osseointegration. (Plate 7)

Once the apical extent of the defect was identified, the depth of the defect was measured in microns from the collar of the implant. This distance was divided into 3 sections of equal dimensions and labeled coronal, middle, and apical AOI as in the radiographic study. (Plate 8 A) The amount of osseointegration in the defect region was then calculated first by tracing the implant surface that did not have any visible light or interposed connective tissue between the implant and bone in each AOI. Second, the surface of the implant, both osseointegrated and non-integrated was determined for each AOI. Osseointegration for each individual AOI and the entire defect region were calculated for mesial and distal surfaces by dividing the total osseointegrated surface by the total implant surface. This same calculation was repeated for the entire non-defect region to derive one figure for osseointegration. Implant vents were not included in the analysis.

65

Plate 7.   Demonstration of Defect and Non-defect Areas Selected for Analysis of
Trabeculation and Osseointegration. (Magnification 10x)
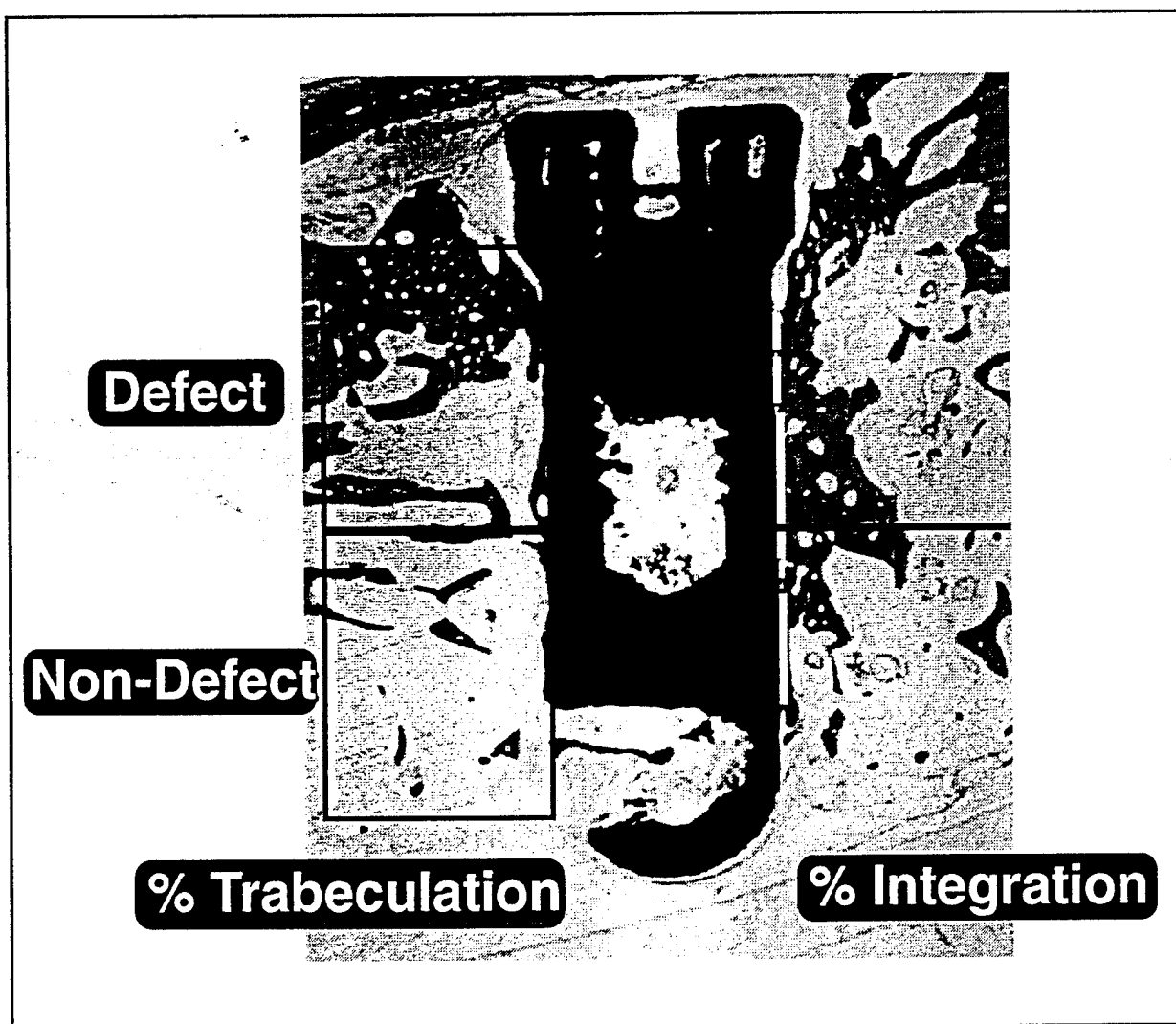
Plate 8.

A.   Demonstration of the Defect Area Divided into Coronal, Middle, and Apical AOIs for Analysis of Osseointegration. Yellow Tracings Represent Osseointegrated Implant Surface. (Magnification 21x)

B.   Demonstration of Tracing Technique Used for Analysis of Trabeculation. Red Lines Represent Borders of Original Defect Determined through Reversal Lines or Verification by Reflective Epifluorescence. Yellow Lines Represent Tracings of Trabeculae. Note the Numerous Small Marrow Spaces within Newly Formed Bone in Upper Half of Defect. Marrow spaces > 170 μm in Size Were Traced (Yellow) and Subtracted from Total Percent Trabeculation. Marrow Spaces < 170 μm Were Not Subtracted. (Magnification 21x)

Coronal

Middle

Apical

A

B
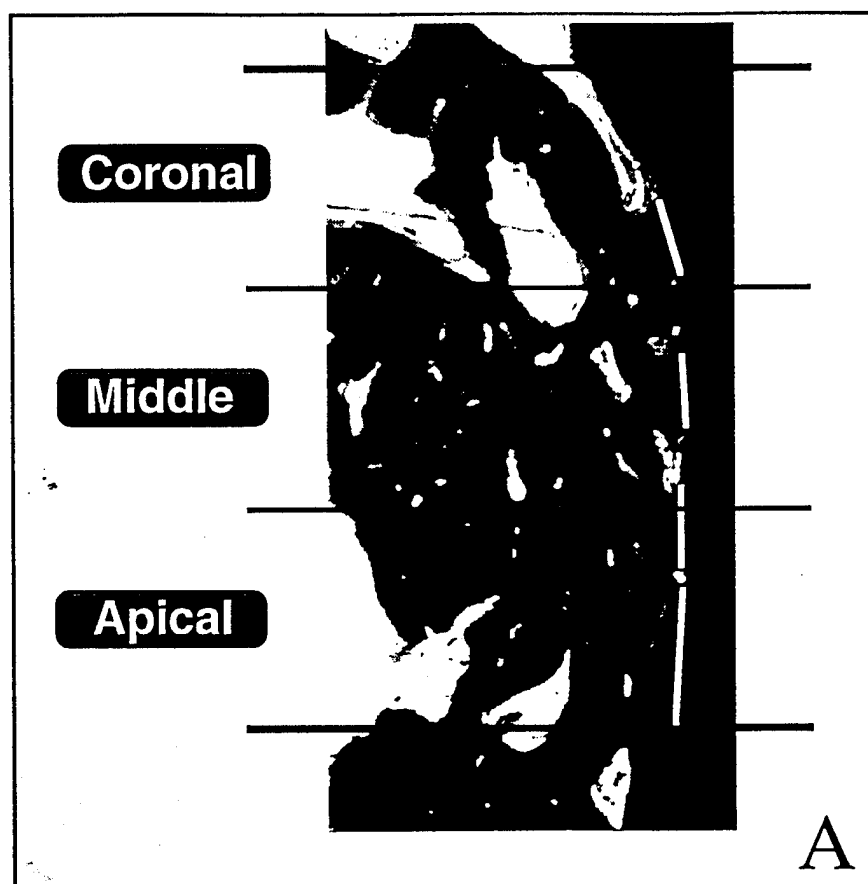
For trabeculation in the defect region, the total area of the defect was calculated by tracing from the implant collar to the lateral defect border, to the junction of the lateral and apical borders, to the implant surface, and finally tracing the implant surface back to the collar. The area of the trabeculae in the defect was then determined by tracing the borders of the trabeculae and summing the area of all trabeculae in the defect. The area of marrow spaces greater than 5 mm in diameter (as viewed on the monitor at 30x magnification- actual size greater than 170 μm) within trabeculae were subtracted from the total area derived for trabeculae. Marrow spaces less than 170 μm in diameter (actual size) were ignored in the calculation and included as part of the measured trabeculae. Trabeculation was calculated by dividing the total defect area of trabeculation by the total area of the defect. (Plate 8 B)

For trabeculation in the non-defect region, an area with similar dimension to the defect region was selected below the mesial and distal apical extent of the defect adjacent to the implant. The percent trabeculation was determined for the non-defect region as previously described.

Residual DFDBA particles in the defect region were identified by the Masson-Trichrome-Goldner stain as golden brown. The area of these particles were summed and divided by the total area of the defect previously determined to calculate the percentage of residual DFDBA. (Plate 9)

Finally, the distance from the advancing bone front to the Ti implant surface was measured within each AOI. The defect was divided into AOIs and the closest point from the bone front in any direction to the implant surface was measured in microns.

68

Plate 9.   Demonstration of Technique Used for Analysis of Residual DFDBA. Outer
            Red Lines Represent Borders of Original Defect Determined through Reversal
            Lines or Verification by Reflective Epifluorescence. Inner Red Circles
            Represent Tracings of Residual DFDBA. (Magnification 22x)

IV. <u>RESULTS</u>

A. Clinical

The post-operative course was uneventful in the DFDBA/e-PTFE group. Of these 20 sites, none fenestrated and the soft tissue integrity was maintained throughout the length of the study. Conversely, in 3 of 20 e-PTFE alone sites, membrane exposures were present at the 6 week time point, including 1 Ti implant (anterior location) and 2 HA-coated implants (posterior locations). Of the 20 control sites, in which no membrane was placed over the defect, 6 implants fenestrated through the mucosa at some time point between 4 and 10 weeks, including 3 Ti implants and 3 HA-coated implants. Two of the animals that had fenestrated the control site by 4 weeks also subsequently fenestrated the contralateral control site at the 6 and 10 week time point. The two animals with both of their control implants fenestrated also demonstrated a site with membrane exposure. (Table 1) In many of the animals the zone of attached gingiva remaining on the edentulous ridge was quite narrow. Upon refection of the buccal and lingual mucoperiosteal flaps deep into the vestibule, the tissue tended to relax buccally and the attached tissue would not reside directly over the crest of the ridge. In some cases the tissue was properly oriented; however, by the first POT attached gingiva was in a more buccal location. In these animals the implants remained covered by mucosa for the duration of the study and did not pose a problem.

In the 4 animals examined clinically by flap refection and membrane removal, all implants were judged to be clinically integrated through lack of mobility when tested by mirror handles. Membranes had to be dissected from the ridge after flap reflection and solid bone-like structure had replaced the defect during the 4 month healing period. Tapping on the cover screws with a mirror handle produced a characteristic "ring" associated with integrated implants.

Control sites consistently demonstrated a loss of ridge height and width. Crestal resorption occurred to such an extent that the ridges sloped gradually toward the apical extent of the

Table 1

NUMBER OF SITES PER ANIMAL WITH FENESTRATED IMPLANT OR e-PTFE

EXPOSURE

ANIMAL	DFDBA/E-PTFE	E-PTFE ALONE	CONTROL
0870	0	0	0
1045	0	0	0
1125	0	0	1 (HA @ WK 10)
1127	0	0	1 (TI @ WK 4)
1136	0	0	0
1479	0	0	0
1496	0	0	0
1647	0	1 (TI @ WK 6)	0
1700	0	1 (HA @ WK 6)	2 (HA @ WK 4, TI @ WK 6)
1702	0	1 (HA @ WK 6)	2 (HA @ WK 4, TI @ WK 4)
TOTAL	0	3 (HA X 2, TI X 1)	6 (HA X 3, TI X 3)

defect. Some regeneration of the defect had occurred in these areas, but certainly not like the other treatment sites.

e-PTFE alone sites had maintained most of the ridge height to approximately the level of the fixture table. There was not an increase in bone volume as seen with the DFDBA/e-PTFE sites. Faciolingual ridge dimension often was less than the original ridge width in areas of dehiscence and the implant surface could be seen through the thin facial and lingual walls.

Those sites with DFDBA/e-PTFE had bone to the level of the cover screw and in some instances the cover screw was completely covered. The bone regenerating the defect had proliferated under the membrane to the extent that after membrane removal, an exacerbation of bone mimicked the shape of the membrane. This bone growth in some instances had increased the dimension of the original ridge in both a buccolingual and apicocoronal direction. (Plate 10)

B. Visual interpretation of radiographs

Radiographically, all 60 implants appeared to be integrated in their apical portion below the defect. In the defect region, control sites demonstrated some regeneration of the defect area, while HA-coated and Ti implants had approximately equal ranges of defect fill. There was an equal number of sites with defect fill of 1/3, 1/2, and 2/3. (Table 2) In general, crestal resorption occurred both mesial and distal to the implant creating a gradual slope to the coronal portion of the regenerated defect. The dimensions of the original defect were not always discernible nor was the visual determination of density gain relative to the surrounding alveolus.

Visually, DFDBA/e-PTFE sites appeared to have an increase in density compared to the surrounding alveolus for both HA-coated and Ti implants compared to membrane alone sites. (Table 3) The alveolar crest at DFDBA/e-PTFE sites appeared to have regenerated to the level of the cover screw and beyond more often than to the level of the fixture table and below compared to membrane alone sites. (Table 4) Regarding level of alveolar regeneration, there

72

Plate 10.   Clinical Appearance Prior to Sacrifice after Flap Reflection and e-PTFE
               Membrane Removal. This Implant Site Received DFDBA/e-PTFE and
               Demonstrates the Characteristic Increase in Bone Volume seen after 4 Months
               of Healing at these Sites.
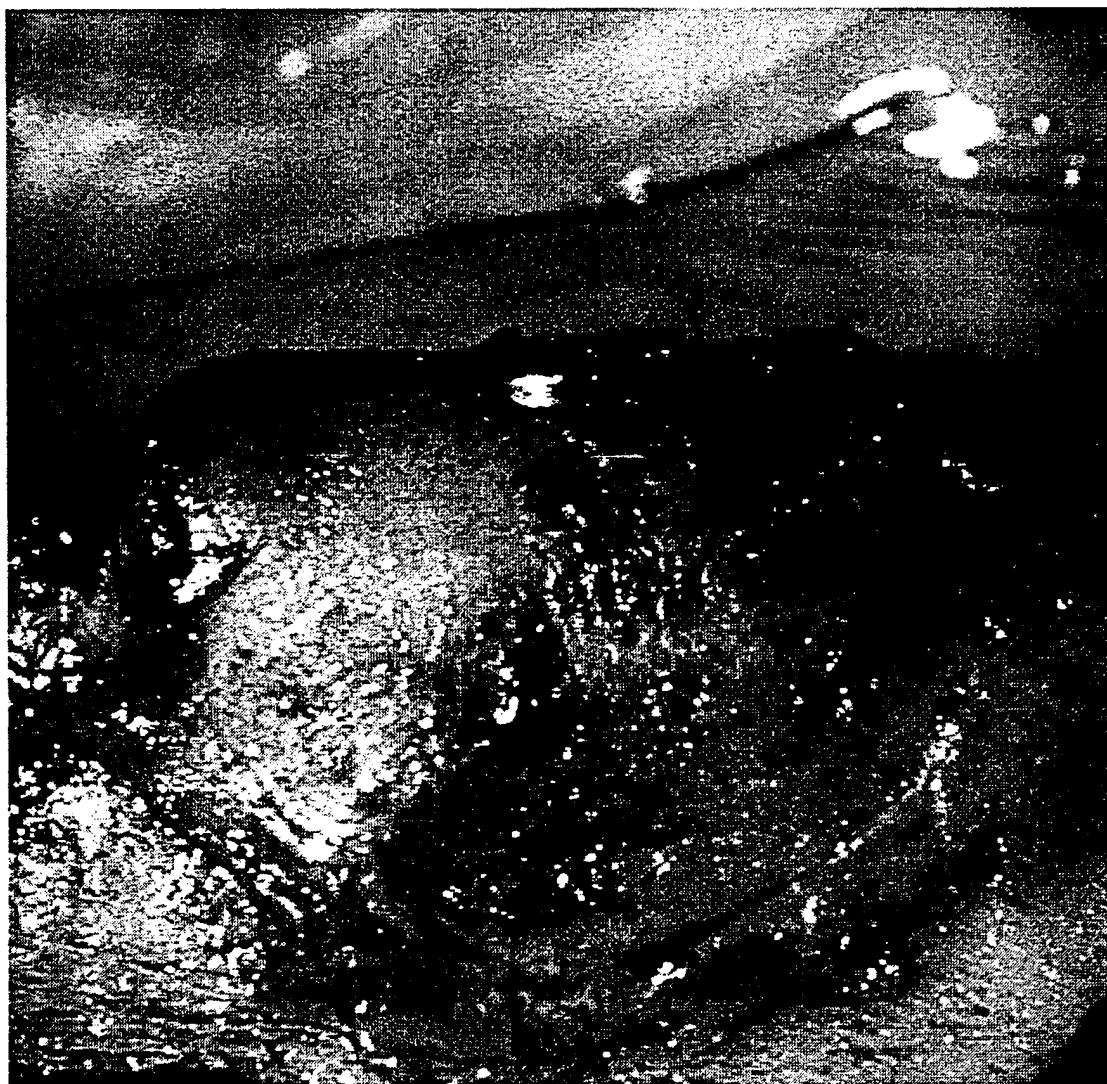
Table 2

CLINICAL INTERPRETATION OF PRE-SACRIFICE RADIOGRAPHS FOR DEFECT FILL
IN CONTROL IMPLANTS BY LEVEL OF REGENERATION ACHIEVED

Level of defect fill	HA	Ti	HA + Ti
1/1 (Complete)	0	0	0
2/3	3	3	6
1/2	4	2	6
1/3	3	3	6
0	0	2	2

Table 3

COMPARISON OF APPARENT DENSITY GAIN BASED ON VISUAL
INTERPRETATION OF RADIOGRAPHS, DEFECT SITE VERSUS NON-DEFECT
ALVEOLAR BONE

	Density gain	DFDBA/membrane	Membrane alone	Total for DFDBA/membrane and membrane alone
HA	> alveolus	6	2	8
	= alveolus	2	2	4
	< alveolus	2	6	8
Ti	> alveolus	5	1	6
	= alveolus	1	3	4
	< alveolus	4	6	10

Table 4

VISUAL RADIOGRAPHIC DETERMINATION OF LEVEL OF ALVEOLAR CREST
REGENERATION IN THE DEFECT COMPARED TO STANDARD POINTS ON THE
IMPLANTS FOR DFDBA/e-PTFE SITES AND e-PTFE ALONE SITES

Bone level	DFDBA/membrane	Membrane alone
≥ cover screw	15	5
= implant fixture table	5	10
< implant fixture table	0	5

was no apparent difference between HA-coated and Ti implants. (Table 5) The HA-coated implants appeared to be integrated to the level of the collar, at which point a lamina dura was present that cupped away from the neck of the implant to the crest of the ridge. Ti implants also had cupping at the collar of the implant.

Peri-implant radiolucencies in the healed defect were noted adjacent to 14 Ti implants but were not seen adjacent HA-coated implants. (Table 6) e-PTFE alone sites had a greater incidence of vertical peri-implant radiolucencies than DFDBA/e-PTFE sites. Ti controls demonstrated 3 out of 10 sites with peri-implant radiolucencies which was fewer than DFDBA/e-PTFE or e-PTFE alone sites. Peri-implant radiolucencies could only be identified when new bone had formed within the defect; therefore, results with Ti controls may be misleading since few of the controls had any bone in the healed defect.

C. Quantitative assessment with CADIA

The CADIA values were analyzed by 4-way ANOVA using JMP™ statistical program (SAS Institute, Cary, NC) on a Power Macintosh 9500 computer with 32 MB of RAM (Apple Computer Co., Cupertino, CA).

1. Analysis of defect by mean

The CADIA values for the recall films #1 and #2 were calculated for each implant AOI. No effort had been made to identify in which order the 2 recall films were taken. The intent of making the duplicate films was to assess the measurement error in CADIA. The CADIA values for each AOI varied in relation to the corresponding area in the corresponding recall film. The recall #1 group gave a mean CADIA of 40.7 and a standard deviation of 34.7. Recall #2 group gave a mean of 45.6 and standard deviation of 35.1. A one factor ANOVA revealed there was no difference between the 2 sets of films (p= 0.0751). Since differences between recall #1 and recall #2 films were not statistically significant, recall #1 films were selected by coin flip as the set to analyze. (Table 7)

Table 5

VISUAL RADIOGRAPHIC DETERMINATION OF LEVEL OF ALVEOLAR CREST
REGENERATION IN THE DEFECT COMPARED TO STANDARD POINTS ON THE
IMPLANTS FOR DFDBA/e-PTFE SITES AND e-PTFE ALONE SITES BY IMPLANT TYPE

Bone level	HA	Ti	HA + Ti
≥ cover screw	12	9	21
= implant fixture table	6	8	14
< implant fixture table	2	3	5

Table 6

IMPLANTS WITH VISUALLY DETECTABLE VERTICAL PERI-IMPLANT
RADIOLUCENCY IN THE DEFECT REGION BY TREATMENT SITE AND IMPLANT TYPE

	HA	Ti
DFDBA/e-PTFE	0/10	4/10
e-PTFE alone	0/10	7/10
Control	0/10	3/10
Totals	0/30	14/30

Table 7

ANOVA FOR RADIOGRAPHIC COMPARISON OF MEAN GROUP CADIA VALUE FOR

RECALL FILM GROUP #1 AND #2

	F-value	p-value
Recall film #1 versus recall #2	3.178	0.0751

CADIA was performed for each of the implants using 6 areas of interest. (Plate 6 A) A repeated measures ANOVA was performed utilizing the dog as the unit of analysis to evaluate the effects of different treatments (DFDBA/e-PTFE, e-PTFE alone, or control) with regard to the change in density of healing bone in the surgically created defects. When all 10 dogs were analyzed, statistically significant differences in density gains were seen relative to the treatments used (p<0.0001), the overall mean density change values for each dog (p<0.0001), and AOI positions (p<0.0001). (Table 8) DFDBA/e-PTFE sites demonstrated the greatest bone density increase followed by e-PTFE alone, with control sites having the least density gain. (Table 9, Figure 3) Contrasts were constructed within this significant effect for DFDBA/e-PTFE versus control (p<0.0001) and DFDBA/e-PTFE versus e-PTFE alone (p<0.0001). (Table 9, Figure 3) Significant differences between the AOI positions demonstrate greater bone density increases in the apical regions followed by the middle region, with the coronal region gaining the least density. (Table 9, Figure 4) Contrasts were also constructed within this significant effect for apical versus middle (p<0.01) and middle versus coronal (p<0.0001) AOI position. (Table 9, Figure 4) There were no significant differences (p=0.1424) in radiographic bone density changes adjacent to Ti versus HA-coated implants. (Tables 8 and 9, Figure 5) No significant interactions existed between treatments, AOI position, and/or implant types. (Table 8)

Two of the 3 implant sites with membrane exposure during healing demonstrated a loss or negligible gain in bone density when compared to other similarly treated sites and may have introduced a confounding variable. In order to alleviate any influence of adverse healing at membrane exposure sites on the final results, the data were reanalyzed using only the 7 animals without soft tissue complications at the test sites involving membranes. The results were similar to the analysis performed on all 10 dogs. Repeated measures ANOVA demonstrated statistically significant differences in bone density increase relative to treatments used (p<0.0001), AOI positions (p<0.0001) and the overall mean density values for each dog (p<0.0001). (Table 8) DFDBA/e-PTFE sites again demonstrated the greatest

Table 8

ANOVA SUMMARY FOR RADIOGRAPHIC PORTION OF STUDY FOR N=10 AND N=7
ANIMALS

	N = 10*		N = 7†	
	F-value	p-value	F-value	p-value
Treatments	52.2871	0.0000	41.043	0.0000
Implant type	2.1741	0.1424	4.698	0.0325
Dogs	5.7022	0.0000	7.906	0.0000
AOI Position	29.9214	0.0000	20.1317	0.0000
Interactions				
Treatment*Implant type	0.4574	0.6338	1.0589	0.3506
Treatment*AOI Position	1.0376	0.3898	0.4980	0.7372
Implant Type*AOI Position	0.5585	0.5732	0.4712	0.6256
Implant Type*AOI Position*Treatments	0.2128	0.9310	0.1086	0.9793

* Complete data set

† 3 dogs eliminated from data set due to membrane complications

Table 9

MEAN CADIA VALUES FOR EACH TREATMENT FOR N=10 AND N=7 ANIMALS

	CADIA Values (± SE)	
	n=10*	n=7†
Treatment		
DFDBA/e-PTFE	63.6 ± 3.7	64.4 ± 4.1
e-PTFE alone	41.2 ± 4.1	46.2 ± 4.9
Control	21.6 ± 3.0	22.3 ± 3.5
AOI Position		
Coronal	25.2 ± 3.6	27.9 ± 4.5
Middle	44.5 ± 4.3	48.3 ± 4.9
Apical	56.7 ± 3.7	56.6 ± 4.5
Implant Type		
Ti	39.7 ± 3.3	40.1 ± 3.9
HA	44.6 ± 3.6	48.4 ± 4.1

* Complete data set

† 3 dogs eliminated from data set due to membrane complications

Figure 3.   Mean CADIA Values by Treatment (DFDBA/e-PTFE, e-PTFE Alone, and Control) for n=10 and n=7. The Overall Treatment Effect was Significant at $p<0.0001$ by ANOVA.
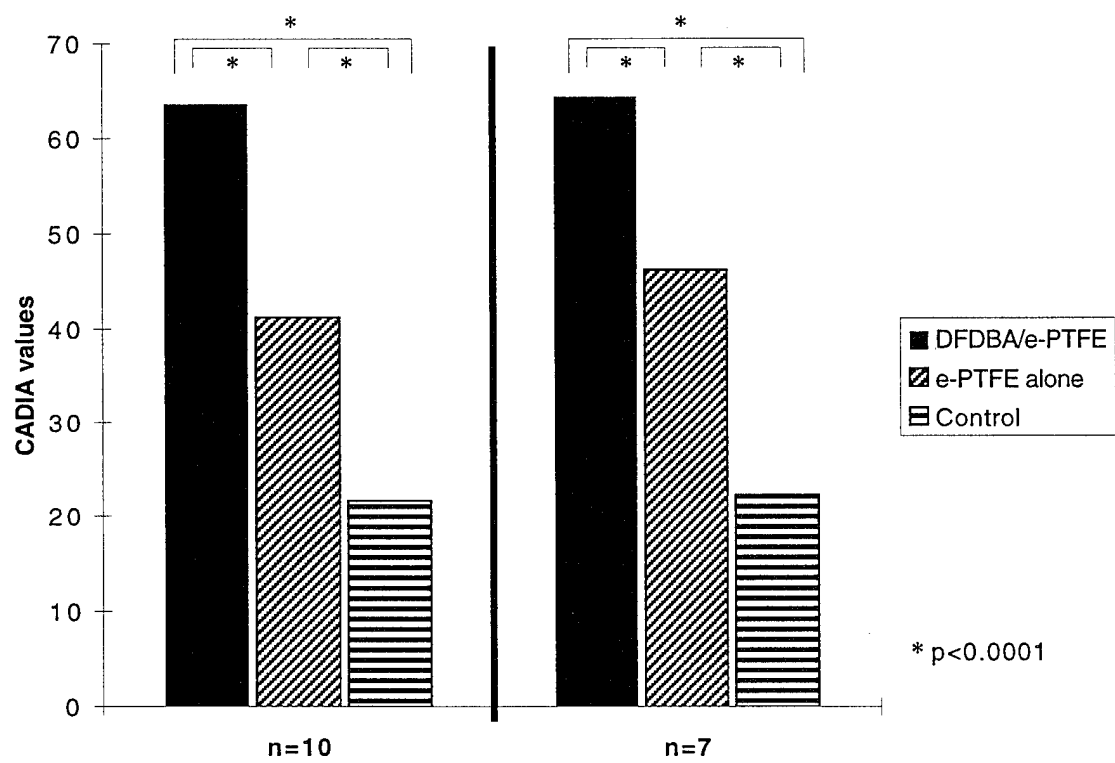
Figure 4.   Mean CADIA Values by Area of Interest (AOI [Coronal, Middle, and Apical]) for n=10 and n=7. The Overall Effect of AOI Position was Significant at p<0.0001 by ANOVA.
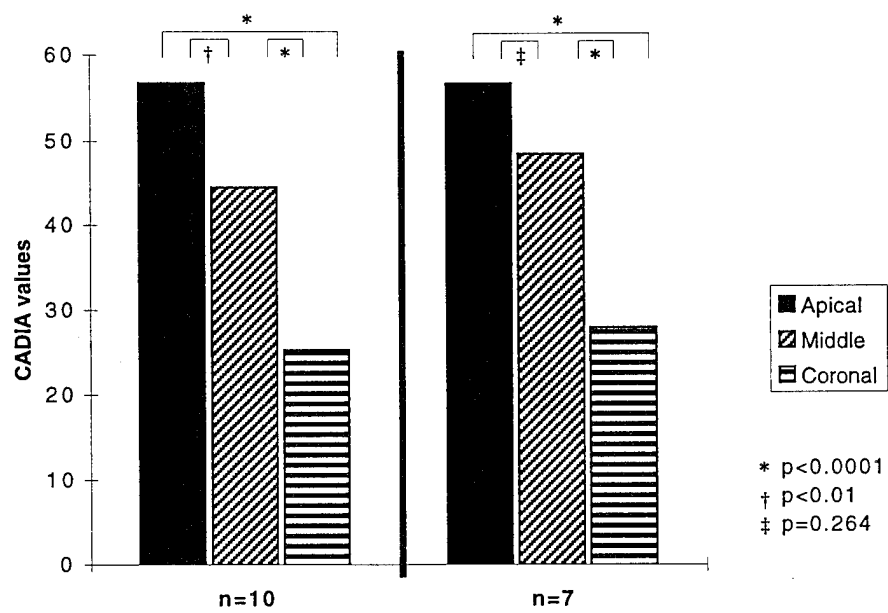
Figure 5.   Mean CADIA Values for Implant Surface for n=10 and n=7. The overall effect
of the Implant Surface was Not Significant when Analyzed by ANOVA for
n=10, but was Significant when Analyzed for n=7.
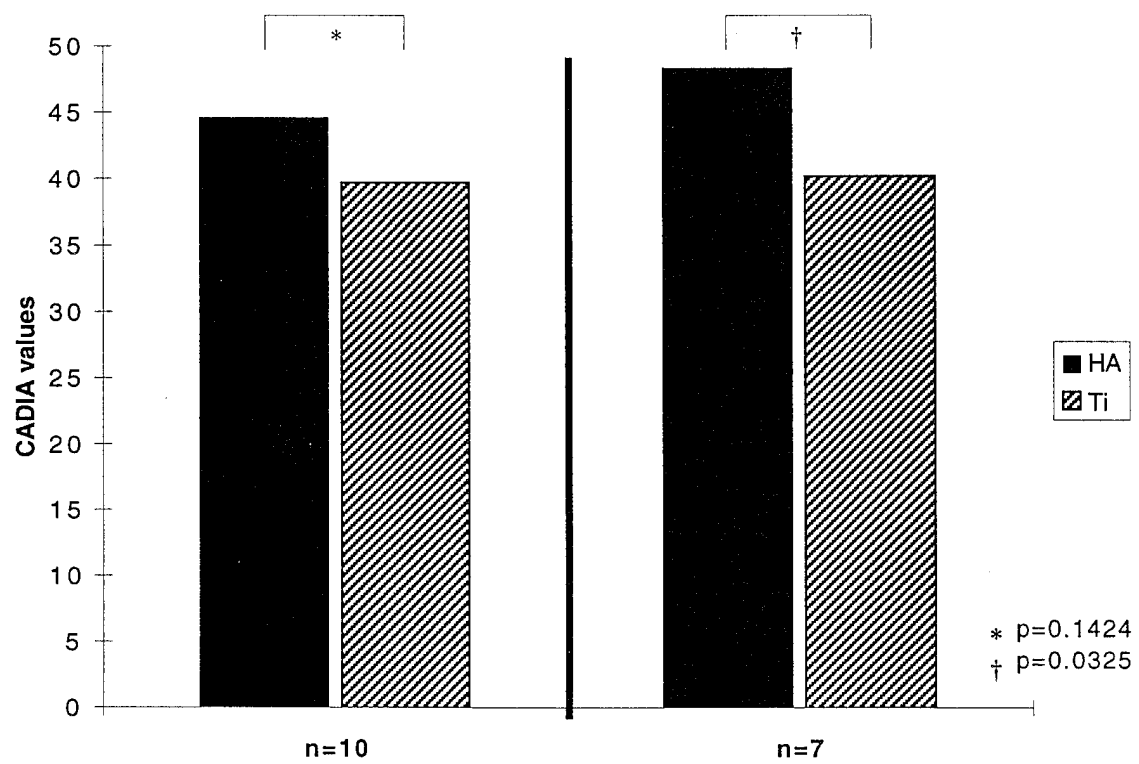
density gain followed by e-PTFE alone, with controls sites having the least density increase. (Table 9, Figure 3) Likewise, bone density gain was greatest in the most apical AOI followed by the middle AOI, with the least density seen in the coronal AOI. (Table 9, Figure 4) In contrast to the analysis including all 10 animals, when the 3 dogs with membrane complications were eliminated from the data set, there was significantly greater bone density increase adjacent to HA-coated implants than was seen adjacent to Ti implants (p=0.0325). (Table 9, Figure 5) When potential interactions between treatments, AOI position, and implant type were analyzed by ANOVA, no statistically significant interactions were detected. (Table 8)

2. Analysis by region

Dividing the defect into coronal, middle, and apical regions revealed a trend in CADIA values regarding the regions and implant type. (Table 10) Differences between e-PTFE alone and control sites for n=10 animals were smaller in the apical AOI (51.5 versus 42.3) than similar differences in middle (44.7 versus 19.5) and coronal (27.5 versus 3.7) AOIs. A similar trend was noted for analysis of n=7 animals. Data in Table 10 also reveal that the smallest difference in radiographic density gain between treatment groups were noted when comparing e-PTFE alone and control in the apical AOI (51.5 versus 42.3) in the analysis for all 10 animals. Additionally, there was a trend for a greater increase in density with HA-coated implants compared to Ti across all treatment groups within apical and middle AOIs. In coronal AOIs, the difference in density gain between implant types were generally small. (Table 10)

D. Tetracycline Labeling

Tetracycline labeling was very adequate with both methods used. The oral preparation given over 3 days appeared to have a slightly wider band of label than the single IM preparation. This labeling indicated the areas of mineralization at 7 days post implant

Table 10

AVERAGE CADIA VALUE FOR EACH AOI BY TREATMENT AND IMPLANT TYPE
(± S.E.)

Treatment (Implant type)	AOI for n = 10 dogs			AOI for n = 7 dogs		
	Coronal	Middle	Apical	Coronal	Middle	Apical
DFDBA/e-PTFE	45.1 ± 8.9	69.3 ± 7.8	76.6 ± 6.9	48.4 ± 9.8	69.6 ± 9.6	75.1 ± 8.1
DFDBA/e-PTFE (Ti)	45.1 ± 10.3	60.9 ± 9.9	70.8 ± 7.8	48.9 ± 12.1	63.2 ± 11.4	71.1 ± 9.0
DFDBA/e-PTFE (HA)	45.0 ± 7.4	77.7 ± 5.6	82.3 ± 5.9	47.8 ± 7.5	75.9 ± 7.7	79.1 ± 7.2
e-PTFE alone	27.5 ± 8.9	44.7 ± 10.9	51.5 ± 9.4	32.0 ± 11.3	51.7 ± 12.1	54.9 ± 11.6
e-PTFE alone (Ti)	26.8 ± 7.6	43.8 ± 9.9	47.7 ± 8.4	26.7 ± 10.4	44.4 ± 12.3	43.9 ± 10.8
e-PTFE alone (HA)	28.1 ± 10.2	45.5 ± 11.8	55.3 ± 10.4	37.3 ± 12.1	59.0 ± 11.9	65.8 ± 12.3
Control	3.7 ± 1.2	19.5 ± 5.8	42.3 ± 7.7	3.3 ± 1.2	23.7 ± 7.5	39.8 ± 18.2
Control (Ti)	3.7 ± 1.3	18.9 ± 4.9	39.4 ± 8.1	3.5 ± 1.2	21.2 ± 6.6	38.4 ± 9.4
Control (HA)	2.7 ± 1.0	20.1 ± 6.6	45.1 ± 7.2	3.1 ± 1.2	26.2 ± 8.4	41.2 ± 8.8

placement and demonstrated the delineation of the surgically created defect. (Plate 11 A) At 7 days, around several of the HA-coated implants, labeling at the HA surface could be seen along with labeling inside of the vent holes. This indicates very early bone deposition in areas were there was no adjacent host bone. This same phenomenon was not seen at Ti implant surfaces or vent holes. (Plate 11 B) Focal areas of labeling were also noted around DFDBA crystals in the defect and around particles lying over the cover screw. (Plate 11 C) This represents bone deposition in areas not adjacent to the host bone.

The xylenol orange label was unsuccessful and no evidence of it was seen in any of the specimens. During the preparation of the xylenol orange solution 1.0 N HCl was used to buffer the solution from pH 11.0 to 7.2 and this may have destroyed the activity of the compound. A recent study by White et al.[142] used this label; however, the labeling technique was radically different, using 60 mg/kg with administration of a second dose on an 8-hour interval, compared to the single 20 mg/kg dose used for this study.[143]

E. Gross Description of Light Microscopy

For control implants, in the non-defect region, focal areas of osseointegration were seen; however, for the HA-coated implants there appeared to be considerably greater areas of osseointegration. In the defect region, the amount of defect regeneration was minimal for Ti implants and no osseointegration to the Ti surface was seen. For the HA-coated implants, there was more regeneration of the defect and some osseointegration at the implant surface. (Plates 12 A and B)

For e-PTFE alone sites, in the non-defect region, focal areas of osseointegration were seen. Again, a greater degree of osseointegration was noted for HA-coated implants. In the defect region, regeneration of the defect occurred generally to the level of the fixture table; however, there was no osseointegration to the Ti surface. For the HA-coated implants, there was regeneration to the level of the fixture table and there appeared to be considerable osseointegration to the HA surface. (Plates 13 A and B)

Plate 11.

A. Reflective Epifluorescence Demonstrating the Boundaries of the Surgically Created Defect Through Tetracycline Labeling (glows yellow). (Original Magnification 50x)

B. Reflective Epifluorescence Demonstrating Osteoinduction through Tetracycline Labeling at 7 Days Post-implant Placement in the Vent Area of an HA-coated Implant. This Area was Void of Host Bone at Implant Placement. (Original Magnification 100x)

C. Reflective Epifluorescence Demonstrating Osteoinduction Around DFDBA Particles through Tetracycline Labeling at 7 Days Post-implant Placement in the Defect Area. This Area was Void of Host Bone at Implant Placement. (Original Magnification 50x)

Plate 12.

A.   Control HA-coated Implant after 16 Weeks of Healing. Same Animal as Plate 12 B. (Magnification 13x)

B.   Control Ti Implant after 16 Weeks of Healing. Same Animal as Plate 12 A. (Magnification 13x)
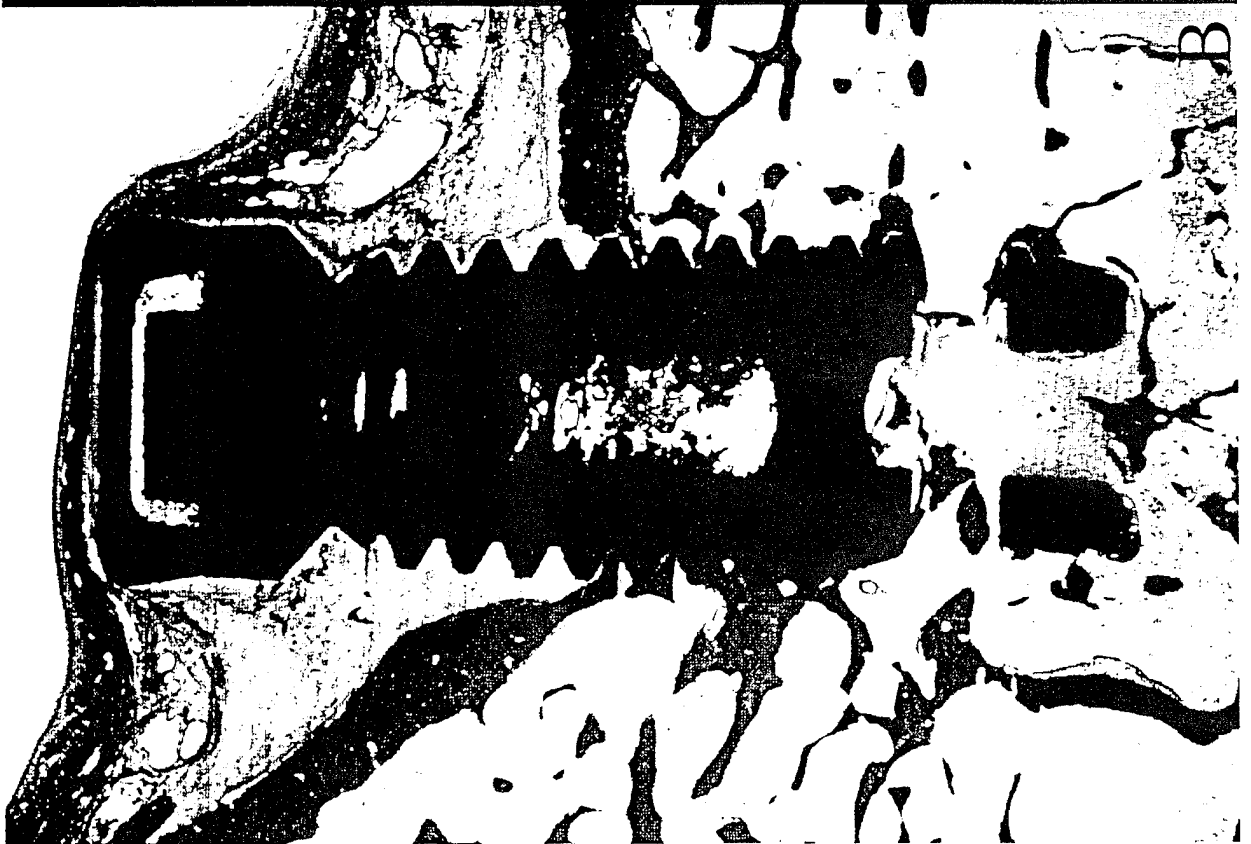
Plate 13.

A.   e-PTFE Alone Treated HA-coated Implant after 16 Weeks of Healing. Same
            Animal as Plate 13 B. (Magnification 13x)

B.   e-PTFE Alone Treated Ti Implant after 16 Weeks of Healing. Same Animal as
            Plate 13 A. (Magnification 13x)

Finally, for DFDBA/e-PTFE sites in the non-defect region, focal areas of osseointegration were noted for the Ti implant. This was similarly true for the HA-coated implant but to a greater degree. In the defect region, regeneration of the defect extended coronally beyond the level of the cover screw and in some cases new bone completely covered the implant; however, there was no osseointegration to the Ti surface in the defect region. For the HA-coated implants, there was similar regeneration above the level of the cover screw, but notably more osseointegration was apparent at the HA-coated surface from the apical extent of the defect to the collar of the implant. Residual DFDBA was seen in both specimens and was either incorporated into the regenerating trabeculae or existed free in the marrow spaces. (Plates 14 A and B, 15 A and B)

The defect adjacent to Ti implants often regenerated with bone; however, the bone did not fill into the threads of the implant and consistently appeared to stop short of the implant surface. (Plates 12 B, 13 B, 14 B, and 15 B)

F. Histomorphometric Analysis

Histomorphometry was performed for each of the implants. A repeated measures ANOVA, using JMP™ statistical program (SAS Institute, Cary, NC) on a Power Macintosh 9500 computer with 32 MB of RAM (Apple Computer Co., Cupertino, CA), utilizing the dog as the unit of analysis, was accomplished to evaluate the amount of osseointegration and trabeculation in non-defect and defect regions. Additionally, the amount of residual DFDBA remaining in DFDBA/e-PTFE sites was determined.

When all 10 dogs were analyzed in the non-defect region, statistically significant differences in percent osseointegration were found for each dog (p<0.0001) and implant type (p<0.0001). (Table 11) As expected in the non-defect region, no significant differences in osseointegration were seen relative to the treatments used (p=0.4654). HA-coated implants demonstrated significantly greater osseointegration than Ti (p<0.0001). (Tables 11 and 12, Figure 6) No significant interactions existed between treatments and implant type (p=0.7817).

Plate 14.

A.   DFDBA/e-PTFE Alone Treated HA-coated Implant after 16 Weeks of Healing. Same Animal as Plate 14 B. (Magnification 13x)

B.   DFDBA/e-PTFE Treated Ti Implant after 16 Weeks of Healing. Same Animal as Plate 14 A. (Magnification 13x)

94
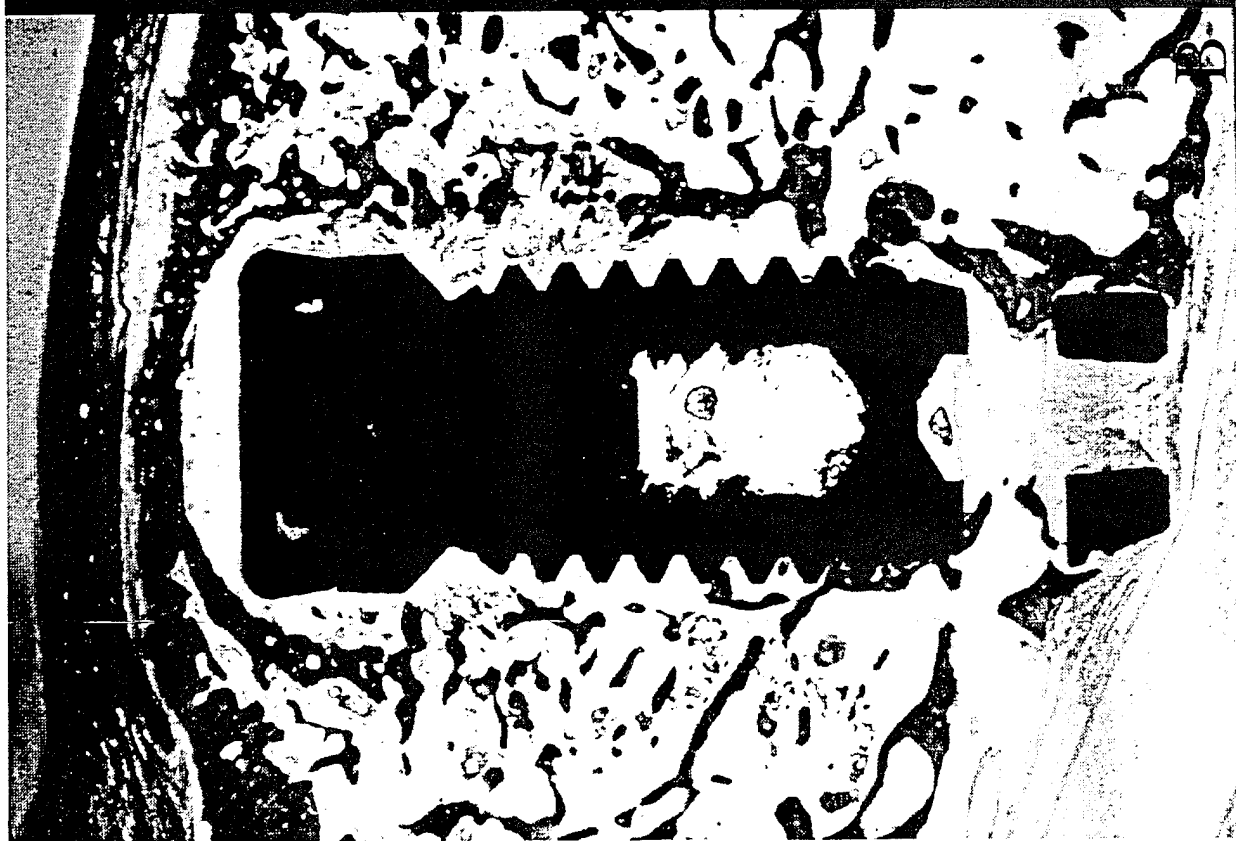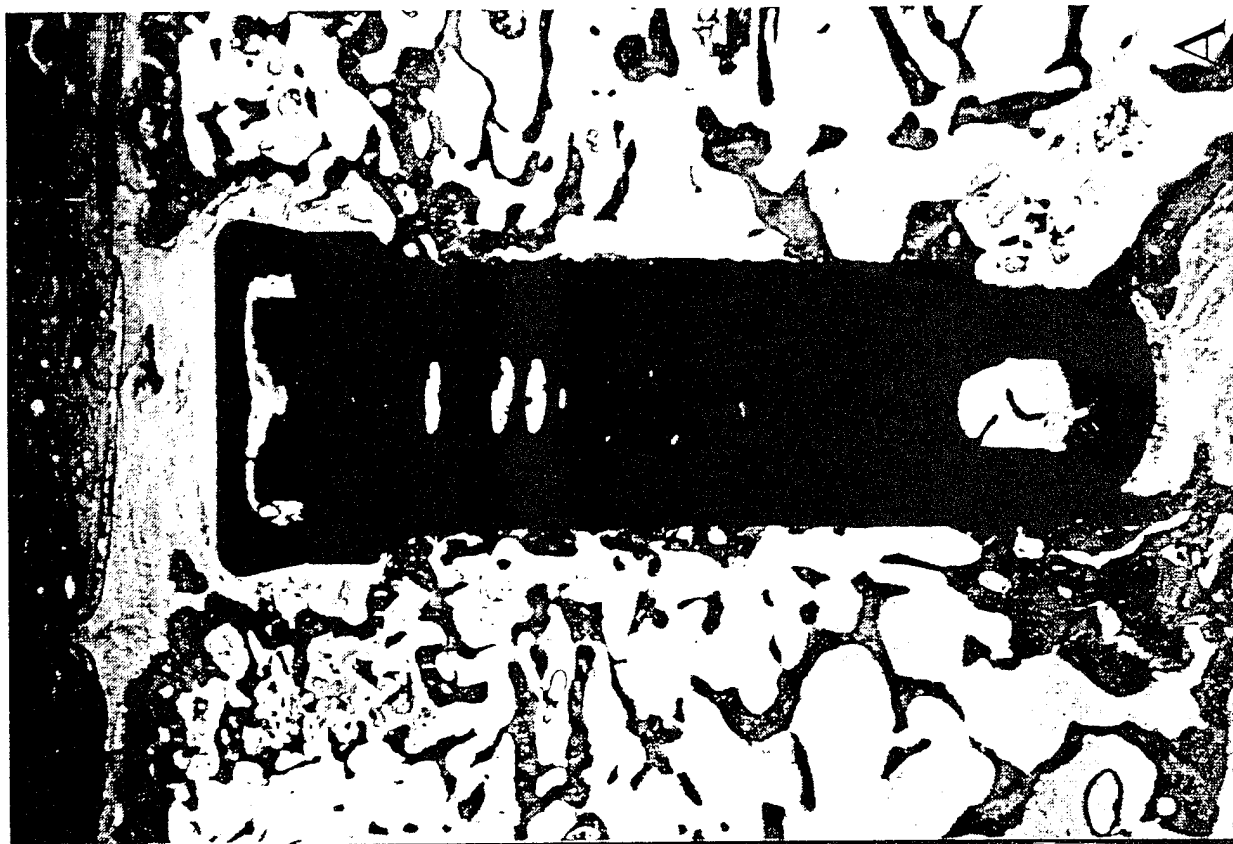
Plate 15.

A.   DFDBA/e-PTFE Treated HA-coated Implant after 16 Weeks of Healing.
           Specimens are from an Animal Examined Clinically Prior to Sacrifice. Same
           Animal as Plate 15 B. (Magnification 13x)

B.   DFDBA/e-PTFE Treated Ti Implant after 16 Weeks of Healing. Specimens are
           from an Animal Examined Clinically Prior to Sacrifice. Same Animal as Plate
           15 A. (Magnification 13x)

Table 11

ANOVA SUMMARY FOR HISTOLOGIC PORTION OF STUDY REGARDING PERCENT OSSEOINTEGRATION FOR N=10 AND N=7 ANIMALS

| | N = 10* | | | | N = 7† | | | |
| | Defect | | Non-defect | | Defect | | Non-defect | |
	F-value	p-value	F-value	p-value	F-value	p-value	F-value	p-value
Treatments	20.1979	0.0001	0.7780	0.4654	9.2309	0.0001	0.5329	0.5923
Implant type	453.1331	0.0001	158.8489	0.0001	413.251	0.0001	96.2085	0.0001
Dogs	6.1454	0.0001	5.2831	0.0001	6.4020	0.0001	3.0544	0.0188
AOI Position	31.8717	0.0001	-	-	26.3091	0.0001	-	-
Interactions								
Treatment*Implant type	20.4733	0.0001	0.2476	0.7817	9.3109	0.0001	0.0223	0.9780
Treatment*AOI Position	1.2667	0.2855	-	-	1.6229	0.1742	-	-
Implant Type*AOI Position	27.1795	0.0001	-	-	22.4467	0.0001	-	-
Implant Type*AOI Position*Treatments	0.9284	0.4491	-	-	1.3850	0.2444	-	-

* Complete data set
† 3 dogs eliminated from data set due to membrane complications

Table 12

MEAN PERCENT OSSEOINTEGRATION FOR EACH TREATMENT, POSITION AND IMPLANT TYPE FOR N=10 AND N=7 ANIMALS (± S.E.)

	N = 10*		N = 7†	
	Defect	Non-defect	Defect	Non-defect
Treatment				
DFDBA/e-PTFE	32.0 ± 2.1	37.5 ± 5.0	32.3 ± 2.7	35.6 ± 5.7
HA	63.7 ± 4.0	59.2 ± 6.6	64.2 ± 5.0	55.9 ± 8.0
Ti	0.3 ± 0.2	16.1 ± 3.4	0.4 ± 0.3	15.3 ± 3.3
e-PTFE alone	21.6 ± 3.1	37.8 ± 5.7	24.6 ± 3.7	36.6 ± 5.8
HA	42.0 ± 5.5	56.6 ± 6.0	48.0 ± 6.4	56.7 ± 7.3
Ti	1.2 ± 0.7	19.0 ± 5.3	1.2 ± 0.9	16.4 ± 4.3
Control	15.8 ± 2.9	42.0 ± 4.4	19.6 ± 3.5	40.6 ± 5.7
HA	31.3 ± 5.5	62.0 ± 3.9	38.8 ± 6.7	61.7 ± 5.4
Ti	0.2 ± 0.2	21.9 ± 4.9	0.3 ± 0.3	19.4 ± 5.9
AOI Position				
Apical	32.6 ± 2.6	-	35.1 ± 2.6	-
HA	63.4 ± 4.4	-	68.4 ± 4.3	-
Ti	1.8 ± 0.7	-	1.9 ± 0.9	-
Middle	24.7 ± 2.7	-	27.6 ± 3.1	-
HA	49.4 ± 5.3	-	55.1 ± 6.1	-
Ti	0.0 ± 0.0	-	0.0 ± 0.0	-
Coronal	12.1 ± 2.3	-	13.8 ± 2.7	-
HA	24.2 ± 4.5	-	27.5 ± 5.4	-
Ti	0.0 ± 0.0	-	0.0 ± 0.0	-
Implant Type				
HA	45.6 ± 5.0	59.3 ± 5.5	50.3± 6.0	58.1± 6.9
Ti	0.6 ± 0.4	19.0 ± 4.5	0.7 ± 0.6	17.1 ± 4.5

* Complete data set
† 3 dogs eliminated from data set due to membrane complications

Figure 6.   Mean Percent Osseointegration by Implant Type (Ti and HA-coated) for Defect and Non-defect Regions for n=10 and n=7 Animals.
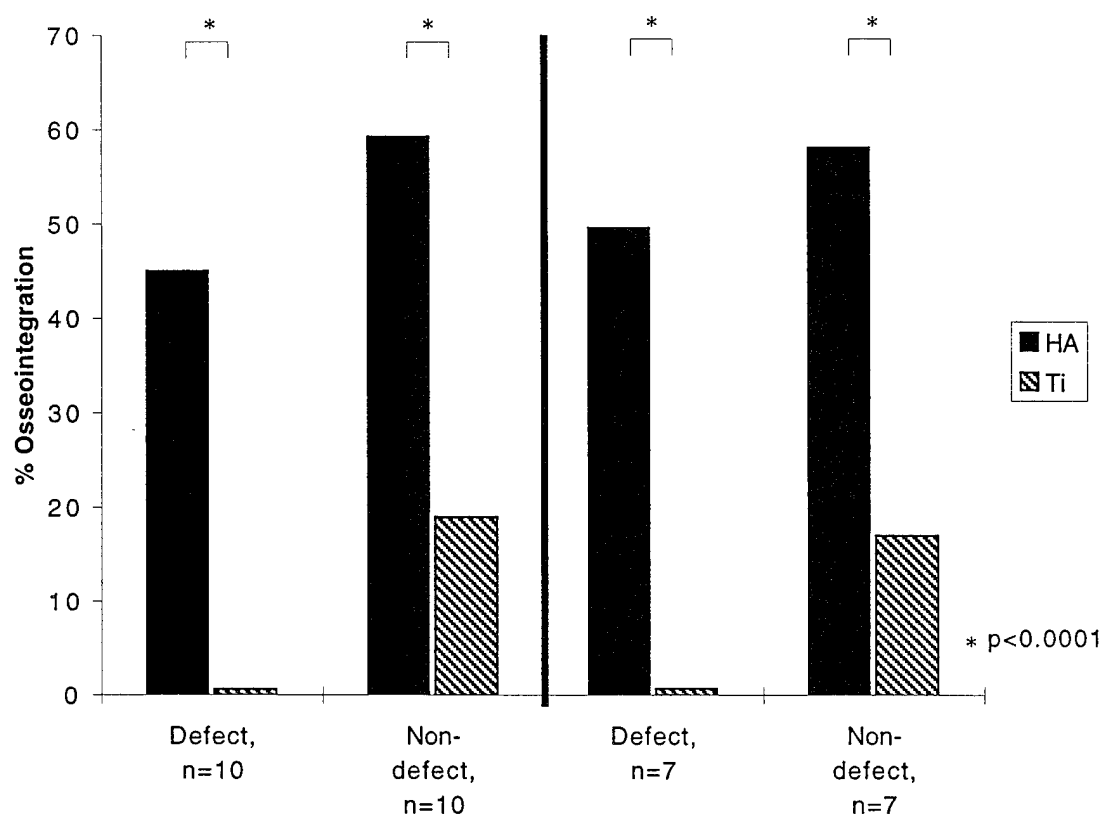
(Table 11) Regarding trabeculation in the non-defect region, statistically significant differences were seen relative to the overall mean non-defect trabeculation for each dog (p<0.0001). No significant differences in trabeculation were seen relative to the treatments used (p=0.0776) or implant type (p=0.2126). (Table 13, Figures 7 and 8) No significant interactions existed between treatments and implant type (p=0.9752). (Table 13)

When all 10 dogs were analyzed for osseointegration within the defect region, statistically significant differences were seen relative to the treatments used (p<0.0001), implant type (p<0.0001), the overall mean osseointegration for each dog (p<0.0001), and AOI position (p<0.0001). (Table 11) DFDBA/e-PTFE sites demonstrated the greatest degree of osseointegration followed by e-PTFE alone, with control sites having the least osseointegration. (Table 12) Since Ti implants had minimal osseointegration, contrasts were constructed within this significant treatment effect for HA-coated implants only. Significantly greater osseointegration in the defect area around HA-coated implants was noted for DFDBA/e-PTFE (63.7%) compared to e-PTFE alone (42.0%) (p<0.0001) or to controls (31.3%) (p<0.0001). No significant difference was noted in percent osseointegration in the defect around HA-coated implants when e-PTFE alone (42.0%) was compared to control (31.3%) (p=0.0912). (Table 12, Figure 9) HA-coated implants demonstrated significantly greater osseointegration within the defect than Ti (p<0.0001). (Table 12, Figure 6) Significant differences existed between AOI positions, with apical regions demonstrating the greatest degree of osseointegration followed by the middle region, and the coronal region having the least osseointegration. (Table 12) Since Ti implants had minimal osseointegration, contrasts were only constructed within this significant effect for HA-coated implants, comparing percent osseointegration in apical, middle, and coronal AOIs. The percent osseointegration in the apical (63.4%) AOI was significantly greater than either the middle (49.4%) (p<0.001) or coronal (24.2%) AOI (p<0.0001). Significantly greater osseointegration was seen in middle (49.4%) AOI compared to coronal (24.2%) AOI (p<0.0001). (Table 12, Figure 10)
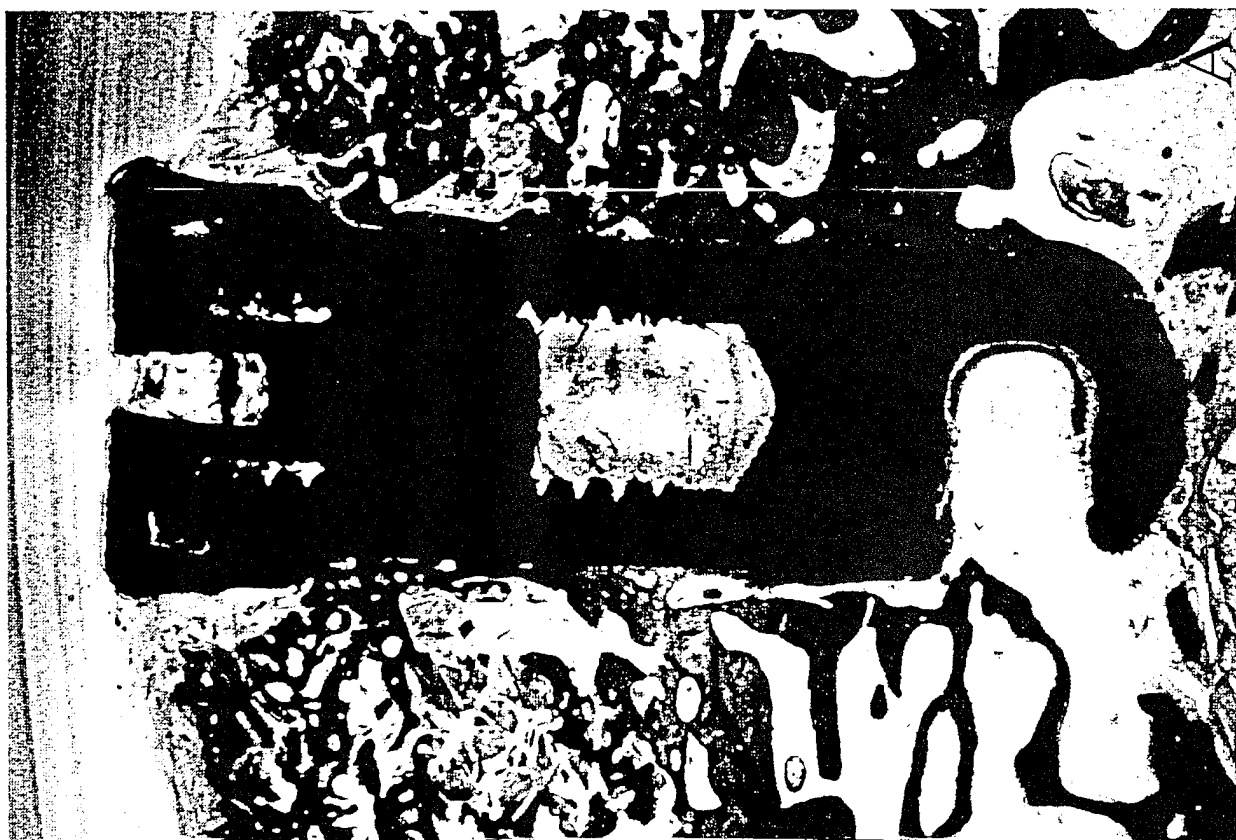
Table 13

ANOVA SUMMARY FOR HISTOLOGIC PORTION OF STUDY REGARDING PERCENT TRABECULATION FOR N=10 AND N=7 ANIMALS

| | N = 10* | | | | N = 7† | | | |
| | Defect | | Non-defect | | Defect | | Non-defect | |
	F-value	p-value	F-value	p-value	F-value	p-value	F-value	p-value
Treatments	2.0935	0.1351	2.7076	0.0776	0.1810	0.8354	3.3240	0.0501
Implant type	20.7039	0.0001	1.5983	0.2126	24.8501	0.0001	0.5649	0.4581
Dogs	2.7919	0.0109	4.4424	0.0001	3.5079	0.0095	1.2626	0.3039
Interactions								
Treatment*Implant type	1.5415	0.2252	0.0251	0.9752	0.5248	0.5970	0.0515	0.9499

* Complete data set
† 3 dogs eliminated from data set due to membrane complications

Figure 7.   Mean Percent Trabeculation by Treatment (DFDBA/e-PTFE, e-PTFE alone, and Control) for Defect and Non-defect Regions for n=10 and n=7 Animals.
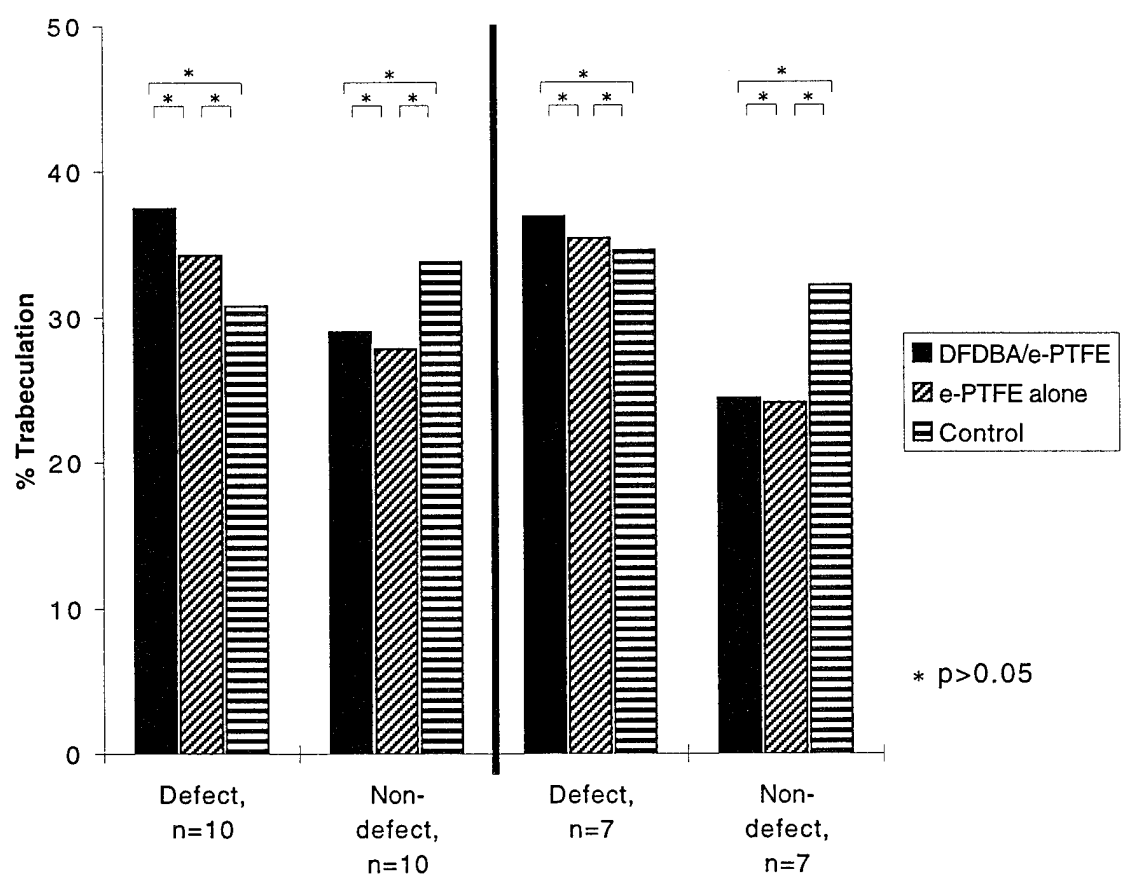
Figure 8.   Mean Percent Trabeculation by Implant Type (Ti and HA-coated) for Defect and
              Non-defect Regions for n=10 and n=7 Animals.
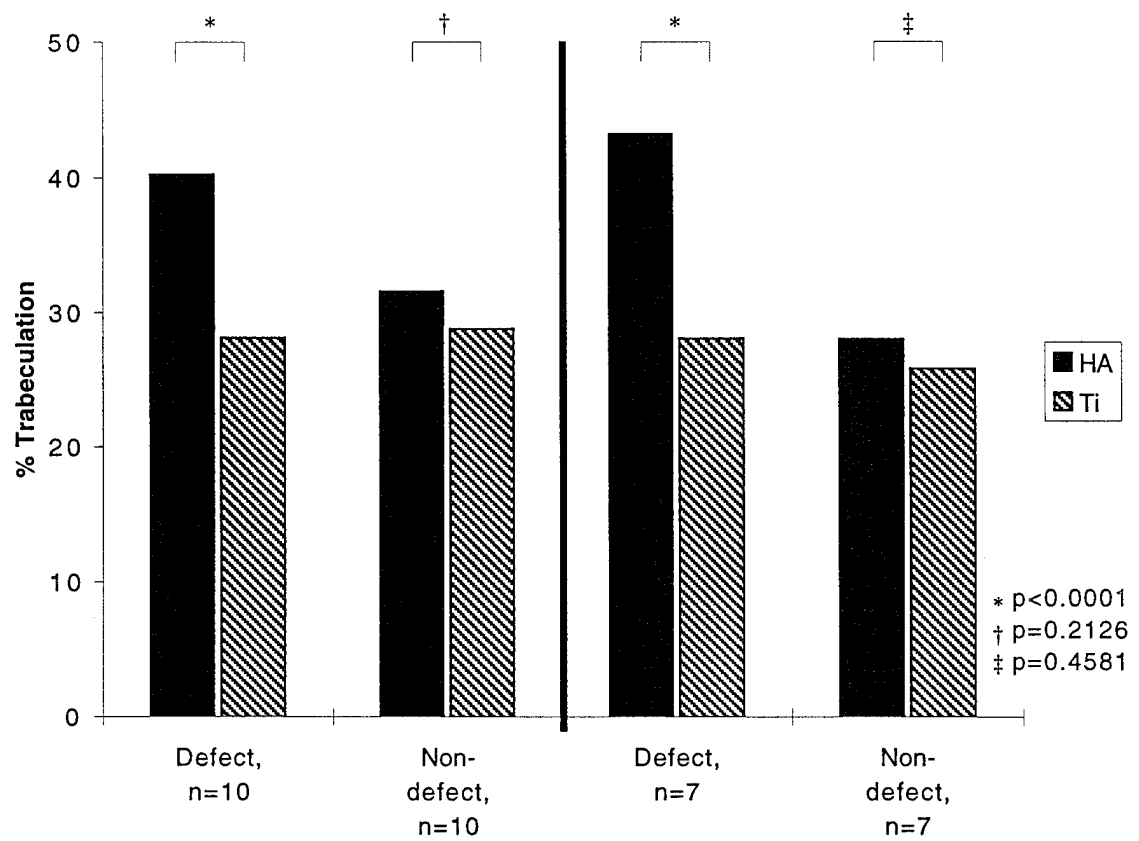
Figure 9.   Mean Percent Osseointegration by Treatment and Implant Type (DFDBA/e-
             PTFE/HA, DFDBA/e-PTFE/Ti, e-PTFE alone/HA, e-PTFE alone/Ti,
             Control/HA and Control/Ti) for Defect and Non-defect Regions for n=10 and
             n=7 Animals.
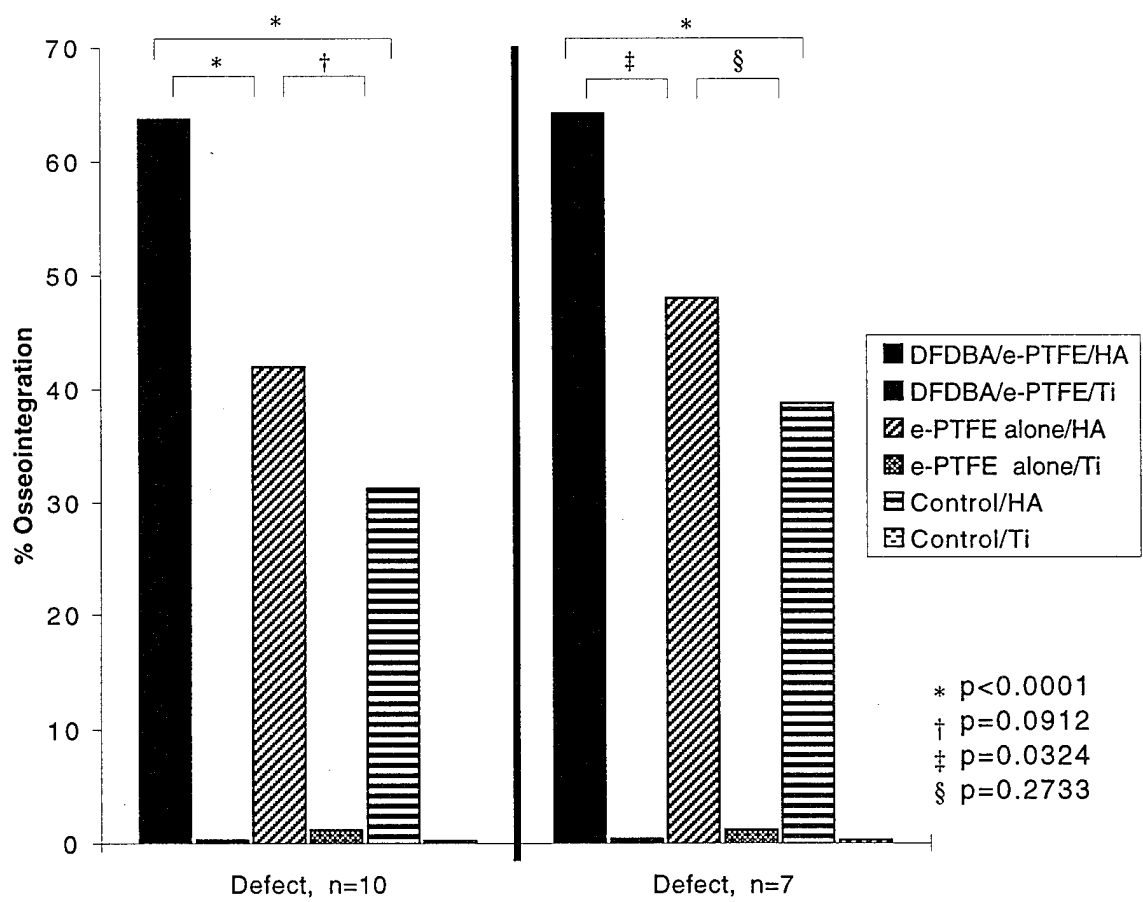
Figure 10.   Mean Percent Osseointegration by AOI Region and Implant Type (Apical/HA, Apical/Ti, Middle/HA, Middle/Ti, Coronal/HA and Coronal/Ti) for Defect and Non-defect Regions for n=10 and n=7 Animals.
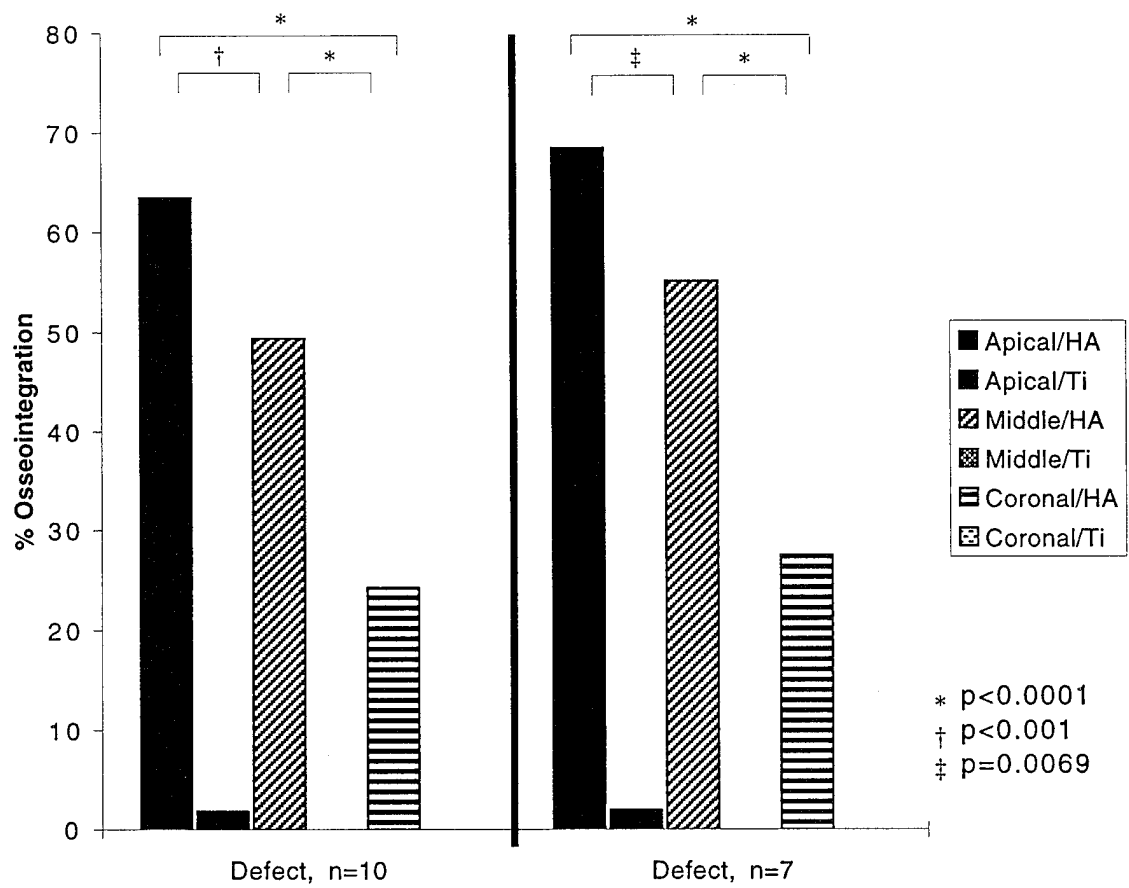
Significant interactions existed between treatments and implant type (p<0.0001) and implant type and AOI position (p<0.0001). (Table 11)

A trend was noted in the analysis for 10 dogs when osseointegration was examined by AOI and treatment. (Table 14) All DFDBA/e-PTFE sites demonstrated greater osseointegration than e-PTFE alone and control sites. Likewise, apical AOIs had greater osseointegration than coronal and middle AOIs in all treatment groups. (Table 14)

Additionally, for the defect region, statistically significant differences in trabeculation were seen relative to the overall mean defect trabeculation for each dog (p=0.0109) and implant type (p<0.0001). No significant differences in trabeculation were seen relative to the treatments used (p=0.1351). (Table 13, Figure 7) HA-coated implants demonstrated significantly greater trabeculation within the healed defect than Ti (p<0.0001). (Tables 13 and 15, Figure 8) No significant interactions existed between treatments and implant type (p=0.2252). (Table 13)

Finally, for the defect region, when all 10 dogs were analyzed in the defect area for residual DFDBA particles, Ti implants demonstrated significantly greater residual DFDBA than HA-coated implants (p=0.0355); however, differences between dogs were not significant (p=0.0578). (Tables 16 and 17, Figure 11)

Three out of 40 implant sites with membranes had exposure of the membrane during the healing period which may have introduced a confounding variable. In order to alleviate any influence of adverse healing at membrane exposure sites on the final results, the data were reanalyzed using only the 7 animals without soft tissue complications at the test sites involving membranes. The results were identical to the analysis performed on all 10 dogs except for overall mean trabeculation for dogs in the non-defect region which demonstrated no significant difference (p=0.3039 for n=7 versus p<0.0001 for n=10) (Table 13) and percent residual DFDBA which revealed no significant difference (p=0.1027 for n=7 versus p=0.0355 for n=10) between Ti and HA-coated implants with 7 dogs. (Table 16)

When 7 dogs were analyzed for the percent osseointegration in the non-defect region, statistically significant differences were found for each dog (p=0.0188) and implant type

Table 14

AVERAGE PERCENT OSSEOINTEGRATION VALUE FOR EACH AOI BY TREATMENT

($\pm$ S.E.)

Treatment	AOI for n = 10 dogs			AOI for n = 7 dogs		
	Coronal	Middle	Apical	Coronal	Middle	Apical
DFDBA/e-PTFE	24.0 $\pm$	32.5 $\pm$	36.9 $\pm$	24.8 $\pm$	36.1 $\pm$	36.1 $\pm$
e-PTFE alone	8.6 $\pm$	22.1 $\pm$	34.3 $\pm$	11.5 $\pm$	24.7 $\pm$	37.5 $\pm$
Control	3.8 $\pm$	16.9 $\pm$	26.7 $\pm$	5.0 $\pm$	21.9 $\pm$	31.9 $\pm$

Table 15

MEAN PERCENT TRABECULATION FOR EACH TREATMENT, POSITION, AND IMPLANT TYPE FOR N=10 AND N=7 ANIMALS (± S.E.)

	N = 10*		N = 7†	
	Defect	Non-defect	Defect	Non-defect
Treatment				
DFDBA/e-PTFE	37.5 ± 3.1	29.0 ± 3.0	36.9 ± 3.5	24.4 ± 2.0
HA	46.1 ± 3.8	30.5 ± 3.6	46.6 ± 4.4	25.6 ± 3.1
Ti	28.9 ± 2.4	27.4 ± 2.4	27.1 ± 2.5	23.3 ± 0.9
e-PTFE alone	34.3 ± 3.7	27.8 ± 3.0	35.4 ± 3.9	24.1 ± 3.1
HA	37.2 ± 4.0	29.4 ± 3.8	41.4 ± 3.2	24.6 ± 3.9
Ti	31.3 ± 3.3	26.2 ± 2.1	29.4 ± 4.6	23.6 ± 2.2
Control	30.8 ± 4.3	33.8 ± 4.0	34.6 ± 5.5	32.2 ± 4.8
HA	37.5 ± 4.1	34.8 ± 4.4	41.7 ± 5.0	33.9 ± 6.1
Ti	24.1 ± 4.5	32.7 ± 3.5	27.6 ± 6.0	30.6 ± 3.5
Implant Type				
HA	40.3 ± 4.0	31.6 ± 4.0	43.2 ± 4.2	28.0 ± 4.4
Ti	28.1 ± 3.4	28.8 ± 2.7	28.0 ± 4.3	25.8 ± 2.2

* Complete data set
† 3 dogs eliminated from data set due to membrane complications

Table 16.

MEAN PERCENT RESIDUAL DFDBA IN DEFECT AREA

	N = 10[*]		N = 7[†]	
	F-value	p-value	F-value	p-value
Implant type	6.1070	0.0355	3.9757	0.1027
Dogs	3.0163	0.0578	2.7160	0.1484

* Complete data set
† 3 dogs eliminated from data set due to membrane complications

Table 17

MEAN PERCENT RESIDUAL DFDBA BY IMPLANT TYPE IN DEFECT AREA (± S.E.)

Implant type	Percent Residual DFDBA	
	n=10[*]	n=7[†]
HA	4.1 ± 0.9	3.0 ± 1.0
Ti	8.2 ± 2.1	7.7 ± 3.0

* Complete data set
† 3 dogs eliminated from data set due to membrane complications

Figure 11.   Percent Residual DFDBA by Implant Type (Ti and HA-coated) for Defect and Non-defect Regions for n=10 and n=7 Animals.
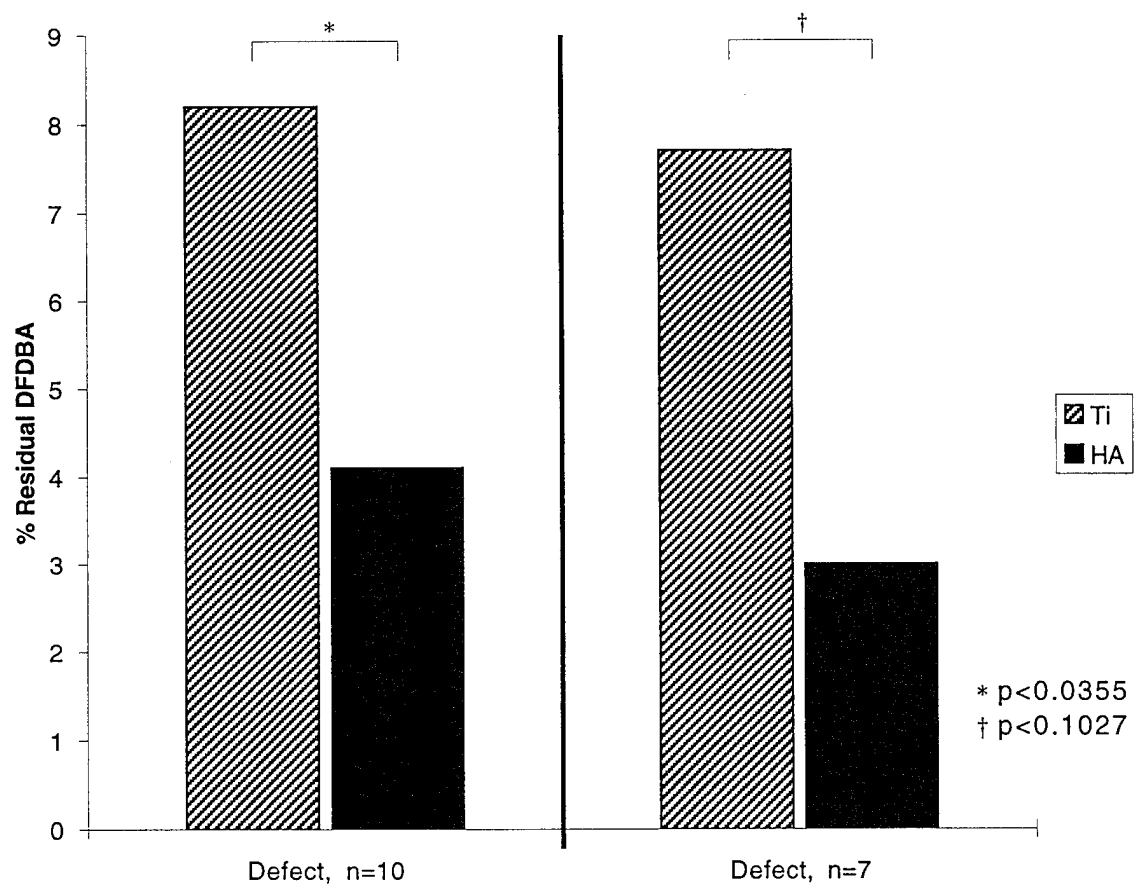
(p<0.0001). (Table 11) As expected in the non-defect region, no significant differences in osseointegration were seen relative to the treatments used (p=0.5923). HA-coated implants demonstrated significantly greater osseointegration than Ti (p<0.0001). (Tables 11 and 12, Figure 6) No significant interactions existed between treatments and implant type (p=0.9780). (Table 11) Regarding trabeculation in the non-defect region, no significant differences in trabeculation were seen relative to treatments (p=0.0501), implant type (p=0.4581) or dogs (p=0.3039). (Tables 13 and 15, Figures 7 and 8) No significant interactions existed between treatments and implant type (p=0.9499). (Table 13)

When 7 dogs were analyzed for osseointegration in the defect region, statistically significant differences in osseointegration were seen relative to the treatments used (p<0.0001), implant type (p<0.0001), the overall mean osseointegration for each dog (p<0.0001), and AOI position (p<0.0001). (Table 11) DFDBA/e-PTFE sites demonstrated the greatest degree of osseointegration followed by e-PTFE alone, with control sites having the least osseointegration. (Table 12) Since Ti implants had minimal osseointegration, contrasts were constructed within this significant treatment effect for HA-coated implants only. Significantly greater osseointegration in the defect area around HA-coated implants was noted for DFDBA/e-PTFE (64.2%) compared to e-PTFE alone (48.0%) (p≤0.0324) or to controls (38.8%) (p<0.0001). No significant difference was noted in percent osseointegration in the defect around HA-coated implants when e-PTFE alone (48.0%) was compared to control (38.8%) (p=0.2733). (Table 12, Figure 9) HA-coated implants demonstrated significantly greater osseointegration within the defect than Ti (p<0.0001). (Tables 11 and 12, Figure 6) Significant differences existed between AOI positions, with apical regions demonstrating the greatest degree of osseointegration followed by the middle region, and the coronal region having the least osseointegration. (Table 12) Since Ti implants had minimal osseointegration, contrasts were only constructed within this significant effect for HA-coated implants, comparing percent osseointegration in apical, middle, and coronal AOIs. The percent osseointegration in the apical (68.4%) AOI was significantly greater than either the middle

(55.1%) (p≤0.0069) or coronal (27.5%) AOI (p<0.0001). Significantly greater osseointegration was seen in middle (55.1%) AOI compared to coronal (27.5%) AOI (p<0.0001). (Table 12, Figure 10) Significant interactions existed between treatments and implant type (p<0.0001) and implant type and AOI position (p<0.0001). (Table 11)

A trend was noted in the analysis for 7 dogs when osseointegration was examined by AOI and treatment. (Table 14) All DFDBA/e-PTFE sites demonstrated greater osseointegration than e-PTFE alone and control sites (except in the apical region compared to e-PTFE alone sites- 36.1 versus 37.5%). Likewise, apical AOIs had greater osseointegration than coronal and middle AOIs in the e-PTFE alone and the control groups. In the DFDBA/e-PTFE group, osseointegration in apical and middle AOIs was identical (36.1%). (Table 14)

Additionally, for the defect region, statistically significant differences in trabeculation were seen relative to the overall mean defect trabeculation for each dog (p=0.0095) and implant type (p<0.0001). No significant differences in trabeculation were seen relative to the treatments used (p=0.8354). (Table 13, Figure 7) HA-coated implants demonstrated significantly greater defect trabeculation than Ti (p<0.0001). (Tables 13 and 15, Figure 8) No significant interactions existed between treatments and implant type (p=0.5970). (Table 13)

Finally, for the defect region, when 7 dogs were analyzed for residual DFDBA particles, there was no difference in residual DFDBA between HA-coated and Ti implants (p=0.1027). Differences between dogs were also not significant (p=0.1484). (Tables 16 and 17, Figure 11)

In examining histologic sections for this study, an interesting finding was the pattern of bone regeneration within the healing defect. Frequently, the newly regenerating bone grew from the mesial or distal wall of the defect toward the implant but did not enter the threads of the Ti implant, forming a wall or front of bone. Within each AOI, the shortest distance from the bone front in any direction to the implant was recorded in microns. Data were grouped in categories of 0 (defined as osseointegration at some point in the AOI), 1 to 200 μm, and greater than 200 μm. Mesial measurements were chosen by coin flip for examination. Thirty implants of each type (HA-coated or Ti) with 3 AOI regions per implant resulted in 90 areas for

consideration with each implant type. HA-coated implants demonstrated osseointegration at at least one point in 86.7% of all AOIs. The bone front was 1 to 200 μm away from the HA-coated implant 5.5% of AOIs. In only 7.8% of all AOIs was the bone front at a distance greater than 200 μm from HA-surface. Conversely, Ti implants demonstrated at least one point of osseointegration in only 12.2% of all AOIs, while the advancing bone front was 1 to 200 μm away from the Ti surface in 38.9% of AOIs. In 48.9% of all AOIs, the bone front was greater than 200 μm from the Ti implant surface. (Table 18)

Table 18

COMPARISON BETWEEN HA-COATED AND Ti IMPLANTS REGARDING THE
DISTANCE FROM THE ADVANCING BONE FRONT TO THE IMPLANT SURFACE

	% of Bone Distance from Implant by Type	
Distance (μm)	HA	Ti
0	86.7	12.2
1-200	5.5	39.9
> 200	7.8	48.9

V. __DISCUSSION__

The results of this study demonstrate that the combination of DFDBA and e-PTFE barrier membranes in treating surgically created defects adjacent to dental implants promotes a denser healing of bone when measured radiographically than either e-PTFE membranes alone or no regenerative treatment. While radiographic data are not the only indicator for clinical success in implant dentistry, radiographs provide a non-invasive tool for assessment of implant success prior to abutment connection and are also useful for long-term evaluation.

In an evidence-based review of the literature relative to GBR, Mellonig and Nevins[144] determined that barrier membranes alone and DFDBA plus membranes produce similar positive clinical results when implants are placed into extraction sockets and are surrounded by a spacemaking defect, a situation similar to the design of this study. While the evidence-based review determined relative clinical equivalence between DFDBA/membrane and membrane alone, the radiographic portion of this study provides evidence supporting use of DFDBA to increase peri-implant bone density during healing. The histologic results of this study verify the radiographic assumption that the combination of DFDBA and e-PTFE barrier membranes in treating surgically created defects adjacent to dental implants promotes a greater healing through increased osseointegration when measured histologically than either e-PTFE membranes alone or no treatment. Furthermore, the type of implant surface selected in this model is critical in obtaining osseointegration in the defect region.

This study was designed to create a large defect adjacent to the dental implant in order to simulate those defects often seen following placement of implants into recent extraction sites or other anatomically challenging areas. As seen in humans, variability in ridge anatomy was found in the animal model used for this study. In some animals, the peri-implant defect was surrounded in its entirety by bony walls. In other animals, facial and lingual bony dehiscences were produced during defect creation. While this variability in ridge anatomy precluded complete standardization

114

of all defects, randomization of treatments and implant types allowed evaluation of the effects of each therapeutic modality in both dehiscence and non-dehiscence defects. Since mesiodistal sections were planned for the histologic analysis, presence or absence of facial or lingual bony dehiscences may be of little consequence. Furthermore, the mesial and distal aspects of each peri-implant defect were standardized, and both mesial and distal bony walls were always present. Other authors have studied surgically created facial defects; however, the results of treatment were not analyzed radiographically.[10,60,63] In this study, the effect of loss of facial or lingual bony walls on bone density during healing is unknown. During placement of implants into immediate extraction sites in humans, the peri-implant space may be entirely surrounded by bony walls or may have varying degrees of dehiscence or fenestration. In this regard, the surgically created defects produced in this study may mimic those defects frequently seen clinically in humans. Interestingly, a recent report in the literature evaluated facial dehiscences in 6 edentulous humans treated with and without e-PTFE membranes. Implants were allowed to integrate and then were removed with a trephine after 5 months of healing. Results showed 95 to 100% regeneration of the defect in 4 of the 6 cases treated with e-PTFE; however, differences in clinical and histologic measurements between membrane and non-membrane sites were not statistically significant.[54] In the current study there were significant differences between sites with and without e-PTFE membranes implying the use of barrier membranes at large defects sites is critical to maximizing the potential for regeneration.

In order to assess the effects of the two treatments (DFDBA/e-PTFE versus e-PTFE alone), the defects had to be of sufficient size to prevent complete spontaneous healing. Knox et al.[15] determined in dogs that any circumferential peri-implant defect larger than 0.5 mm healed with significantly more residual defect remaining than sites prepared conventionally. Peri-implant defects of 0.5, 1.0, and 2.0 mm widths resulted in significantly larger defects remaining and a more apical level of osseointegration than conventionally prepared implant sites. In the current study using peri-implant defects with 3.0 mm widths, the minimal radiographic changes and the minimal regeneration and osseointegration seen histologically at untreated control sites confirms

that the surgically created defects were large enough to prevent spontaneous healing to the implant fixture table. (Plate 6B)

Standardized radiographs were taken 1 week post-surgery with the membranes and DFDBA in place. Since membranes were in place for both the baseline and follow-up radiographs, any effect of the membrane would have been controlled in calculation of the CADIA value. The DFDBA was likewise present in the defect at the time of both the initial and follow-up radiographs. Any radiographic change at DFDBA sites would therefore be related to an increase in density during the healing period.

The question exists as to whether DFDBA has an inherent density that would be detectable on radiographs. If so, the density of DFDBA itself may create artificial differences between DFDBA/e-PTFE sites and either e-PTFE alone or control sites. Guillemin et al.[145] reported that DFDBA placed in a 6 mm deep cylindrical defect oriented buccolingually in a dry mandible produced a CADIA value of only 6.8 (S.D. = 1.4). Further measurements of the defect with and without an e-PTFE membrane produced a change in CADIA value of 0.67 (S.D. = 0.9), implying the membrane had little effect on density. Therefore, the presence of DFDBA and e-PTFE may have a slight influence on the CADIA values if baseline films are taken prior to DFDBA and membrane placement and are then compared with subsequent films taken after material placement. Baseline radiographs in the current study were made after placement of the material, negating any concern for the inherent density of materials used for these guided bone regeneration procedures.

Subtraction radiography techniques may be useful in determining the ultimate success or failure of implant integration and maintenance by providing a noninvasive method of demonstrating changes in density adjacent to implants after placement or loading.[146] Radiographic bone density is a valuable endpoint determinant in implant therapy which, with the advent and refinement of CADIA techniques, is readily quantifiable. Subtraction radiography has been used to demonstrate evidence of peri-implant bone loss in humans which was not apparent by conventional radiographic observation.[147] However, subtraction radiography provides only a subjective visual image of bone density loss without quantitation. In this study, the relative changes apparent in

defect healing were quantified using CADIA in addition to visual interpretation of radiographic changes. Since two different implant types with differing surface morphology were evaluated, it was deemed impractical to measure density changes in a standardized area at the immediate implant surface. In addition, placing the AOIs too close to the implant may have introduced error due to the radiographic brightness of the implant or projection problems with the sharp angles of the Ti screw or with the undulating surfaces of the HA coating. Using standardized AOIs for both implant types allowed for direct comparison of the effect of the different implant surfaces on bone density within the healing defect. However, the radiographic method used did not permit determination of bone density changes in the 0.2 mm region immediately juxtaposed to the implant surface. The possible effect of the implant surface material or texture on the healing of bone directly adjacent to the implant is not revealed by this technique.

Clinical evaluation revealed that, over the 4 month healing period, the ridge anatomy changed as the control implants and the e-PTFE alone sites appeared to lose ridge height and width. Ridge width at DFDBA/e-PTFE sites increased compared to the original anatomy. Becker *et al.*[59] also determined that the use of e-PTFE membranes augments ridge width compared to non-membrane controls. Another clinical study in humans also demonstrated e-PTFE significantly increased bone formation around implants placed in immediate extraction sockets.[119] Caudill and Lancaster[148] found crestal bone apposition and greater defect fill with e-PTFE over HA-coated implants compared to defects with implants alone. In the current study, at sites with buccal or lingual defect dehiscences there was a tendency for the membrane to collapse toward the implant if DFDBA was not used. Use of DFDBA appeared to maintain the ridge width at these dehiscence sites. Prior to sacrifice, a perfectly raised outline of the membrane could frequently be seen clinically at DFDBA sites, indicating maintenance of or an increase in osseous bulk under the membrane. (Plate 10) Radiographically, clinically, and histologically, the use of e-PTFE with or without DFDBA maintained the radiographic, clinical, and histologic ridge height and prevented the bone from significantly resorbing at the defect/alveolar ridge junction, a phenomenon frequently encountered at control sites. (Plates 6 B and 12 - 15 A and B)

At the time of sacrifice, the 4 animals evaluated clinically appeared to have integrated implants, although there was significant thread or implant surface exposure at control sites. All implants were non-mobile and emitted the characteristic "ring" when percussed by an instrument. However, clinical and radiographic examination of Ti implants at DFDBA/e-PTFE sites was misleading. Visual radiographic assessment revealed only 40% of the Ti implants at DFDBA/e-PTFE sites had any indication of a peri-implant defect, while histologic evaluation found basically no osseointegration in the defect region for all Ti implants. This casts some doubt on the reliability of our current standards for clinical implant evaluation in sites with peri-implant defects at the time of placement. Sunden et al.[149] recently reported on radiographic interpretation of peri-implant radiolucencies, where the positive predictive value for fixture instability was only 17%. Consequently, over 80% of the unstable fixtures would remain undetected radiographically.

The increase in peri-implant bone density was greatest in the apical region of the defect followed by the middle and then the coronal AOIs. The healing response in the defects may be dependent on the presence of a blood clot that was protected by the membrane.[103] Following implant placement, the defects filled with blood and no attempt was made to place additional venous blood into the defects as in some healing studies.[103,150] The newly formed blood clot may be relatively stable in the most apical portion of the defects; thus, the addition of a barrier membrane may have minimal effect on healing in this area. Conversely, use of a membrane may enhance clot stability in the middle and coronal portions of the defect, especially in the absence of facial or lingual bony defect walls. The membrane then serves to protect the clot and maintain the space for cellular ingrowth. The addition of DFDBA may enhance clot formation throughout the defect and aid in stabilizing the clot during initial healing.[151]

The phenomenon of DFDBA enhancing healing was seen in both the radiographic and histologic portions of this study when data were viewed by treatment and AOI position. For DFDBA/e-PTFE sites, a trend exists for the apical portion to have a greater increase in density as measured by CADIA (76.6) relative to e-PTFE alone (51.5) and control (42.3) for all 10 animals. There appears to be little difference in the apical portion of the defect in density changes between

the e-PTFE alone and control sites. (Table 10) Histologically, when data were viewed by treatment and AOI position, the presence of DFDBA resulted in a greater increase in osseointegration than e-PTFE alone and control sites. In contrast to the radiographic analysis where the apical AOI had the greatest increase in density (Table 10), the benefit of DFDBA on osseointegration was much greater in the middle AOI (32.5 versus 22.1 and 16.96) and coronal AOI (24.0 versus 8.6 and 3.8) AOIs rather than in the apical AOI. (Table 14) Although the trends are not clear cut and it would be inappropriate to single out the various AOIs and analyze them statistically by region, the presence of DFDBA appears to be beneficial in wound healing when measured radiographically and histologically. Reports in the literature concerning the use of DFDBA in conjunction with e-PTFE membranes for both peri-implantitis and peri-implant defects have indicated the use of DFDBA was not significantly different from a membrane alone.[137,152] It seems the use of DFDBA in certain regenerative situations is critical and future research will have to delineate the clinical situations were allograft material is recommended.

Much controversy exists in the periodontal literature concerning the efficacy of DFDBA. As discussed in the literature review, significant work has been accomplished concerning DFDBA and BMP. However, the use of DFDBA around dental implants has had equivocal clinical results. Clinically the material appears beneficial in maintaining space for regeneration under membranes. However, animal research testing clinical regeneration of facial dehiscence defects found DFDBA and e-PTFE membranes not to perform as well as control sites with membranes only.[113] The authors found differences between the control (80% regeneration) and DFDBA (75%); however, this should not be considered clinically significant and no osseointegration values were discussed. Histologic sections presented in the article demonstrate bone regeneration but as in the current study, minimal bone ingrowth into the threads and resultant lack of osseointegration appeared along the Ti implant in the defect region.

In the previous study, much is discussed about residual DFDBA in the regeneration sites amounting to 40 to 50% of the bone volume, how the allograft appears to be recalcifying, and how it appears non-vital. In the current research project, residual DFDBA particles were also found in

the defects. Some particles were free in the marrow space while others were contiguous with forming trabeculae and appeared to be recalcifying. Although present, the DFDBA particles were only occupying between 4.1 and 8.2% of the defect volume in all 10 animals. The Ti implants had a greater amount of residual DFDBA compared to the HA-coated implants and the difference was statistically significant. Initially, the defect was full of DFDBA and no host bone was present at implant placement. Therefore, the vast majority of DFDBA was not present in the defects 4 months after placement. Whether or not it is non-vital or recalcifying, in this model the presence of DFDBA in surgically created defect was beneficial to healing. Residual amounts of only 4 to 8% are not clinically significant compared to the 100% lack of bone at defect preparation.

Becker and co-workers[60] had previously looked at a similar model in dogs using DFDB xenograft (human source) with e-PTFE membranes, along with other regenerative combinations. The DFDB was found to have the least desirable results and questioned the use of the material compared to membrane therapy alone. Again, Ti implants were used and only clinical defect regeneration by the number of exposed threads was reported. This study received much criticism from the periodontal community since the DFDB was a xenograft and not an allograft. Sampath and Reddi[115] have described how the BMP is homologous between species; however, xenografts are prone to failure due to immunogenic or inhibitory components present in the extracellular bone matrix. In the current study efforts were made to ensure DFDB allograft was the material of choice for grafting. Both of the Becker *et al.* studies evaluated the regeneration in a facial dehiscence defect and demonstrated little benefit of DFDB around Ti implants. Perhaps the same results are true in the current study in a buccolingual orientation; however, buccolingual sections were not performed. It may also be that the size of the defect was so large that the natural healing ability of the animal could not compensate and spontaneously heal, permitting the presence of the DFDBA to be critical to wound healing.

Becker *et al.*[153] have also examined placement of DFDBA from commercial tissue banks in ectopic sites in athymic mice. Results indicate that DFDBA sites had minimal bone formation and significant amounts of non-vital bone chips. BMP is thought to decrease with aging and

commercial bone banks usually procure their bone from older individuals and do not quantify the amount of BMP in the specimens. This may explain the lack of ectopic bone formation in DFDBA sites. The authors felt the use of DFDBA needs to be re-evaluated since the presence of BMP may be too low to be osteoinductive and, therefore, the DFDBA is only osteoconductive. Reflective epifluorescence used in the current study identified areas of labeling activity at 7 days post-implant placement around DFDBA particles and within some of the vents of the HA-coated implants. This provides strong evidence of the osteoinductive properties of both HA and DFDBA in this animal model. The osteoinductive activity described within 7 days falls within the time parameters of Regional Accelerated Phenomenon (RAP) that occurs within a few days of surgery in humans. Yaffe et al.[154] describes RAP as an extensive regional intracortical bone remodeling, recruiting cellular activity necessary for activation of the subsequent healing process.

The effect of the implant surface on the density of healing bone is difficult to discern from the data in this study. When all 10 animals were analyzed, there was no significant difference in bone density gain adjacent to HA-coated implants compared to Ti implants. However, when 3 dogs with membrane complications were eliminated from the analysis, the bony density adjacent to HA-coated implants was significantly greater than the density adjacent to Ti implants. Gher et al.[45] have reported no significant differences between titanium plasma sprayed (TPS) and HA-coated implants based on clinical observations. Zablotsky et al.[10] demonstrated significantly greater histologic repair in surgically created dehiscence defects adjacent to HA-coated implants than grit-blasted titanium implants whether or not an e-PTFE membrane was used. The equivocal results in the radiographic portion of the study preclude definitive conclusions relative to the effect of the implant surface on bone density following GBR procedures, when measured radiographically.

However, the histologic results unquestionably demonstrate that the implant surface in this model was a significant factor in the amount of osseointegration achieved in both the defect and non-defect regions. Kohri et al.[25] compared threaded Ti implants and HA-coated cylinders in a split-mouth design in dogs. Although there was a trend for greater osseointegration around HA-coated implants, the results were not significantly different. In this study, the Ti implants obtained

a mean of 19.0% osseointegration in the non-defect regions which was well below the mean of 47.3 reported by Kohri *et al.* The mean percent osseointegration of 59.3 reported in this study in non-defect regions for HA-coated implants was equivalent to the 57.2 mean reported by the same investigators. Answers to why the osseointegration in non-defect regions of Ti implants was lower than anticipated or how much osseointegration is needed to create a stable implant are only conjecture. Perhaps the loss of the coronal cortical plate and lack of bicortical plate stabilization may have increase the mobility of the implant during initial healing and reduced the potential amount of osseointegration. Becker and Becker[114] recommended in immediate implant placement that the apical portion of the implant be at least 3 to 5 mm into bone. The defects in this study allowed 5 mm into bone for stabilization, but the majority of these animals had poor trabeculation in their mandibles and might be considered type 4 bone. Steflik *et al.*[14] reported that several investigations have determined osseointegration between 40 and 60% in different implant systems. Roberts *et al.*[67] have reported osseointegration in dogs around 50% with brightfield microscopy while the same specimens with microradiographic assessment demonstrated only 23.6% osseointegration. Another publication by Roberts and co-workers used orthodontic forces on integrated implants and found osseointegration values of less than 10% were able to withstand orthodontic continuous loads of 3 Newtons (>300 grams).[155] Therefore, the absolute amount of osseointegration with Ti implants may or may not be a major factor in determining the success of these implants clinically.

Unfortunately, HA-coated implants have been associated with failure 3-5 years after placement, secondary to HA coating dissolution.[36] These problems were associated with first generation HA coatings. Newer sintering techniques may have resolved this problem; however, further clinical research is needed to follow-up and test this phenomenon. The answer to the HA coating dissolution question was beyond the scope of this project, especially since it was designed as a healing study. Hopefully, this research will lay the ground work to build an extensive data base of clinical results with HA-coated surfaces.

In this study, the statistical effect of the dogs on osseointegration and increased bone density was significant both radiographically and histologically, implying that the dogs healed differently from one another. This is exemplified in the variability of mean CADIA values for the dogs which ranged from 18.72 to 60.78 and mean osseointegration in the defect for HA-coated implants which ranged from 20.0% to 76.0%. Several variables may explain these findings: the type of mandibular bone quality varied naturally at implant placement from type 2 to 4; the breed of dog was not standardized; and, the dogs ranged in age from 1 to 5 calendar years. Furthermore, as with any animal model, the health and/or healing capacity of the individual dogs exhibited individual variation. Additionally, there were no significant interactions in the radiographic study implying each variable was acting independently of the others. However, in the histologic analysis, significant interactions occurred in treatment and implant type along with implant type and AOI position. This is a result of the AOI and treatment effects only demonstrating an effect for the HA-coated implants (implant type) since there was virtually no integration of the Ti implants in the defect regions.

New directions for implant therapy include the use of vertical ridge augmentation using e-PTFE with Ti reinforcement,[50] or e-PTFE with Ti miniscrews to tent the membrane and Memfix fixation screws to stabilized the membrane,[130] or e-PTFE with autogenous bone or DFDBA under the membrane.[156] It has recently been established that bone regenerated in membrane-protected defects is able to physiologically respond to implant procedures similarly to non-regenerated host bone.[110] Research is also needed to determine if the implant surface makes a difference in the quality of regeneration achieved, including comparisons of smooth surface Ti, Ti plasma sprayed surfaces, or HA coatings. Additionally, as implant therapy becomes more common place, research in regeneration will be needed concerning the treatment of ailing and failing implants. Sound research describing the histologic events following peri-implantitis have been reported.[152,157] The future is exciting for implant dentistry and associated regenerative techniques.

VI. <u>SUMMARY</u>

In clinical situations where significant peri-implant defects are present, such as voids commonly seen between immediately placed implants and the bony wall of an extraction socket, the results of this study would suggest that use of GBR techniques with e-PTFE will produce a denser healing of the newly formed bone and greater osseointegration at defect-implant surfaces than no regenerative therapy. Furthermore, the addition of DFDBA to the defect site enhances the gain in bone density and increases the amount of osseointegration at the defect-implant surface. Data suggest HA-coated implants produce significantly greater osseointegration than Ti implants under the tested treatment options. Overall, clinical and radiographic observations may be misleading when evaluating osseointegration in peri-implant defects. Animal histology suggest both treatment and implant selection are important in obtaining optimum osseointegration with implant therapy.

APPENDIX A

Osteo-Bed Infiltration

Technique

Xylene		48 hours
Xylene:Osteo-Bed	(3:1)	24 hours
Xylene:Osteo-Bed	(2:1)	24 hours
Xylene:Osteo-Bed	(1:1)	24 hours
Xylene:Osteo-Bed	(1:2)	24 hours
Xylene:Osteo-Bed	(1:3)	24 hours
Osteo-Bed Resin	(100%)	24 hours (change solution)
Osteo-Bed Resin	(100%)	24 hours
Catalyzed Resin II		48 hours
Catalyzed Resin III		48 hours
Catalyzed Resin III		Until Polymerized (~48 hours)

Osteo-Bed infiltration resin II and III are catalyzed with the addition of Benzoyl Peroxide. These mixtures can be stored in the refrigerator for several weeks.

Catalyzed Mix Part II	Catalyzed Mix Part III
Osteo-Bed Resin 100 ml	Osteo-Bed Resin 100 ml
Benzoyl Peroxide 1 gm	Benzoyl Peroxide 2.5 gm

APPENDIX B

Paragon/Alizarin Red Stains

Materials

Paragon Stain:	Toluidine Blue O	0.73 gm
	Basic Fuchsin	0.27 gm
	30% EtOH	100 ml

Alizarin Red:	Alizarin Red S	1.0 gm
	Distilled water	100 ml
	0.1% ammonium hydroxide	10 ml

Technique

Place sections in Paragon stain for 2 hours, rinse in water and differentiate in acid alcohol. Rinse with water again. Place sections in Alizarin Red stain for 1 to 5 minutes, rinse with water, and air dry.

APPENDIX C

Masson-Trichrome-Goldner Stain[158]

1. Stain 15 minutes in Weigerts ferric hematoxylin

2. Rinse 5 minutes in running tap water

3. Stain 7 minutes in Masson-solution (Goldner I)

4. Rinse with 2% acetic acid

5. Stain 5 minute phosphormolybdanum-acid-orange-G

6. Rinse with 2% acetic acid

7. Stain 15 minute in "light green", 60 degree C incubator

8. Rinse with 2% acetic acid

9. Dip slide briefly in distilled water, to wash off the acetic acid

10. Dry slide and coverslip

To consider: Prepare Weigerts ferric hematoxylin shortly before use. Use equal parts of 1 and 2

  solutions.

Ingredients:

  acid fuchsin (Rubin S, Merck)

  xylidine-Ponceau (1B 207, Chroma)

  azophloxin (1 B 103, Chroma)

  light green (yellowish, Merck)

Production of the solutions:

A. Masson-Solution (Goldner I)

1. Dissolve 1 g acid fuchsin in 100 ml distilled water and 1 ml glacial acetic acid

2. Dissolve 1 g Xylidine-Ponceau in 100 ml distilled water and 1 ml glacial acetic acid

3. dissolve 0.5 g azophloxin in 100 ml distilled water and 0.2 ml glacial acetic acid

Mix 33 ml of the acid fuchsin in solution and 66 ml Xylidine-Ponceau-solution.

Mix 100 ml of the solution with 20 ml azophloxin in 100 ml distilled water and 0.2 acetic acid.

The finished mixture is identical with the Masson-Goldner-Solution (Goldner I).

B. Orange-G

1. Dissolve 10 g orange-G in 500 ml distilled water

2. Dissolve 15 gm molybdatophosphor acid (Merck) in above (1) solution

C. Light Green

1. Mix 0.5 g light green and 1 ml glacial acetic acid into 500 ml distilled water.

LITERATURE CITED

1.   Albrektsson, T. and U. Lekholm. 1989. Osseointegration: Current state of the art. Dental Clinics of North America, 33: 537-554.

2.   Brånemark, P. I., U. Breine, R., Adell, B. O. Hansson, J. Lindström and A. Olsson. 1969. Intraosseous anchorage of dental prostheses. I. Experimental studies. Scandinavian Journal of Plastic and Reconstructive Surgery and Hand Surgery, 3: 879-903.

3.   Krauser, J. T. 1989. Hydroxylapatite-coated dental implants: Biologic rationale and surgical technique. Dental Clinics of North America, 33: 879-903.

4.   Weinlaender, M. 1991. Bone growth around dental implants. Dental Clinics of North America, 35: 585-601.

5.   Binon, P. P., D. J. Weir and S. J. Marshall. 1992. Surface analysis of an original Brånemark implant and three related clones. International Journal of Oral and Maxillofacial Implants, 7: 168-174.

6.   Donley, T. G. and W. B. Gillette. 1991. Titanium endosseous implant-soft tissue interface: a literature review. Journal of Periodontology, 62: 153-160.

7.   Bernard, G. W. 1991. Healing and repair of osseous defects. Dental Clinics of North America, 35: 469-477.

8.   Thomsen, P. 1989. Titanium and the Inflammatory Response. In: T. Albrektsson and G. A. Zarb, editors. The Brånemark Osseointegrated Implant. Chicago: Quintessence Publishing Co., Inc. 262 p.

9.   Lynch, S. E., D. Buser, R. A. Hernandez, H. P. Weber, C. H. Fox and R. C. Williams. 1991. Effects of the platelet-derived growth factor/insulin-like growth factor-I combination on bone regeneration around titanium dental implants. Results of a pilot study in beagle dogs. Journal of Periodontology, 62: 710-716.

10. Zablotsky, M., R. Meffert, R. Caudill and G. Evans. 1991. Histological and clinical comparisons of guided tissue regeneration on dehised hydroxylapatite-coated and titanium endosseous implant surfaces: A pilot study. International Journal Oral and Maxillofacial Implants, 6: 294-303.

11. Denissen, H. W., W. Kalk, H. M. de Nieuport, J. C. Maltha and A. van de Hooff. 1990. Mandibular bone response to plasma-sprayed coatings of hydroxyapatite. International Journal of Prosthodontics, 3: 53-58.

12. Schepers, E., M. De Clercq, P. Ducheyne. 1988. Histological and histomorphometrical analysis of bioactive glass and fibre reinforced bioactive glass dental root implants. Journal of Oral Rehabilitation, 15: 473-487.

13. Albrektsson, T. 1985. Bone Tissue Response. In: P. I. Brånemark, G. A. Zarb and T. Albrektsson, editors. Tissue integrated-prostheses: Osseointegration in clinical dentistry. Chicago: Quintessence Publishing Co. 350 p.

14. Steflik, D. E., P. J. Hanes, A. L. Sisk, G. R. Parr, M. J. Song, F. T. Lake and R. V. McKinney. 1992. Transmission electron microscopic and high voltage electron microscopic observations of the bone and osteocyte activity adjacent to unloaded dental implants placed in dogs. Journal of Prosthetic Dentistry, 63: 443-452.

15. Knox, R., R. Caudill and R. Meffert. 1991. Histologic Evaluation of Dental Endosseous Implants Placed in Surgically Created Extraction Defects. International Journal of Periodontics and Restorative Dentistry, 11: 365-375.

16. Golec, T. S. and J. T. Krauser. 1992. Long-term retrospective studies on hydroxyapatite coated endosteal and subperiosteal implants. Dental Clinics of North America, 36: 39-65.

17. Jarcho, M. 1992. Retrospective analysis of hydroxyapatite development for oral implant applications. Dental Clinics of North America, 36: 19-26.

18. Brånemark, P.I. 1985. Introduction to Osseointegration. In: P. I. Brånemark, G. A. Zarb and T. Albrektsson, editors. Tissue-integrated prostheses: Osseointegration in clinical dentistry. Chicago: Quintessence Publishing Co. p 11-76.

19. Arvidson, K., H. Bystedt and I. Ericsson. 1990. Histometric and ultrastructural studies of tissues surrounding Astra dental implants in dogs. International Journal of Oral and Maxillofacial Implants, 5: 127-134.

20. Lum, L. B. and O. R. Beirne. 1986. Viability of the retained bone core in the core-vent dental implant. Journal of Oral and Maxillofacial Surgery, 44: 341-345.

21. Roberts, W. E., F. R. Helm, K. J. Marshall and R. K. Gongloff. 1989. Rigid endosseous implants for orthodontic and orthopedic anchorage. Angle Orthodontist, 59: 247-256.

22. Adell, R., U. Lekholm, B. Rockler and P. I. Brånemark. 1990. A long-term follow-up of osseointegrated implants in the treatment of the totally edentulous jaw. International Journal of Oral and Maxillofacial Surgery, 5: 347-359.

23. Zarb, G. A. and A. Schmitt. 1990. The longitudinal clinical effectiveness of osseointegrated implants. The Toronto Study. Part I: Surgical results. Journal of Prosthetic Dentistry, 63: 451-457.

24. Zarb, G. A. and A. Schmitt. 1993. The longitudinal clinical effectiveness of osseointegrated dental implants in anterior partially edentulous patients. International Journal of Prosthetic Dentistry, 6: 180-189.

25. Kohri, M., E. P. Cooper, J. L. Ferracane and D. F. Waite. 1990. Comparative study of hydroxyapatite and titanium dental implants in dogs. Journal of Oral and Maxillofacial Surgery, 48: 1265-1273.

26. Block, M.S., I. M. Finger, M. G. Fontenot and J. N. Kent. 1989. Loaded hydroxylapatite-coated and grit-blasted titanium implants in dogs. International Journal of Oral and Maxillofacial Implants, 4: 219-225.

27. Cooley, D. R., A. F. Van Dellen, J. O. Burgess and A. S. Windeler. 1992. The advantages of coated titanium implants prepared by radiofrequency sputtering from hydroxyapatite. Journal of Prosthetic Dentistry, 67: 93-100.

28. Zablotsky, M. 1992. The surgical management of osseous defects associated with endosteal hydroxyapatite-coated and titanium dental implants. Dental Clinics of North America, 36: 117-149.

29. Ohno, K., A. Sugimoto, T. Shirota, K. Michi, S. Ohtani, K. Yamagata and K. Donath. 1991. Histologic findings of apatite-titanium complex dental implants in the jaws of dogs. Oral Surgery, Oral Medicine, Oral Pathology, 71: 426-429.

30. Block, M. S., A. Delongo, M. G. Fontenot. 1990. The effect of diameter and length of hydroxylapatite-coated dental implants on ultimate pullout force in dog alveolar bone. Journal of Oral and Maxillofacial Surgery, 48: 174-178.

31. Meffert, R. M., B. Langer and M. E. Fritz. 1992. Dental implants. A review. Journal of Periodontology, 63: 859-870.

32. Kay, J. F. 1992. Calcium phosphate coatings for dental implants. Current status and future potential. Dental Clinics of North America, 36: 1-18.

33. Pilliar, R. M., D. A. Deporter, P. A. Watson, M. Pharoah, M. Chipman, N. Valiquette, S. Carter and K. DeGroot. 1991. The effect of partial coating with hydroxyapatite on bone remodeling in relation to porous-coated titanium-alloy dental implants in the dog. Journal of Dental Research, 70: 1338-1345.

34. Buser, D. and U. Belser. 1994. Anatomic, surgical, and esthetic considerations in implant dentistry. In: D. Buser, C. Dahlin and R. Schenk, editors. Guided bone regeneration in implant dentistry. Chicago: Quintessence Publishing Co., Inc. p 13-30.

35. Meffert, R. M., M. S. Block, J. N. Kent. 1987. What is osseointegration? International Journal of Periodontics and Restorative Dentistry, 7: 9-21.

36. Johnson, B. W. 1992. HA-coated dental implants: Long-term consequences. California Dental Association Journal, 20: 33-41.

37. Cook, S. D., J. F. Kay, K. A. Thomas and M. Jarcho. 1987. Interface mechanics and histology of titanium and hydroxylapatite-coated titanium for dental implant applications. International Journal of Oral and Maxillofacial Implants, 2: 15-22.

38. Gottlander, M. and T. Albrektsson. 1991. Histomorphometric studies of hydroxylapatite-coated and uncoated CP titanium threaded implants in bone. International Journal of Oral and Maxillofacial Implants, 6: 399-404.

39. Krauser, J., P. Bertholdt, I. Tamary and R. Seckinger. 1991. A scanning electron microscopy study of failed root form dental implants [abstract]. Journal of Dental Research, 70: 274. Abstract nr 65.

40. Rams, T. E., T. W. Roberts, D. Feik, A. K. Molzan and J. Slots. 1991 Clinical and microbiological findings of newly inserted hydroxylapatite-coated and pure titanium human dental implants. Clinical Oral Implant Research, 2: 121-127.

41. Ducheyne, P., L. L. Hench, A. Kogan, M. Martens, A. Bursens and J. C. Mulier. 1980. Effect of hydroxyapatite impregnated on skeletal bonding of porous coated implants. Journal of Biomedical Research, 14: 225-237.

42. Rivero, D. P., J. Fox, A. K. Skipor, R. M. Urban and J. O. Galante. 1988. Calcium phosphate-coated porous titanium implants for enhanced skeletal fixation. Journal of Biomaterial Research, 22: 191-201.

43. de Groot, K., R. G. T. Geesink, C. P. A. T. Klein and P. Serekian. 1987. Plasma sprayed coatings of hydroxylapatite. Journal of Biomedical Material Research, 21:1375-1381.

44. Block, M. S. and J. N. Kent. 1992. Prospective review of Integral implants. Dental Clinics of North America, 36: 27-37.

45. Gher, M., G. Quintero, D. Assad, E. Monaco and A. Richardson. 1994. Bone grafting and guided bone regeneration for immediate dental implants in humans. Journal of Periodontology, 65: 881-891.

46. Landsberg, C., A. Grosskopf and M. Weinreb. 1994. Clinical and biologic observations of demineralized freeze-dried bone allografts in augmentation procedures around dental implants. International Journal of Oral and Maxillofacial Implants, 9: 568-592.

47. Becker, W. and B. E. Becker. 1990. Guided tissue regeneration for implants placed into extraction sockets and for implant dehiscences: Surgical techniques and case reports. International Journal of Periodontics and Restorative Dentistry, 10: 376-391.

48. Becker, W., B. E. Becker, G. Polizzi and C. Bergstrom. 1994. Autogenous bone grafting of bone defects adjacent to implants placed into immediate extraction sockets in patients: A prospective study. International Journal of Oral and Maxillofacial Implants, 9: 389-396.

49. Vlassis, J. M. 1993. Guided bone regeneration at a fenestrated dental implant: histologic assessment of a case report. International Journal of Periodontics and Restorative Dentistry, 8: 447-451.

50. Simion, M., P. Trisi and A. Piattelli. 1994. Vertical ridge augmentation using a membrane technique associated with osseointegrated implants. International Journal of Periodontics and Restorative Dentistry, 14: 497-511.

51. Takeshita, F., H. Kuroki, A. Yamasaki and T. Suetsugu. 1995. Histopathologic observation of seven removed endosseous dental implants. International Journal of Oral and Maxillofacial Implants, 10: 367-372.

52. Hansson, H. A., T. Albrektsson, P. I. Brånemark. 1983. Structural aspects of the interface between tissue and titanium implants. Journal of Prosthetic Dentistry, 50: 108-113.

53. Piattelli, A., P. Trisi, N. Romasco and M. Emanuelli. 1993. Histologic analysis of a screw implant retrieved from man: Influence of early loading and primary stability. Journal of Oral Implantology, 19: 303-306.

54. Palmer, R. M., P. D. Floyd, P. J. Palmer, B. J. Smith, C. B. Johansson and T. Albrektsson. 1994. Healing of implant dehiscence defects with and without expanded polytetrafluoroethylene membranes: A controlled clinical and histological study. Clinical Oral Implant Research, 5: 98-104.

55. Gratz, K. W., A. P. Zimmermann and H. F. Sailer. 1994. Histological evidence of osseointegration 4 years after implantation. A case report. Clinical Oral Implants Research, 5: 173-176.

56. Rohrer, M., R. Bulard and M. Patterson. 1995. Maxillary and mandibular titanium implants 1 year after surgery: Histologic examination in a cadaver. International Journal of Oral and Maxillofacial Implants, 10: 466-473.

57. GaRey, D. J., J. M. Whittaker, R. A. James and J. L. Lozada. 1991. The histologic evaluation of the implant interface with heterograft and allograft materials--an eight-month autopsy report, Part II. Journal of Oral Implantology, 17: 404-408.

58. Warrer, K., K. Gotfredsen, E. Hjorting-Hansen and T. Karring. 1991. Guided tissue regeneration ensures osseointegration of dental implants placed into extraction sockets. An experimental study in monkeys. Clinical Oral Implants Research, 2: 166-171.

59. Becker, W., B. Becker, M. Handelsman, C. Ochsenbein and T. Albrektsson. 1991. Guided tissue regeneration for implants placed into extraction sockets. A study in dog. Journal of Periodontology, 62: 703-709.

60. Becker, W., S. E. Lynch, U. Lekholm, B. E. Becker, R. Caffesse, K. Donath and R. Sanchez. 1992. A comparison of ePTFE membranes alone or in combination with platelet-derived growth factors and insulin-like growth factor-I or demineralized freeze-dried bone in promoting bone formation around immediate extraction socket implants. Journal of Periodontology, 63: 929-940.

61. Caudill, R. F. and R. M. Meffert. 1991. Histologic analysis of the osseointegration of endosseous implants in simulated extraction sockets with and without e-PTFE barriers. 1. Preliminary Findings. International Journal of Periodontics and Restorative Dentistry, 11: 207-215.

62. Lekholm, U., W. Becker, C. Dahlin, B. Becker, K. Donath and E. Morrison. 1993. The role of early versus late removal of E-PTFE membranes on bone formation at oral implants placed into immediate extraction sockets. An experimental study in dogs. Clinical Oral Implants Research, 4: 121-129.

63. Becker, W., B. E. Becker, M. Handlesman, R. Celletti, C. Ochsenbein, R Hardwick and B. Langer. 1990. Bone formation at dehised dental implant sites treated with implant

augmentation material: a pilot study in dogs. International Journal of Periodontics and Restorative Dentistry, 10: 93-101.

64. Messadi, D. V. and C. N. Bertolami. 1991. General principles of healing pertinent to the periodontal problem. Dental Clinics of North America, 35: 443-457.

65. Schenk, R. 1994. Bone regeneration: Biologic basis. In: D. Buser, C. Dahlin and R. Schenk, editors. Guided bone regeneration in implant dentistry. Chicago: Quintessence Publishing Co., Inc. p 49-100.

66. Steflik, D. E., R. V. McKinney and D. L. Koth. 1989. Ultrastructural comparisons of ceramic and titanium dental implants in vivo: a scanning electron microscopic study. Journal of Biomedical Materials Research, 23: 895-909.

67. Roberts, W. E. 1988. Bone tissue interface. Journal of Dental Education, 52: 804-809.

68. Deporter, D. A., P. A. Watson, R. M. Pilliar, M. L. Chipman and N. Valiquette. 1990. A histological comparison in the dog of porous-coated versus threaded dental implants. Journal of Dental Research, 69: 1138-1145.

69. Ravaglioli, A., A. Krajewski, V. Biasini, R. Martinetti, C. Mangano and G. Venini. 1992. Interface between hydroxyapatite and mandibular human bone tissue. Biomaterials, 13: 162-167.

70. Nyman, S., J. Lindhe, T. Karring and H. Rylander. 1982. New attachment following surgical treatment of human periodontal disease. Journal of Clinical Periodontology, 9: 290-296.

71. Minabe, M. 1991. A critical review of the biologic rationale for guided tissue regeneration. Journal of Periodontology, 62: 171-179.

72. Nyman, S., J. Gottlow, T. Karring and J. Lindhe. 1982. The regenerative potential of the periodontal ligament. An experimental study in the monkey. Journal of Clinical Periodontology, 9: 257-265.

73. Caton, J. G., E. L. DeFuria, A. M. Polson and S. Nyman. 1987. Periodontal regeneration via selective cell repopulation. Journal of Periodontology, 58: 546-552.

74. Gottlow, J., S. Nyman, T. Karring and J. Lindhe. 1984. New attachment formation as the result of controlled tissue regeneration. Journal of Clinical Periodontology, 11: 494-503.

75. Aukhil, I., D. M. Simpson and T. V. Schaberg. 1983. An experimental study of new attachment procedure in beagle dogs. Journal of Periodontal Research, 18: 643-654.

76. Magnusson, I., S. Nyman, T. Karring and J. Egelberg. 1985. Connective tissue attachment formation following exclusion of gingival connective tissue and epithelium during healing. Journal of Periodontal Research, 20: 201-208.

77. Claffey, N., S. Motsinger, J. Ambruster, and J. Egelberg. 1989. Placement of a porous membrane underneath the mucoperiosteal flap and its effect on periodontal wound healing in dogs. Journal of Clinical Periodontology, 16: 12-16.

78. Gottlow, J., S. Nyman, J. Lindhe, T. Karring and J. Wennstrom. 1986. New attachment formation in the human periodontium by guided tissue regeneration. Case reports. Journal of Clinical Periodontology, 13: 604-616.

79. Pontoriero, R., S. Nyman, J. Lindhe, E. Rosenberg and F. Sanavi. 1987. Guided tissue regeneration in the treatment of furcation defects in man. Journal of Clinical Periodontology, 14: 618-620.

80. Becker, W., B. E. Becker, J. F. Prichard, R. Caffesse, E. Rosenberg and J. G. Grasso. 1987. Root isolation for new attachment procedures. A surgical and suturing method: Three case reports. Journal of Periodontology, 58: 819-826.

81. Becker, W., B. E. Becker, L. Berg, J. Prichard, R. Caffesse and E. Rosenberg. 1988. New attachment after treatment with root isolation procedures: report for treated Class III and Class II furcations and vertical osseous defects. International Journal of Periodontics and Restorative Dentistry, 8: 8-23.

82. Caffesse, R. G., B. A. Smith, B. Duff, E. C. Morrison, D. Merrill and W. Becker. 1990. Class II furcations treated by guided tissue regeneration in humans: case reports. Journal of Periodontology, 61: 510-514.

83. Lekovic, V., E. B. Kenney, K. Kovacevic and F. A. Carranza. 1989. Evaluation of guided tissue regeneration in Class II furcation defects. A clinical re-entry study. Journal of Periodontology, 60: 694-698.

84. Pontoriero, R., J. Lindhe, S. Nyman, T. Karring, E. Rosenberg and F. Sanavi. 1989. Guided tissue regeneration in the treatment of furcation defects in mandibular molars. A clinical study of degree III involvements. Journal of Clinical Periodontology, 16: 170-174.

85. Pontoriero, R., J. Lindhe, S. Nyman, T. Karring, E. Rosenberg and F. Sanavi. 1988. Guided tissue regeneration in degree II furcation-involved mandibular molars. A clinical study. Journal of Clinical Periodontology, 15: 247-254.

86. Dahlin, C., L. Sennerby, U. Lekholm, A. Linde and S. Nyman. 1989. Generation of new bone around titanium implants using a membrane technique: an experimental study in rabbits. International Journal of Oral and Maxillofacial Implants, 4: 19-25.

87. Mellonig, J. T. 1991. Freeze-dried bone allografts in periodontal reconstructive surgery. Dental Clinics of North America, 35: 505-520.

88. Shetty, V. and T. J. Han. 1991. Alloplastic materials in reconstructive periodontal surgery. Dental Clinics of North America, 35: 521-530.

89. Hurt, W. C. 1968. Freeze-dried bone homografts in periodontal lesions in dogs. Journal of Periodontology, 39: 89-92.

90. Hancock, E. B., editor. 1989. Regeneration Procedures. Proceedings of the World Workshop in Clinical Periodontics; 1989 Jul 23-27; Princeton. Chicago: The American Academy of Periodontology. pVI1-VI20.

91. Mellonig, J. T., G. M. Bowers and W. R. Cotton. 1981. Comparison of bone graft materials. Part II. New bone formation with autografts and allografts: a histological evaluation. Journal of Periodontology, 52: 297-302.

92. Urist, M. R., R. J. DeLange and G. A. M. Finerman. 1983. Bone Cell Differentiation and Growth Factors. Science, 220: 680-686.

93. Werbitt, M. 1987. Decalcified freeze-dried bone allografts: a successful procedure in the reduction of intrabony defects. International Journal of Periodontics and Restorative Dentistry, 7: 57-63.

94. Quintero, G., J. T. Mellonig, V. M. Gambill and G. B. Pelleu. 1982. A six-month clinical evaluation of decalcified freeze-dried bone allografts in periodontal osseous defects. Journal of Periodontology, 53: 726-730.

95. Bowers, G. M., B. Chadroff, R. Carnevale, J. Mellonig, R. Corio, J. Emerson, M. Stevens and E. Romberg. 1989. Histologic evaluation of new attachment apparatus formation in humans. Part III. Journal of Periodontology, 60: 683-693.

96. Seibert, J. and S. Nyman. 1990. Localized ridge augmentation in dogs: a pilot study using membranes and hydroxyapatite. Journal of Periodontology, 61: 157-165.

97. Guillemin, M. R., J. T. Mellonig and M. A. Brunsvold. 1993. Healing in periodontal defects treated by decalcified freeze-dried bone allografts in combination with ePTFE membranes. I. Clinical and scanning electron microscopic analysis. Journal of Clinical Periodontology, 20: 528-536.

98. Anderegg, C.R., S. J. Martin, J. L. Gray, J. T. Mellonig and M. E. Gher. 1991. Clinical evaluation of the use of decalcified freeze-dried bone allograft with guided tissue regeneration in the treatment of molar furcation. Journal of Periodontology, 62: 264-268.

99. Becker, W., M. R. Urist, L. M. Tucker, B. E. Becker and C. Ochsenbein. 1995. Human demineralized freeze-dried bone: Inadequate induced bone formation in athymic mice. A preliminary report. Journal of Periodontology, 66: 822-828.

100. Sendax, V. I. 1992. Postscript: hydroxyapatite-coated implants. Dental Clinics of North America, 36: 227-232.

101. Yukna, R. A. 1991. Clinical comparison of hydroxyapatite-coated titanium dental implants placed in fresh extraction sockets and healed sites. Journal of Periodontology, 62: 468-472.

102. Buser, D., K. Dula, U. Belser, H. Hirt and H. Berthold. 1993. Localized ridge augmentation using guided bone regeneration. I. Surgical procedure in the maxilla. International Journal of Periodontics and Restorative Dentistry, 13: 29-45.

103. Schenk, R. K., D. Buser, W. R. Hardwick and C. Dahlin. 1994. Healing pattern of bone regeneration in membrane-protected defects. A histologic study in the canine mandible. International Journal of Oral and Maxillofacial Implants, 9: 13-29.

104. Dahlin, C., U. Lekholm and A. Linde. 1991. Membrane-induced bone augmentation at titanium implants. A report on ten fixtures followed from 1 to 3 years after loading. International Journal of Periodontics and Restorative Dentistry, 11: 273-281.

105. Dahlin, C., U. Lekholm, W. Becker, B. Becker, K. Higuchi, A. Callens and D. van Steenberghe. 1995. Treatment of fenestration and dehiscence bone defects around oral implants using the guided tissue regeneration technique: A prospective multicenter study. International Journal of Oral and Maxillofacial Implants, 10: 312-318.

106. Nyman, S., N. P. Lang, D. Buser and U. Brägger. 1990. Bone regeneration adjacent to titanium dental implants using guided tissue regeneration: a report of two cases. International Journal of Oral and Maxillofacial Implants, 5: 9-14.

107. Jovanovic, S. A., H. Spiekermann and E. J. Richter. 1992. Bone regeneration around titanium dental implants in dehisced defect sites: A clinical study. International Journal of Oral and Maxillofacial Implants, 7: 233-245.

108. Jovanovic, S. and Buser D. 1994. Guided bone regeneration in dehiscence defects and delayed extraction sockets. In: D. Buser, C. Dahlin and R. Schenk, editors. Guided bone regeneration in implant dentistry. Chicago: Quintessence Publishing Co., Inc. p 155-188.

109. Kenney, E. B. and S. Jovanovic. 1993. Osteopromotion as an adjunct to osseointegration. International Journal of Prosthodontics, 6: 131-136.

110. Buser, D., J. Ruskin, F. Higginbottom, R. Hardwick, C. Dahlin and R. Schenk. 1995. Osseointegration of titanium implants in bone regenerated in membrane-protected defects: A

histologic study in the canine mandible. International Journal of Oral and Maxillofacial Implants, 10: 666-681.

111. Jensen, O. 1994. Guided bone graft augmentation. In: D. Buser, C. Dahlin and R. Schenk, editors. Guided bone regeneration in implant dentistry. Chicago: Quintessence Publishing Co., Inc. p 235-264.

112. Nevins, M. and J. Mellonig. 1992. Enhancement of the damaged edentulous ridge to receive dental implants: A combination of allograft and the Gore-Tex membrane. International Journal of Periodontics and Restorative Dentistry, 12: 97-111.

113. Becker, W., R. Schenk, K. Higuchi, U. Lekholm and B. Becker. 1995. Variations in bone regeneration adjacent to implants augmented with barrier membranes alone or with demineralized freeze-dried bone or autologous grafts: A study in dogs. International Journal of Oral and Maxillofacial Implants, 10: 143-154.

114. Becker, W. and Becker B. E. 1994. Bone promotion around e-PTFE augmented implants placed in immediate extraction sockets. In: D. Buser, C. Dahlin and R. Schenk, editors. Guided bone regeneration in implant dentistry. Chicago: Quintessence Publishing Co., Inc. p 137-154.

115. Sampath, T. K. and A. H. Reddi. 1983. Homology of bone-induced proteins from human, monkey, bovine, and rat extracellular matrix. Cell Biology, 80: 6591-6595.

116. Gotfredsen, K., J. Warrer, E. Horting-Hansen and T. Karring. 1991. Effect of membranes and hydroxyapatite on healing in bone defects around titanium implants. An experimental study in monkeys. Clinical Oral Implants Research, 2: 172-178.

117. Lazzara, R. J. 1989. Immediate implant placement into extraction sites: surgical and restorative advantages. International Journal of Periodontics and Restorative Dentistry, 9: 333-343.

118. Nyman, S., N. P. Lang, D. Buser, and U. Brägger. 1990. Bone regeneration adjacent to titanium dental implants using guided tissue regeneration: A report of two cases. International Journal of Oral and Maxillofacial Implants, 5: 9-14.

119. Becker, W., C. Dahlin, B. Becker, U. Lekholm, D. van Steenberghe and K. Higuchi. 1994. The use of e-PTFE barrier membranes for bone promotion around titanium implants placed into extraction sockets: A prospective multicenter study. International Journal of Oral and Maxillofacial Implants, 9: 31-40.

120. Block, M.S. and J. N. Kent. 1991. Placement of endosseous implants into tooth extraction sites. Journal of Oral and Maxillofacial Surgery, 49: 1269-76.

121. Ashman, A. 1990 An immediate tooth root replacement: an implant cylinder and synthetic bone combination. Journal of Oral Implantology, 16: 28-38.

122. Tolman, D. E. and E. E. Keller. 1991. Endosseous implant placement immediately following dental extraction and alveoloplasty: Preliminary report with 6-year follow-up. International Journal of Oral and Maxillofacial Implants, 6: 24-28.

123. Augthin, M., M. Yildirim, H. Spiekermann and S. Biesterfeld. 1995. Healing of bone defects in combination with immediate implants using the membrane technique. International Journal of Oral and Maxillofacial Implants, 10: 421-428.

124. Reddy, M. S. 1992. Radiographic methods in the evaluation of periodontal therapy. Journal of Periodontology, 63: 1078-1084, .

125. Bender, I. B. and S. Seltzer. 1961. Roentgenographic and direct observation of experimental lesions in bone (I). Journal of the American Dental Association, 62: 152-160.

126. Bender, I. B. and S. Seltzer. 1961. Roentgenographic and direct observation of experimental lesions in bone (II). Journal of the American Dental Association, 6: 708-716.

127. Van der Stelt, P. F. 1985. Experimentally produced bone lesions. Oral Surgery, Oral Medicine, Oral Pathology, 59: 306-312.

128. Ortman, L. F., K. McHenry and E. Hausmann. 1982. Relationship between alveolar bone measured by 125I absorptiometry with analysis of standardized radiographs. 2. Bjorn technique. Journal of Periodontology, 53: 311-314.

129. Grondahl, K., B. Kullendorff, K. G. Strid, H. G. Grondahl and C. O. Henrickson. 1988. Detectability of artificial marginal bone lesions as a function of lesion depth. A comparison

between subtraction radiography and conventional radiographic technique. Journal of Clinical Periodontology, 15: 156-162.

130. Brägger, U. 1988. Digital imaging in periodontal radiography. Journal of Clinical Periodontology, 15: 551-557.

131. Jeffcoat, M. K., M. S. Reddy, R. L. Webber, R. C. Williams and U. E. Ruttiman. 1987. Extraoral control of geometry for digital subtraction radiography. Journal of Periodontal Research, 22: 396-402.

132. Brägger, U., L. Pasquali, H. Rylander, D. Carnes and K. S. Kornman. 1988. Computer assisted densitometric image analysis for the quantitation of radiographic alveolar bone changes. Journal of Periodontal Research. 15: 27-37.

133. Brägger, U., J. Litch, L. Pasquali and K. S. Kornman. 1987. Computer assisted densitometric image analysis for the quantitation of radiographic alveolar bone changes. Journal of Periodontal Research, 22: 227-229.

134. Remington, R. D. and M. A. Schork. 1970. Statistics with application to the biological and health science. Englewood Cliffs: Prentice-Hall, Inc. 418 p.

135. Brägger, U., W. Burgin, I. Fourmoussis and N. P. Lang. 1992. Image processing for the evaluation of dental implants. Dento-maxillo-facial Radiology, 21: 208-212.

136. Yukna, R. A. 1992. Placement of hydroxyapatite-coated implants into fresh or recent extraction sites. Dental Clinics of North America, 36: 97-115.

137. Shanaman, R. 1994. A retrospective study of 237 sites treated consecutively with guided tissue regeneration. International Journal of Periodontics and Restorative Dentistry, 14: 293-301.

138. Mellonig, J. T., A. B. Prewett and M. P. Moyer. 1992. HIV inactivation in a bone allograft. Journal of Periodontology, 63: 979-983.

139. Dove, S. B., W. D. McDavid and C. D. Wilcox. 1988. C.A.R.E. [computer program]. San Antonio (TX): University of Texas Health Science Center at San Antonio.

140. Dove, S. B., W. D. McDavid and D. Wilcox. 1990. RADWORKS [computer program]. San Antonio (TX): University of Texas Health Science Center at San Antonio.

141. Ruttimann, U. E., R. L. Webber and E. Schmidt. 1986. A robust digital method for film contrast correction in subtraction radiography. Journal of Periodontal Research, 21: 486-495.

142. White, C., E. Hancock., L. Garetto and A. Kafrawy. 1994. A histomorphometric study on the healing of class III furcations utilizing bone labelling in beagle dogs. Journal of Periodontology, 65: 84-92.

143. Lillie, R. D. 1977. H. J. Conn's biological stains. 9th ed. Baltimore: Williams and Wilkins Co. 692 p.

144. Mellonig, J. R. and M. Nevins. 1995. Guided bone regeneration of bone defects associated with implants. International Journal of Periodontics and Restorative Dentistry, 15: 168-185.

145. Guillemin, M. R. 1993. Healing in periodontal defects treated by decalcified freeze-dried bone allografts in combination with e-PTFE membranes. Assessment by computerized densitometric analysis. Journal of Clinical Periodontology, 20: 520-527.

146. Brägger, U., W. Burgin, N. P. Lang and D. Buser. 1991. Digital subtraction radiography for the assessment of changes in peri-implant bone density. International Journal of Oral and Maxillofacial Implants, 6: 160-166.

147. Jeffcoat, M. K. and M. S. Reddy. 1993. Digital subtraction radiography for longitudinal assessment of peri-implant bone change: method and validation. Advances in Dental Research, 7: 196-201.

148. Caudill, R. and D. Lancaster. 1993. Histologic analysis of the osseointegration of endosseous implants in simulated extraction sockets with and without e-PTFE barriers. Part II: Histomorphometric findings. Journal of Oral Implantology, 19: 209-215.

149. Sunden S., K. Grondahl and H. Grohndahl. 1995. Accuracy and precision in the radiographic diagnosis of clinical instability in Brånemark dental implants. Clinical Oral Implants Research, 6: 220-226.

150. Jovanovic, S. A., R. K. Schenk, M. Orsini and E. B. Kenney. 1995. Supracrestal bone formation around dental implants: An experimental dog study. International Journal of Oral and Maxillofacial Implants, 10: 23-31.

151. Cortellini, P. and G. Bowers. 1995. Periodontal regeneration of intrabony defects: An evidence-based treatment approach. International Journal of Periodontics and Restorative Dentistry, 15: 128-145.

152. Hurzeler, M., C. Quinones, E. Morrison and R. Caffesse. 1995. Treatment of peri-implantitis using guided bone regeneration and bone grafts, alone or in combination, in beagle dogs. Part 1: Clinical findings and histologic observations. International Journal of Oral and Maxillofacial Implants, 10: 474-484.

153. Becker, W., M. R. Urist, L. M. Tucker, B. E. Becker and C. Ochsenbein. 1995. Human demineralized freeze-dried bone: Inadequate induced bone formation in athymic mice. A preliminary report. Journal of Periodontology, 66: 822-828.

154. Yaffe, A., N. Fine and I. Binderman. 1994. Regional accelerated phenomenon in the mandible following mucoperiosteal flap surgery. Journal of Periodontology, 65: 79-83.

155. Roberts, W. E., F. R. Helm, K. J. Marshall and R. K. Gongloff. 1989. Rigid endosseous implants for orthodontic and orthopedic anchorage. Angle Orthodontist, 59: 247-255.

156. Jensen, O., R. Greer, L. Johnson and D. Kassebaum. 1995. Vertical guided bone-graft augmentation in a new canine mandibular model. International Journal of Oral and Maxillofacial Implants, 10: 335-344.

157. Schupbach, P., M. Hurzeler and U. Grunder. 1994. Implant-tissue interfaces following treatment of peri-implantitis using guided tissue regeneration. A light and electron microscopic study. Clinical Oral Implant Research, 5: 55-65.

158. Donath, K. 1987. Preparation of histologic sections. Norderstedt: Exakt-Kulzer Publication. p 13.

VITA

William Cyrus Stentz, Jr. was born in New Orleans, Louisiana on March 9, 1957 to William Cyrus Stentz and Anita Stewart Stentz. Following graduation from Alfred Bonnabel High School in Metairie, Louisiana, in May 1975, he attended The University of New Orleans in New Orleans, Louisiana, receiving the degree of Bachelor of Arts in Biology in 1979. In August 1979, he was admitted to the Louisiana State University School of Dentistry in New Orleans. In May 1983, he received the degree of Doctor of Dental Surgery and in July 1983, he began a General Practice Residency at the Wright-Patterson USAF Medical Center, Wright-Patterson AFB, Ohio. In July 1984, he was assigned as a staff general dentist to USAF Hospital, 36th TFW, Bitburg AB, Germany. In August 1987, he was reassigned as a staff dentist to Wilford Hall USAF Medical Center, Lackland AFB, Texas. In July 1992, he entered the Post-Doctoral Periodontics program at the University of Texas Health Science Center at San Antonio in conjunction with Wilford Hall USAF Medical Center.

Dr. Stentz was married to Maria Lisa Hogan in July 1984 prior to departing for Germany.